ARISTOTLE UNIVERSITY OF THESSALONIKI
Interinstitutional Program of Postgraduate Studies in
PALAEONTOLOGY – GEOBIOLOGY

EMMANOUIL FRAGKIOUDAKIS
Geologist

ECOMORPHOLOGICAL STUDY OF *POTAMOTHERIUM VALLETONI* (MAMMALIA : CARNIVORA)

MASTER THESIS

DIRECTION: Macropalaeontology
Directed by: Aristotle University of Thessaloniki

THESSALONIKI
2023

[page intentionally left blank]

Interinstitutional Program of Postgraduate Studies in PALAEONTOLOGY – GEOBIOLOGY

supported by:

Τμήμα Γεωλογίας ΑΠΘ
School of Geology AUTh

Τμήμα Βιολογίας ΑΠΘ
School of Biology AUTh

National and Kapodistrian University of Athens
Faculty of Geology and Geoenvironment

Τμήμα Γεωλογίας & Γεωπεριβάλλοντος ΕΚΠΑ

Faculty of Geology & Geoenvironment NKUA

Department of GEOLOGY

Τμήμα Γεωλογίας Παν/μίου Πατρών
Department of Geology, Patras Univ.

UNIVERSITY OF THE AEGEAN

Τμήμα Γεωγραφίας Παν/μίου Αιγαίου
Department of Geography, Aegean Univ.

[λευκή σελίδα]

EMMANOUIL FRAGKIOUDAKIS
ΕΜΜΑΝΟΥΗΛ ΦΡΑΓΚΙΟΥΔΑΚΗΣ
Πτυχιούχος Γεωλόγος

ECOMORPHOLOGICAL STUDY OF *POTAMOTHERIUM VALLETONI* (MAMMALIA : CARNIVORA)

ΟΙΚΟΜΟΡΦΟΛΟΓΙΚΉ ΜΕΛΈΤΗ ΤΟΥ *POTAMOTHERIUM VALLETONI* (ΘΗΛΑΣΤΙΚΑ : ΣΑΡΚΟΦΑΓΑ)

Υποβλήθηκε στο ΔΠΜΣ Παλαιοντολογία-Γεωβιολογία

Ημερομηνία Προφορικής Εξέτασης: 13/10/2023
Oral Examination Date: 13/10/2023

Three-member Examining Board

Associate Professor Georgios Lyras, Supervisor
Associate Professor Socrates Roussiakis, Member
Associate Professor Georgios Iliopoulos, Member

Τριμελής Εξεταστική Επιτροπή

Αναπληρωτής Καθηγητής Γεώργιος Λύρας, Επιβλέπων
Αναπληρωτής Καθηγητής Σωκράτης Ρουσιάκης, Μέλος Τριμελούς Εξεταστικής Επιτροπής
Αναπληρωτής Καθηγητής Γεώργιος Ηλιόπουλος, Μέλος Τριμελούς Εξεταστικής Επιτροπής

Citation:
Fragkioudakis E., 2023. – Ecomorphological Study of *Potamotherium valletoni* (Mammalia : Carnivora). Master Thesis, Interinstitutional Program of Postgraduate Studies in Palaeontology-Geobiology. School of Geology, Aristotle University of Thessaloniki, 115 pp.

Cover Figure: Filhol, M. H., 1879. Étude des mammifères fossiles de Saint-Gérand le Puy (Allier) par M. H. Filhol. Bibliothèque de l'Ecole des Hautes Études, Sciences Natural, Paris.

Table of Contents

Abstract

Potamotherium valletoni is a small semi-aquatic carnivore from late Oligocene-Miocene of Europe and North America. Although it is known and described for many years its exact placing within a particular taxonomic group is unclear, with different studies placing it either among the Lutrinae, the semi-aquatic subfamily of Mustelidae, or among stem-pinnipeds the ancestors of the Pinnipedia, the commonly known seals. This study aims to understand the possible foraging behavior of *Potamotherium*. It uses four different approaches: (a) a 3D geometric morphometric analysis of the shape of its skull (b) a 2D geometric analysis of the mandible; (c) the area its infraorbital foramen covered on its face was taken into account as an indicator to understanding how impactful its whiskers were in its foraging behavior; (d) a traditional morphometric analysis of the skull. The results of the first two analyses indicated that *Potamotherium valletoni's* skull had more similarities with skulls of modern Lutrinae. The analysis of the infraorbital foramen showed a possible primitive form of whiskering as a foraging method. The traditional morphometrics analysis placed *P. valletoni* among mouth-oriented predators of Lutrinae which prefer to hunt by swift bites, without using their forelimbs. Nevertheless, elements of cranial morphology remain unique on *P. valletoni*, like the shape of its elongated palate. This study concludes that *Potamotherium valletoni's* foraging had a strong resemblance with modern mouth-oriented hunters among Lutrinae.

Keywords: Mustelidae, Pinnipedia, Lutrinae, Geometric Morphometrics, Foraging habits

Περίληψη

Το *Potamotherium valletoni* είναι ένα μικρό ημιυδρόβιο σαρκοβόρο από το Ανώτερο Ολιγόκαινο εώς το Μειόκαινο της Ευρώπης και της Βορείου Αμερικής. Παρότι είναι γνωστό και έχει περιγραφεί εδώ και πολλά χρόνια η ακριβής τοποθέτηση του σε μία συγκεκριμένη ταξινομική ομάδα είναι αμφιλεγόμενη, με διαφορετικές μελέτες να το τοποθετούν είτε στις Λουτρίνες, την ημιυδροβια υποοικογένεια των Μουστελίδων, είτε στα πρώιμα πτερυγιόποδα, προγόνους των σημερινών πτερυγιοπόδων, των φωκών. Η συγκεκριμένη έρευνα αποσκοπεί στη κατανόηση των πιθανών μεθόδων θήρευσης του P. valletoni. Χρησιμοποιήθηκαν τέσσερις διαφορετικές προσεγγίσεις : α) τρισδιάστατη γεωμετρική μορφομετρία ως μέσο ανάλυσης του σχήματος του κρανίου β) δισδιάστατη γεωμετρική μορφομετρία ως μέσο ανάλυσης του σχήματος της κάτω γνάθους γ) υπολογισμός του εμβαδού του υποκογχικού τρήματος, ως δείκτης πιθανής χρήσεως των μουστακιων κατά τη θήρευση δ) παραδοσιακή μορφομετρική ανάλυση του κρανίου. Τα αποτελέσματα των δύο πρώτων αναλύσεων υποδεικνύουν πως το κρανίο του φέρει ομοιότητες με τα κρανία των σύγχρονων Λουτρίνων. Η ανάλυση του υποκογχικού τρήματος δείχνει πως μία κίνηση των μυστακίων του ανάλογη των σημερινών υδρόβιων και ημιυδρόβιων θηλαστικών ήταν δυνατή, πιθανώς σε μία πιο αρχέγονη μορφή. Η παραδοσιακή μορφομετρική ανάλυση το τοποθέτησε ανάμεσα στις Λουτρίνες που προτιμούν να κυνηγάνε με το στόμα με απότομες δαγκωματιές, χωρίς τη χρήση των εμπρόσθιων άκρων τους. Μολοταύτα, χαρακτήρες του κρανίου του παραμένουν μοναδικοί στο *P. valletoni,* όπως το σχήμα του υπερώιου οστού. Εν κατακλείδι, η έρευνα συμπεραίνει πως η θήρευση του *P. valletoni* έχει έντονες ομοιότητες με τις σύγχρονες Λουτρίνες που κυνηγάνε με το στόμα.

Λέξεις-κλειδιά: Μουστελίδες, Πτερυγιόποδα, Λουτρίνες, Γεωμετρική μορφομετρία, Συνήθειες θήρευσης

Acknowledgments

First of all, I have to thank my parents, Nikolaos and Eleni, my brothers, Stelis and Kotsos, my grandmothers Sofia and Poulcheria, my late grandfathers, Manolis Fragkioudakis and Stelios Damigos and all my extended family (Cousins, Uncles, Aunts, etc, sorry you are just so many to name drop individually).

I would like to heart-fully thank all the following people:

My committee: My supervisor Georgios Lyras from UoA for giving me such an interesting animal to study, all the help and patience he showed against my stupidity. Socrates Roussiakis from UoA, a great professor and my first contact with Palaeontology, back in 2015. Georgios Iliopoulos, University of Patras, one of the most pure scientists in this field.

Dolores Messer, PhD candidate from Technical University of Denmark for giving me permission to use her 3D skull models for this study. Denise Crampton, PhD, Liverpool John Moores University for the extremely helpful video tutorials. Nikolaos Kargopoulos, PhD for providing additional sources.

Dimitris Kostopoulos from AuTH, a man I feel grateful that I had the chance to work, converse and joke with. All the people from the Masters Program (Marina, Vicki, Christina, Nikos, Vaggelis, Christos). You are all great and deserve the best in life. Anastasia Katsagoni from AuTH (Thanks for the company!), George Konidaris from University of Tübingen, one of the kindest guys around. Vasiliki Dimou, Olga Koukousioura, Ioanna Sylvestrou and everybody else I had the pleasure to meet in AuTH.

Lambrini Karapanou and Eleftheria Karampetsou for being the best friends a man can ask for. Mirka Vasileiadi, Master of Paleontology for all the help throughout this period. All the people that I have the pleasure to call friends (Odysseas, Giorgos, Foukos, Chronis, Bagoudo, Ioanna, Thomas, Manos, Foteini, Achilles and all the rest, I love you all). Elli Koumantarou-Malisova and Nikos Nianakas.

The literally thousands of bands, musicians and artists that kept me company, especially Andi Deris, Michael Weikath, Kai Hansen and the rest of Helloween,

James from Hellripper, Iron Maiden, Alicia and Project: Roenwolfe, Rolf Kasparek and Running Wild (BEST riffs ever!), Gamma Ray, King Crimson, Darkthrone, Domine, Mark Shelton (RIP) and Manilla Road, Melissa and Sonja, Seven Sisters, Dave Mustaine, Manowar, Cirith Ungol, Yes, Fates Warning, the Hellacopters, James Rivera and Helstar, Harry Conklin and Jag Panzer, Virgin Steele, Blind Guardian, Warrel Dane (RIP) and Nevermore/Sanctuary, Bolt Thrower and I better stop there because space is limited. Michael Moorcock, Sir Terry Pratchett (GNU), Ursula K. LeGuin, Steven Erikson, Ian C. Esslemont, Don Rosa, NK Jemisin, Douglas Adams, Kazuki Takahashi, Kentaro Miura, Satoshi Tajiri and all my favorite authors and artists which work helped me mold myself.

ShadyPenguinn, MBT, Farfa, Rata, Gage ‘Nyhmnim’ Poljak, Cimooooooooo, Dzeeff and all the content creators that helped me relax with their videos, streams and unfunny jokes (I’m gonna banish a light and a dark, H&M, Agidooo!).

Monty Python, Phoenix Wright Ace Attorney, The Expendables 2 movie, Piotr Kropotkin, Nestor Makhno, Eat Metal Records, Panagiotis and Nellie from Pare Dose 2nd hand store, Metal Era, the creators of Pokemon Radical Red (by far the BEST ROM hack of all time),Ivan Jovanovic, Dimtris Kourbelis and all the Panathinaikos players of 2022-23 season, Erik Ten Hag, Marcus Rashford and Manchester United, Greg Popovich and San Antonio Spurs. Vaggelis ‘The Godfather’ Ioannou, Vasilis ‘Enthen kai Enthen’ Skoudis, Dimitris ‘Grand-guignol’ Chatzigeorgiou and at this point I’m really scraping the bottom of the barrel, aren't I?

And of course the most underrated composer of baroque music in ALL history : Johann Gambolputty de von Ausfern-schplenden-schlitter-crasscrenbon-fried-digger-dingle-dangle-dongle-dungle-burstein-von-knacker-thrasher-apple-banger-horowitz-ticolensic-grander-knotty-spelltinkle-grandlich-grumblemeyer-spelterwasser-kurstlich-himbleeisen-bahnwagen-gutenabend-bitte-ein-nürnburger-bratwustle-gerspurten-mitzweimache-luber-hundsfut-gumberaber-shönendanker-kalbsfleisch-mittler-aucher von Hautkopft of Ulm.

Thank you all.

So Long and Thanks for all the Fish.

1. Introduction

1. 1 General Introduction and aim of this study.

The genus *Potamotherium* has been described in sites ranging from the Late Oligocene to Middle Miocene (Kargopoulos et al., 2022), with the majority of the fossils being excavated from deposits of France, with the site of Saint Gerand-le-Puy (Figure 3B) being the one most abundant, although no complete skeleton has been discovered (Savage, 1957). Other regions that fossils of *Potamotherium* have been unearthed are Germany (Morlo, 1996 ; Mörs and von Koenigswald, 2000; Kargopoulos et al., 2022), Hungary (Rabi et al., 2018), Switzerland (Morlo, 1996) and North America (Baskin, 1998). Most major sites in which *Potamotherium* fossils have been found in Europe are shown in Figure 3A.
It is theorized that *Potamotherium* was one of the carnivorans that migrated from Eurasia to North America on a dispersal wave around 20 Ma through bridges created by tectonic actions (Qiu, 2003 ; Jiang et al., 2015). This migration possibly was directed from Europe to North America via Asia (Rabi et al., 2018). Except *P. valletoni,* the most common one and the focus of this research, a second species of the genus has been identified, *P. miocenicum* Peters, of exclusively Miocene age (Mörs et al., 2000).

There have been multiple theories about the phylogenetic placing of *Potamotherium* within Arctoidea, the superfamily that includes Pinnipedia, Mustelidae and Ursidae (Finarelli, 2008). For many years it was considered a member of Lutrinae, a Mustelidae sub-family (Savage, 1957), with some older references even naming it *Lutra valletoni* (Filhol, 1879), while later classifications put it under another subfamily of Mustelidae, the extinct Oligobuninae (Baskin, 1998) or even its own subfamily, Potamotheriinae (Willemsen, 1992). Another proposed theory was that *Potamotherium* was essentially an in-between genus with characters of both Pinnipeds and Mustelidae and was placed under the

subfamily Semantorinae along the genus *Semantor*, as a possible sister group to Otariidae, the Pinniped family that is consisted of the seals commonly known as sea lions (Tedford, 1976).

Similarities observed between pinnipeds and *Potamotherium* can be traced in different studies for at least a century back and even hinted at a common ancestor of both Mustelidae and pinnipeds related to *Potamotherium*, based on morphological similarities (Kellogg, 1922). An additional theory about its phylogenetic position was that it belonged to a sister clade to Phocidae, among the pinniped families, sharing a common ancestor, a distinction made on the basis of the loss of the alisphenoid canal on both (Wolsan, 1993). Rybczynski et al., (2009) placed *Potamotherium* as an early pinniped along with the basal pinniped genus *Enaliarctos* and the, then recently discovered, terrestrial stem-pinniped *Puijila darwini* based on similarities in characters of their respective morphologies both on the skull and post cranial bones.

A more recent approach by Paterson et al. (2020) using Total-Evidence Dating and synapomorphies of the skull, placed *Potamotherium*, along with *Puijila*, as a sister clade to Pinnipedomorpha and stem pinnipeds, which diverged before Enaliarctos as their own clade on the phylogenetic tree (Figure 1). The term Pinnipedomorpha includes the most recent common ancestor of the *Enaliarctos* and its descendants (Berta, 1991). Both genera seem to be members of Pinnipedomorpha that diverged before *Enaliarctos*, although they don't have many of the synapomorphies that are characteristic of pinnipeds, something that is expected as their position in the phylogenetic tree is as stem pinnipedia (Paterson et al., 2020).

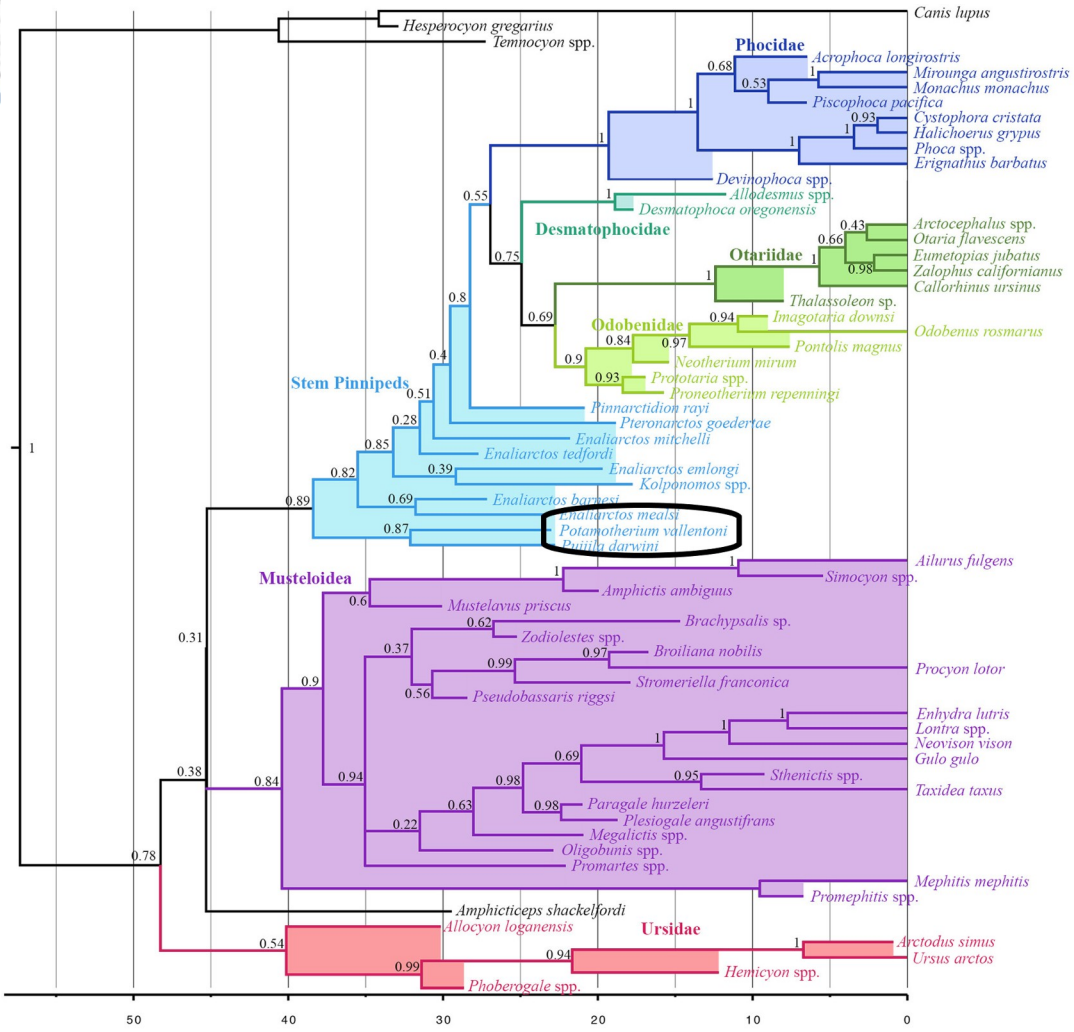

Figure 1: Phylogenetic consensus tree of Arctoidea using Bayesian Inference. Product of Total-Evidence Tip-Dating Analysis. Modified after Paterson et al., (2020).

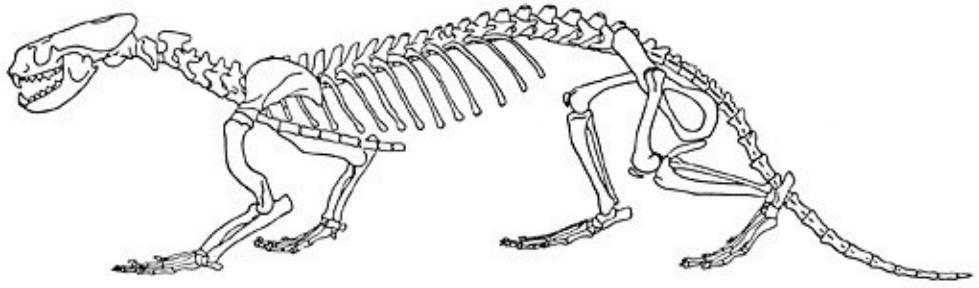

Figure 2: Reconstruction of *P. valletoni's* complete skeleton from individual bones. From Savage (1957)

Potamotherium's habitat seemed to be freshwater, shallow areas either lakes that were surrounded by marshes like the ones on the Saint Gerand-le-Puy site (Savage, 1957) and nearshore areas with subtropical climate (Szabo et al., 2017 ; Rabi et al., 2018). This can be concluded either by sedimentological data (Szabo et al., 2017) or by studying the fauna that accompanies *Potamotherium* on the sites like the fauna of Saint Gerand-le-Puy (Filhol, 1879). In Saint Gerand-le-Puy, ostracods and morphological and functional characters of the different mammals show the possible paleoenvironment as a lake with borders leading to an open background, at the northern part of the Limagne rift basin (Hugueney et al., 1999; Hugueney et al., 2006). The climate of the area was considered as subtropical to tropical with a rotation between dry and drizzly seasons (Cheneval, 1989).

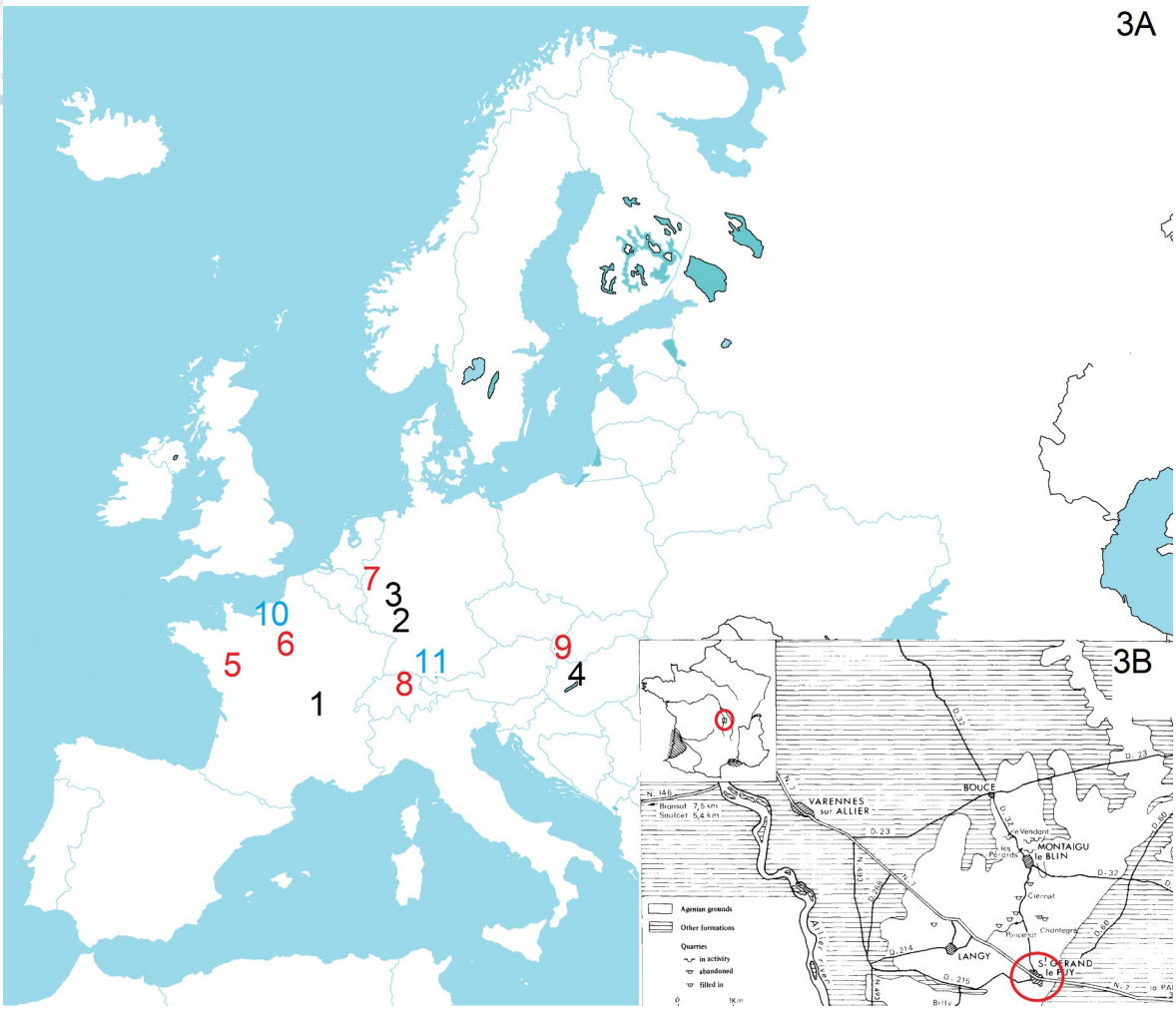

Figure 3: Map of major European sites in which *Potamotherium* has been discovered. 3A. Black numbers indicate *P. valletoni,* Red numbers indicate *P. miocenicum*, Blue numbers indicate *Potamotherium* sp. : 1. St. Gerand-le-Puy, France (Savage, 1957). 2. Mainz Basin, Germany (Morlo, 1996). 3. Espen, Germany (Mors and von Koengiswald, 2000). 4. Máriahalom, Hungary (Rabi et al., 2018). 5. Pontigne, France (Ginsburg and Bonneau, 1995). 6. Artenay, France (Mors et al., 2000). 7. Hambach, Germany (Mors et al., 2000). 8. Elgg, Switzerland (Heer, 1876 ; Bolliger, 2000). 9. Sandberg, Slovakia (Sabol and Holec, 2002). 10: Baigneaux-en-Bause, France (Possible *P. miocenicum*)(Heizmann and Ginsburg, 1980). 11. Hammerschmiede, Germany (Kargopoulos et al., 2022). Map from commons.wikimedia.org. In USA's west coast additional *Potamotherium* sp. fossils have been found. 3B: Map of Saint Gerand-le-Puy in which the cranium and the mandibles used in this study were discovered. Modified after Savage, 1957.

Savage (1957) drafted a thorough analysis and description of *P. valletoni's* morphology using mostly independent fossils from Saint Gerand-le-Puy. He concluded that *P. valletoni* should have a similar appearance to that of the mustelid genus *Lutra* while moving on land ,alas slower than modern otters. While swimming, it seems that *P. valletoni* was pretty agile and fast, and a great predator of the aquatic fauna available, using all of his body parts as tools for locomotion purposes in the water.

His description of *P. valletoni's* teeth led him to the conclusion that, while they have some morphological differences, with those of *Lutra*, in the end do not betray any difference in the eating habits between the two species. However, *P. valletoni's* dentition is more primitive, with an atrophic m2, even though it does not support a difference in function.

Morphologically there are some significant characters that give *P. valletoni* its unique identity (Savage, 1957). Baskin (1998) compiled a number of cranial and dental characters that distinguish *Potamotherium* and help for its identification: Its frontal bone is elongated, the premolars have a cingulum, P1 and p1 can be found on the skull, P4 is extended while M1 is narrow with parallel anterior and posterior margins and around its protocone there is a noticeable parastylar shelf and a well-developed internal cingulum that extend anteriorly and posteriorly respectively, M2 and m2 are single rooted, p4 has prominent anterior and posterior accessory cups, the metaconid of m1 is small in comparison to its paraconid, while its talonid is narrow and semi trenchant, the auditory bulla its flattened and small, its posterior carotid foramen is of considerable size and adjacent to a larger posterior lacerate foramen, while its postglenoid foramen is almost absent.

Today there are many papers concerning the ecomorphological and feeding habits of Pinnipeds and Mustelidae are released on a worldwide scope. However, no study has been focused exclusively on *P. valletoni.* The fact that these two groups are the ones are the most commonly compared with *P. valletoni* and the absence of a thorough, modern examination of it are the motives behind the following analyses which could help in understanding both the lifestyle and the phylogenetic placement of *P. valletoni* within Arctoidea.

1. 2 Related groups and their feeding habits

1. 2. 1. Musteloidea and Pinnipedia

Musteloidea are the richest superfamily within the order Carnivora, with 84 extant species and more than 400 described extinct species, representing approximately 30% of the diversity of the order (Sato et al., 2012 ; Law et al., 2018). Musteloidea are an exceptionally diverse superfamily on an ecological level as they include members that are fully terrestrial and arboreal to species with an aquatic lifestyle and a cornucopia of intermediate lifestyles between different subfamilies and species (Fabre et al., 2013). That means that their feeding strategies and diets can be pretty different between species of the superfamily ranging from herbivorous animals to fully carnivorous members (Dumont et al., 2016).

Among Musteloidea, the family Mustelidae is the one that has been compared morphologically to *Potamotherium* in the bibliography throughout the years based on their similarities and is the largest one among Carnivora with 22 genera and 59 species among them (Koepfli et al., 2008) and a distribution that spans every continent bar Antarctica and Oceania (Yu et al., 2011), although some species can be found in New Zealand as invasive animals introduced by humans, dangerous to the ecological balance (Byrom et al., 2015). It is consisted of eight extant subfamilies, each one with distinctive features (Lutrinae, Mustelinae, Guloinae, Melinae, Ictonychinae, Helictindinae, Taxidiinae, Mellivorinae) (Law et al., 2018b) and the extinct Oligobuninae (Baskin, 2017). Among Musteloidea, Mustelidae is the richest family, far outnumbering the others that are part of the superfamily (Ailuridae, Mephitidae, Procyonidae) (Law et al., 2018). Their high geographical diversity lead to a high locomotion diversity, with members of the family which are fossorial, semi-aquatic and semi-arboreal (Koepfli et al., 2008).

Pinnipeds are classified under the order Carnivora with three distinct, extant families and one extinct family being part of them. Odobenidae, that includes one extant member, *Odobenus rosmarus* (walrus), Otariidae which includes sea lions and fur seals, Phocidae, which includes the earless seals and Desmatophocidae,

the extinct family that lived at the North Pacific in the Miocene (Demere and Berta, 2001 ; Berta et al., 2018 ; Boessenecker and Churchill, 2018). Their geographic diaspora is nearly global, with around 28% of marine mammals nowadays being Pinnipeds that are distributed in 33 different species, not including the recently extinct *Monachus tropicalis* (Stirling, 1983 ; Higdon et al., 2007 ; Berta et al., 2018). They are associated mainly with environments which have low temperature waters that rarely exceed 20°C, with some exceptions that can be found in warmer areas, like the genus *Monachus* (King, 1956 ; Davies, 1958). The main areas that extant Pinnipeds are concentrated are the subarctic parts of the Atlantic and the Pacific Ocean and around the edges of Antarctica (Davies, 1958).

The genus *Semantor*, often associated with *P. valletoni*, was discovered in Miocenian strata of Central Asia and is only known by post cranial material (Orlov, 1932), meaning that is impossible to compare cranial elements with *P. valletoni* in this study, although it appears that it was a semi-aquatic animal resembling Lutrinae in characters of its morphology and habits (Lavrov et al., 2018).

1. 2. 2. Mustelidae eating habits

Mustelidae, unlike Pinnipedia, which will be described in the next subchapter, do not have clearly defined strategies which they use to eat. Contrariwise, they are highly adaptable animals able to modify their feeding based on the environmental pressures which even inside their subfamilies lead to them having completely different diets from hypercarnivores to omnivores (Derežanin et al., 2022).

As mentioned earlier, the subfamily Lutrinae (otters) is the one with the most morphological similarities to *P. valletoni* (Savage, 1957). In general, Lutrinae are separated in two categories based on their feeding technique: the first one includes otters that use their mouth to catch their prey and are mainly piscivores, and the second includes otters that use their forelimbs to immobilize their prey and are invertebrate specialized hunters (Timm-Davis et al., 2015).

1. 2. 3. Pinnipedia eating strategies

In general, pinnipeds use three different strategies to feed underwater among those used by aquatic mammals (Figure 4), biting their prey with pierce feeding or grip-and-tear, filter feeding and suction feeding (Kienle and Berta, 2019).

Pierce feeding in aquatic quadrupeds is mostly connected with the need of the animals to capture their prey, hold it with their teeth, that are usually small and sharp, and swallow it in its entirety, all in one move, without mastication taking place (Adam and Berta, 2002). Characters that are associated with pierce feeding are the lack of distinct occlusal wear on postcanine teeth, a m1 that is anterior to the midpoint of the dentition, homodonty among its postcanine teeth, and enlarged orbits and infraorbital foramina, with this enlargement being a character found only on mammals that transitioned from terrestrial to aquatic habitats (Adam and Berta, 2002).

Grip-and-tear as a strategy to prey capture is used only by one extant pinniped, the leopard seal, *Hydrurga leptonyx* (Kienle and Berta, 2016). After it captures its prey, mostly penguins it stalks underwater, it tosses it back and forth until its head is mauled, then it eats by biting and hurling the carcass around until only skeletal parts remain (Penney and Lowry, 1967). Because, leopard seals are the only pinniped that uses this strategy to hunt, characters of pinnipeds that are connected to grip-and-tear feeding are based on it and are the enlargement of the incisors, the long and sharp postcanine teeth a long skull with a wide base, large orbits and long parietal bones (Adam and Berta, 2002 ; Kienle and Berta, 2016).

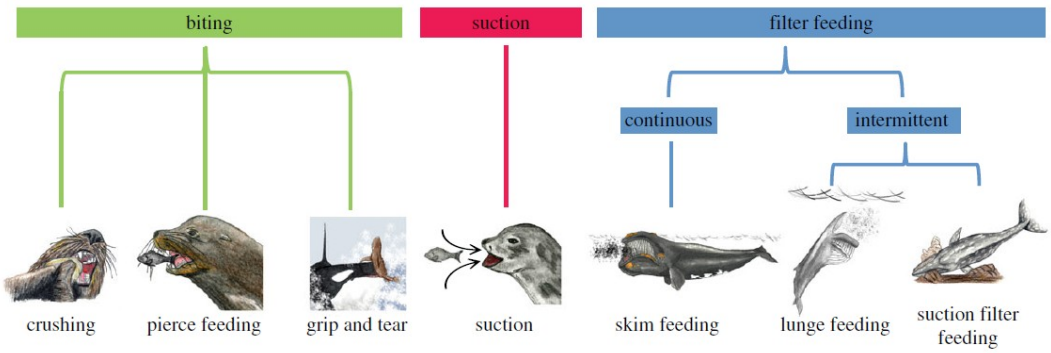

Figure 4: Compilation of basic feeding methods of marine mammals. From Kienle et al., 2017.

Filter feeding as a technique is present in several groups of vertebrate and invertebrate animals and its product of independent evolution, with the mechanisms that different groups use to feed being substantially different at a fundamental level (Riisgard, 2015). It can be defined as the separation of small prey from water with the use of dedicated filtering structures, like baleen on cetaceans or specialized teeth (Hocking et al., 2017). In pinnipeds filter feeding is connected with long, narrow skulls, narrow palates, elongated teeth, thick mandibular symphysis and big postcanine teeth (Berta and Lanzetti, 2020) *Lobodon carcinophaga* is the most characteristic pinniped species that uses it, with its postcanine teeth been used as a sieve when they are interlocked, allowing water to leave its mouth while krill remains in (Werth, 2000).

Suction feeding is a prey capture strategy developed independently in many different aquatic vertebrates, including cetaceans, fishes and pinnipeds and it is a product of independent evolution, though there is no family of marine mammals that use it exclusively (Werth, 2000). It can be defined as the generation of lower intraoral pressure to draw prey into, or transport prey inside, the oral cavity and then swallow it, while shells and remains are dropped (Adam and Berta, 2002 ; Hocking et al., 2017). Specialized suction feeders typically have wide skulls, arched palates and reduced dentition (Berta and Lanzetti, 2020). While walrus is the only extant pinniped that is mainly a suction feeder, other seals, elephant seals and fur seals for example, are able to use suction feeding at a lower level of expertise when they hunt smaller prey (Hocking et al., 2016). In pinnipeds skulls,

suction feeding is connected with arched hard palates, lengthened hard palates, robust pterygoid hamuli that are knob-like, fewer incisors, both upper and lower, and if the mandibular symphysis is ankylosed or not (Adam and Berta, 2002). As the main suction feeder, *Odobenus rosmarus* hunts by moving along the bottom, with its head first, using its hind flippers as a propeller, and its vibrissae as a tool to locate its prey (Fay, 1985).

2. Materials and methods

2. 1 Materials

2. 1. 1 *Potamotherium valletoni* material

***Potamotherium valletoni* Geoffroy, 1833**. NMBA SG2629. Left half of mandible. Collected from Saint Gérand le Puy, France. Figure 6.

***Potamotherium valletoni* Geoffroy, 1833**. NMBA SG21676, Left half of mandible. Collected from Saint Gérand le Puy, France, 1926. Figure 7.

***Potamotherium valletoni* Geoffroy, 1833**. MNHN SG692. Cranium. Collected from Saint-Gérand-le-Puy, France. Downloaded from www. phenome10k. org. Figure 5.

Figure 5: The cranium of *P. valletoni* MNHM SG 692 from Museum of Natural History of Paris collection.

Figure 6: *P. valletoni's* mandible SG 2629. From the Natural History Museum of Basel collection

Figure 7: *P. valletoni's* mandible SG 21676. From the Natural History Museum of Basel collection.

2.1.2 Mandibles

Mandibles used for 2D morphometric analysis

Mustelidae

All the Mustelidae photos used for the study were taken from the mammalian collection of Basel Natural History Museum.

***Aonyx capensis* Schinz, 1821**. NMBA 11499,full mandible.
***Aonyx capensis* Schinz, 1821**. NMBA 14056 (ACA1), full mandible.
***Aonyx congicus* Lönnberg, 1910**. NMBA 14058, full mandible.
***Aonyx congicus* Lönnberg, 1910**. NMBA 14061, full mandible.
***Aonyx cinerea* Illiger, 1815**. NMBA 6099, full mandible. Male. Collected in Java, Indonesia, 1936.
***Aonyx cinerea* Illiger, 1815**. NMBA 8627, full mandible.
***Aonyx cinerea* Illiger, 1815**. NMBA 3785, left half of mandible. Collected in the Indragiri river area, Sumatra, Indonesia, 1905.
***Aonyx cinerea* Illiger, 1815**. NMBA 8801, full mandible.
***Enhydra lutris* Linnaeus, 1758.** NMBA 10738, full mandible.
***Hydrictis maculicollis* Lichtenstein, 1835.** NMBA 14063 (Z1640), full mandible.
***Hydrictis maculicollis* Lichtenstein, 1835**. NMBA 14064 (Z2261), full mandible.
***Hydrictis maculicollis* Lichtenstein, 1835.** NMBA 14065 (Z3220), full mandible.
***Hydrictis maculicollis* Lichtenstein, 1835.** NMBA 14066 (Z3559), full mandible.
***Lontra canadensis* Schreber, 1777.** NMBA 1837 (670), full mandible.
***Lontra canadensis* Schreber, 1777.** NMBA 14068 (scm274), full mandible.
***Lontra canadensis* Schreber, 1777**. NMBA 14069 (scm275), full mandible.
***Lontra canadensis* Schreber, 1777**. NMBA 14070 (scm276), full mandible.
***Lontra canadensis* Schreber, 1777**. NMBA 14071 (scm277), full mandible.
***Lontra canadensis* Schreber, 1777**. NMBA 14073 (scm279), full mandible.
***Lutra lutra* Linnaeus, 1758**. NMBA 5720, full mandible. Collected in Remoulins, Gard, France, 1918 by Biedermann-Imhoof.

***Lutra lutra* Linnaeus, 1758**. NMBA 7451, full mandible. Male. Collected in Toulouse, France.

***Lutra lutra* Linnaeus, 1758**. NMBA 7950, full mandible.

***Lutra lutra* Linnaeus, 1758**. NMBA C4081, full mandible. Collected in 1909.

***Lutra lutra* Linnaeus, 1758**. NMBA C4082, full mandible. Collected in 1909.

***Lutra lutra* Linnaeus, 1758**. NMBA C1795, full mandible. Collected in 1874.

***Lutra lutra* Linnaeus, 1758**. NMBA C. M. 150, full mandible.

***Lutra lutra* Linnaeus, 1758**. NMBA C. M. 402, full mandible.

Pinnipedia

All the Pinnipedia photos used for the study were taken from the Mammals collection of the Museum of Natural History in Paris, France.

***Arctocephalus gazella* Peters, 1875**. MNHM-ZM-MO-2001-2072, left half of mandible.

***Cystophora cristata* Erxleben, 1777**. MNHM-ZM-2007-406, right half of mandible.

***Erignathus barbatus* Erxleben, 1777**. MNHM-ZM-AC-1926-83, right half of mandible.

***Eumetopias jubatus* Schreber, 1776**. MNHM-ZM-MO-1977-775, left half of mandible. Male.

***Halichoerus grypus* Fabricius, 1791**. MNHM-ZM-MO-1991-723, right half of mandible. Male.

***Hydrurga leptonyx* de Blainville**, **1820**. MNHN-ZM-AC-1926-73, full mandible.

***Hydrurga leptonyx* de Blainville, 1820**. MNHM-ZM-MO-1978-346, right half of mandible.

***Leptonychotes weddellii* Lesson, 1826**. MNHM-ZM-AC-1926-67, left half of mandible.

***Lobodon carcinophaga* Hombron and Jacquinoy, 1842**. MNHM-ZM-2005-263, right half of mandible.

***Lobodon carcinophaga* Hombron and Jacquinoy, 1842**. MNHM-ZM-AC-1926-48, full mandible.

***Lobodon carcinophaga* Hombron and Jacquinoy, 1842**. MNHM-ZM-AC-1926-50, left half of mandible.

***Lobodon carcinophaga* Hombron and Jacquinoy, 1842**. MNHM-ZM-AC-1926-51, left half of mandible.

***Mirounga leonina* Linnaeus, 1758.** MNHM-ZM-MO-1971-113, right half of mandible. Male.

***Mirounga leonina* Linnaeus, 1758**. MNHM-ZM-MO-1972-647, right half of mandible. Male.

***Monachus monachus* Hermann, 1779**. MNHM-ZM-AC-1982-142, full mandible.

***Onomatophoca rossii* Gray, 1844**. MNHM-ZM-AC-1924-76, right half of mandible.

***Otaria flavescens* Shaw, 1800.** MNHM-ZM-AC-1907-291, right half of mandible.

***Pusa caspica* Gmelin, 1788.** MNHM-ZM-MO-1992-381, right half of mandible.

***Pagophilus groenlandicus* Erxleben, 1777**. MNHM-ZM-AC-A2910, right half of mandible. Male.

***Pusa hispida* Schreber, 1775**. MNHM-ZM-MO-1934-45, right half of mandible.

***Phoca vitulina* Linnaeus, 1758**. MNHM-ZM-AC-1896-129, left half of mandible.

***Phoca vitulina* Linnaeus, 1758**. MNHM-ZM-ZC-1940-294, right half of mandible. Female.

***Zalophus californianus* Lesson, 1828**. MNHM-ZM-AC-1879-271, right half of mandible.

2. 1. 3. Craniums and Skulls

3D models of skulls used for morphometric analysis. The databases that this study ended up collecting material from were Morphosource (https:/morphosource. org), Sketchfab (https:/sketchfab. com), Digimorph (http:/digimorph. org) and Phenome10K (https:/phenome10k. org).

Mustelidae

***Aonyx capensis* Schinz, 1821**. Cranium. CMNH 17620. MorphoSource Specimen ID 0000S5876 Uploaded by Tseng, J.

***Eira barbara* Linnaeus, 1758**. Cranium. MorphoSource Specimen ID 370801. Uploaded by Dickinson, E. Laboratory of Adam Hartstone-Rose collection.

***Enhydra lutris* Linnaeus, 1758.** Skull. AMNH M-24186. Male. MorphoSource Specimen ID 0000S2718 Uploaded by Tseng, J.

***Enhydra lutris* Linnaeus, 1758**. Cranium. RISD Nature Lab. Accession number 438. 93. Downloaded from www. Sketchfab. com. Uploaded by Edna Lawrence's RISD Nature Lab.

***Enhydra lutris* Linnaeus, 1758.** Skull. Zooarchaeology Lab Collection of the Department of Anthropology, University of Victoria. Male. Downloaded from www. SketchFab. com.

***Gulo gulo* Linnaeus, 1758.** Cranium. MSU 3844. From MSU's Mammalogy, Ornithology and Vertebrate Paleontology Collections. MorphoSource Specimen ID 000S30806. Uploaded by Adams, J.

***Gulo gulo* Linnaeus, 1758**. Cranium MSU 10149. Female. From MSU's Mammalogy, Ornithology and Vertebrate Paleontology Collections. MorphoSource Specimen ID 000S30805 Uploaded by Adams, J.

***Gulo gulo* Linnaeus, 1758**. Cranium. MorphoSource Specimen ID 370812. Uploaded by Dickinson, E. Laboratory of Adam Hartstone-Rose collection.

***Gulo gulo* Linnaeus, 1758**. Cranium. SMNS-Z-MAM-051682. MorphoSource Specimen ID 000S31044 Uploaded by Rovinsky, D.

***Gulo gulo* Linnaeus, 1758**. Cranium. SMNS-Z-MAM-006833. MorphoSource Specimen ID 000S31045 Uploaded by Rovinsky, D.

***Gulo gulo* Linnaeus, 1758**. Skull. RISD Nature Lab. Accession number 460. 06. Downloaded from www. Sketchfab. com. Uploaded by Edna Lawrence's RISD Nature Lab.

***Hydrictis maculicollis* Lichtenstein, 1835.** Cranium AMNH-M-89807. MorphoSource Specimen ID 0000S5879. Uploaded by Tseng, J.

***Lontra canadensis* Schreber, 1777**. Cranium. Downloaded from www. MorphoSource. org , Duke University. MorphoSource Specimen ID 371053. Uploaded by Dickinson, E. Laboratory of Adam Hartstone-Rose collection.

***Lontra canadensis* Schreber, 1777**. Skull. AMNH M-254476. Male. MorphoSource Specimen ID 0000S2722. Uploaded by Tseng, J.

***Lontra canadensis* Schreber, 1777**. Skull. RISD Nature Lab. Accession number 461. 06. Downloaded from www. Sketchfab. com. Uploaded by Edna Lawrence's RISD Nature Lab.

***Lontra canadensis* Schreber, 1777**. Skull. Female. Zooarchaeology Lab Collection of the Department of Anthropology, University of Victoria. Male. Downloaded from www. SketchFab. com.

***Lontra felina* Molina, 1782**. Cranium AMNH M-48193. MorphoSource Specimen ID 0000S5880. Uploaded by Tseng, J.

***Lontra longicaudis* Olfers, 1818.** Cranium. AMNH-M-98589. MorphoSource Specimen ID 0000S5581. Uploaded by Tseng, J.

***Lutra lutra* Linnaeus, 1758**. Cranium. UMZC k. 2768. MorphoSource Specimen ID 0000S36759. Collected from Cambridgeshire. Uploaded by Evers S.

***Lutra lutra* Linnaeus, 1758**. Cranium. AMNH-M-206592. Male. MorphoSource Specimen ID 0000S5882. Uploaded by Tseng, J.

***Lutrogale perspicillata* Geoffroy Saint-Hilaire, 1826**. Cranium AMNH M-204747. Male. MorphoSource Specimen ID 0000S5883. Uploaded by Tseng, J.

***Martes americana* Turton, 1806**. Cranium. MorphoSource Specimen ID 371066. Uploaded by Dickinson, E. Laboratory of Adam Hartstone-Rose collection.

***Martes americana* Turton, 1806.** Skull. Zooarchaeology Lab Collection of the Department of Anthropology, University of Victoria. Male. Downloaded from www. SketchFab. com.

***Martes foina* Erxleben, 1777.** Skull. RISD Nature Lab. Accession number 125. 17. Downloaded from www. Sketchfab. com. Uploaded by Edna Lawrence's RISD Nature Lab.

***Martes martes* Linnaeus, 1758**. Cranium SMNS-Z-MAM-047060. MorphoSource Specimen ID 000S31201. Uploaded by Rovinsky, D.

***Martes martes* Linnaeus, 1758**. Cranium SMNS-Z-MAM-046570. Female. MorphoSource Specimen ID 000S31200. Uploaded by Rovinsky, D.

***Martes martes* Linnaeus, 1758**. Cranium. SMNS-Z-MAM-021806. MorphoSource Specimen ID 000S31055. Uploaded by Rovinsky, D.

***Martes martes* Linnaeus, 1758**. Cranium. SMNS-Z-MAM-021808. Male. MorphoSource Specimen ID 000S31056. Uploaded by Rovinsky, D.

***Mellivora capensis* Schreber, 1777**. Cranium. UMZC k. 1821. MorphoSource Specimen ID 000S36761. Uploaded by Evers, S.

***Meles meles* Linnaeus, 1758**. Cranium. Lapworth Museum of Geology. Downloaded from www. SketchFab. com.

***Meles meles* Linnaeus, 1758**. Cranium. MZB 2011-1034. Female. Museu de Ciències Naturals de Barcelona. Collected from Catalonia, Spain. Downloaded from www. Sketchfab. com.

***Meles meles* Linnaeus, 1758.** Skull. MRI-PAS-170721 From the Zoological collection of Mammal Research Institute, Polish Academy of Sciences. Part of Open Forest Data project. Downloaded from www. SketchFab. com.

***Mustela eversmanii* Lesson, 1827**. Skull. MRI-PAS-91844. From the Zoological collection of Mammal Research Institute, Polish Academy of Sciences. Part of Open Forest Data project. Downloaded from www. SketchFab. com .

***Mustela nivalis* Linnaeus, 1766**. Cranium. MRI-PAS-35262. From the Zoological collection of Mammal Research Institute, Polish Academy of Sciences. Part of Open Forest Data project. Downloaded from www. SketchFab. com.

***Mustela putorius* Linnaeus**, 1758. Skull. MRI-PAS-90420. From the Zoological collection of Mammal Research Institute, Polish Academy of Sciences. Part of Open Forest Data project. Downloaded from www. Sketchfab. com.

***Mustela putorius* Linnaeus, 1758**. Skull. MRI-PAS-27896. From the Zoological collection of Mammal Research Institute, Polish Academy of Sciences. Part of Open Forest Data project. Downloaded from www. Sketchfab. com.

***Mustela sp.* Linnaeus, 1758.** Skul. RISD Nature Lab. Accession Number 77. 85. Downloaded from www. Sketchfab. com. Uploaded by Edna Lawrence's RISD Nature Lab.

***Neovison vison* Schreber, 1777**. Cranium. SMNS-Z-MAM-021831. MorphoSource Specimen ID 000S31204. Uploaded by Rovinsky, D.

***Neovison vison* Schreber, 1777.** Cranium. SMNS-Z-MAM-032536. MorphoSource Specimen ID 000S31205. Uploaded by Rovinsky, D.

***Neovison vison* Schreber, 1777**. Cranium. MorphoSource Specimen ID 371103. Uploaded by Dickinson, E. Laboratory of Adam Hartstone-Rose collection.

***Neovison vison* Schreber, 1777.** Cranium. RISD Nature Lab. Accession Number 91. 85. Downloaded from www. Sketchfab. com. Uploaded by Edna Lawrence's RISD Nature Lab.

***Neovison vison* Schreber, 1777.** Zooarchaeology Lab Collection of the Department of Anthropology, University of Victoria. Male. Downloaded from www. SketchFab. com.

***Pteronura brasiliensis* Gmelin, 1788.** Cranium. AMNH-M98594. Male. Morphosource Specimen ID 0000S5884. Uploaded by Tseng, J.

***Pteronura brasiliensis* Gmelin, 1788**. Cranium. MorphoSource Specimen ID 371144. Uploaded by Dickinson, E. Laboratory of Adam Hartstone-Rose collection.

***Taxidea taxus* Schreber, 1777**. Skull. MorphoSource Specimen ID 371155. Uploaded by Dickinson, E. Laboratory of Adam Hartstone-Rose collection.

***Taxidea taxus* Schreber, 1777.** Skull. LACM 45012. Female. Downloaded from www. digimorph. org Uploaded by Owen, P.

***Taxidea taxus* Schreber, 1777**. Subspecies jeffersonii. Skull. Zooarchaeology Lab Collection of the Department of Anthropology, University of Victoria. Male. Downloaded from www. SketchFab. com.

***Taxidea taxus* Schreber, 1777**. Cranium. IMNH R230. Idaho Museum of Natural History provided access to these data. MorphoSource Specimen ID 000106552. Uploaded by Tyler, J.

Pinnipedia

***Arctocephalus townsendi* Merriam, 1897**. Cranium. LEPBLB-AT-CSL-988-281111. Laboratorio de Ecologia de Pinnipedos ''Burney J. Le Boeuf''. MorphoSource Specimen ID 0000S22561. Uploaded by David Polly, P.

***Callorhinus ursinus* Linnaeus, 1758**. Skull. Zooarchaeology Lab Collection of the Department of Anthropology, University of Victoria. Male. Downloaded from www. SketchFab. com.

***Halichoerus grypus* Fabricius, 1791**. Cranium. NHMUK-ZOO-1961. 1. 23. 7. Natural History Museum (London) Collection Specimens. MorphoSource Specimen ID 392597. Uploaded by Messer, D.

***Halichoerus grypus* Fabricius, 1791.** Cranium. NHMUK-ZOO-1961. 5. 18. 4. Male. Natural History Museum (London) Collection Specimens. MorphoSource Specimen ID 392602. Uploaded by Messer, D.

***Halichoerus grypus* Fabricius, 1791**. Cranium. NHMUK-ZOO-1961. 1. 23. 6. Female. Natural History Museum (London) Collection Specimens. MorphoSource Specimen ID 392592. Uploaded by Messer, D.

***Halichoerus grypus* Fabricius, 1791**. Cranium. NHMUK-ZOO-1961. 5. 18. 30. Female. Natural History Museum (London) Collection Specimens. MorphoSource Specimen ID 390398. Uploaded by Messer, D.

***Halichoerus grypus* Fabricius, 1791**. Cranium. NHMUK-ZOO-1961. 1. 23. 3. Female. Natural History Museum (London) Collection Specimens. MorphoSource Specimen ID 392577. Uploaded by Messer, D.

***Halichoerus grypus* Fabricius, 1791**. Cranium. NHMUK-ZOO-1961. 5. 18. 13. Male. Natural History Museum (London) Collection Specimens. MorphoSource Specimen ID 390276. Uploaded by Messer, D.

***Halichoerus grypus* Fabricius, 1791**. Cranium. NHMUK-ZOO-1951. 11. 28. 1. Natural History Museum (London) Collection Specimens. MorphoSource Specimen ID 390439. Uploaded by Messer, D.

***Halichoerus grypus* Fabricius, 1791**. Cranium. NHMUK-ZOO-1961. 1. 23. 4. Female. Natural History Museum (London) Collection Specimens. MorphoSource Specimen ID 392582. Uploaded by Messer, D.

***Halichoerus grypus* Fabricius, 1791**. Cranium. NHMUK-ZOO-1988. 328. Natural History Museum (London) Collection Specimens. MorphoSource Specimen ID 390429. Uploaded by Messer, D.

***Halichoerus grypus* Fabricius, 1791**. Cranium. NHMUK-ZOO-1961. 5. 18. 36. Female. Natural History Museum (London) Collection Specimens. MorphoSource Specimen ID 390418. Uploaded by Messer, D.

***Halichoerus grypus* Fabricius, 1791**. Cranium. NHMUK-ZOO-1961. 5. 18. 15. Male. Natural History Museum (London) Collection Specimens. MorphoSource Specimen ID 390281. Uploaded by Messer, D.

***Halichoerus grypus* Fabricius, 1791**. Cranium. NHMUK-ZOO-1961. 5. 18. 35. Female. Natural History Museum (London) Collection Specimens. MorphoSource Specimen ID Uploaded by Messer, D.

***Halichoerus grypus* Fabricius, 1791**. Cranium. NHMUK-ZOO-1961. 5. 18. 32. Female. Natural History Museum (London) Collection Specimens. MorphoSource Specimen ID 390408. Uploaded by Messer, D.

***Halichoerus grypus* Fabricius, 1791**. Cranium. NHMUK-ZOO-1961. 5. 18. 37. Natural History Museum (London) Collection Specimens. MorphoSource Specimen ID 390424. Uploaded by Messer, D.

***Halichoerus grypus* Fabricius, 1791**. Cranium. NHMUK-ZOO-1961. 1. 23. 2. Female. Natural History Museum (London) Collection Specimens. MorphoSource Specimen ID 390266 Uploaded by Messer, D.

***Halichoerus grypus* Fabricius, 1791**. Cranium. NHMUK-ZOO-1961. 5. 18. 24. Female. Natural History Museum (London) Collection Specimens. MorphoSource Specimen ID 390286. Uploaded by Messer, D.

***Halichoerus grypus* Fabricius, 1791**. Cranium. NHMUK-ZOO-1961. 5. 18. 31. Female. Natural History Museum (London) Collection Specimens. MorphoSource Specimen ID 390403. Uploaded by Messer, D.

***Halichoerus grypus* Fabricius, 1791**. Cranium. NHMUK-ZOO-1961. 5. 18. 37. Female. Natural History Museum (London) Collection Specimens. MorphoSource Specimen ID 390424. Uploaded by Messer, D.

***Halichoerus grypus* Fabricius, 1791**. Cranium. NHMUK-ZOO-1938. 3. 12. 1. Female. Natural History Museum (London) Collection Specimens. MorphoSource Specimen ID 392572. Uploaded by Messer, D.

***Hydrurga leptonyx* Blainville, 1820**. Skull. DUNUC 2206. D'Arcy Thompson Zoology Museum Collection at the University Of Dundee. Downloaded from www. Sketchfab. com.

***Hydrurga leptonyx* Blainville, 1820**. Skull. USNM-269533. Male. Downloaded from www. digimorph. org. Uploaded by Van Valkenburgh, B.

***Mirounga angustirostris* Gill, 1866**. Cranium. LEPBLB-MA-B-820-000000. Male. Laboratorio de Ecologia de Pinnipedos ''Burney J. Le Boeuf''. MorphoSource Specimen ID 000S22562. Uploaded by David Polly, P.

***Mirounga angustirostris* Gill, 1866**. Cranium. LEPBLB-000000. Female. Laboratorio de Ecologia de Pinnipedos ''Burney J. Le Boeuf''. MorphoSource Specimen ID 000S22588. Uploaded by David Polly, P.

***(Neo)Monachus tropicalis* Gray, 1850**. Skull. USNM-100358. Male. Downloaded from www. digimorph. org. Uploaded by Van Valkenburgh, B.

*(**Neo)Monachus tropicalis* Gray, 1850**. YPM-MAM-008654. Peabody Museum of Natural History, Yale University. MorphoSource Specimen ID 000S29423. Uploaded by Stanley, E.

***Odobenus Rosmarus* Linnaeus, 1758**. DUNUC-2143. D'Arcy Thompson Zoology Museum Collection at the University Of Dundee. Downloaded from www. Sketchfab. com.

***Odobenus rosmarus* Linnaeus, 1758**. Cranium. UAM-14793. Male. Downloaded from www. SketchFab. com. Digitized and Uploaded by Idaho Visualization Laboratory.

***Odobenus rosmarus* Linnaeus, 1758**. Skull. N-C-2-6-158. California Academy of Sciences. Downloaded from www. SketchFab. com.

***Phoca vitulina* Linnaeus, 1758.** Cranium. LEPBLB-PV-CSL-845-170505. Laboratorio de Ecologia de Pinnipedos ‘’Burney J. Le Boeuf’’. MorphoSource Specimen ID 000S22592. Uploaded by David Polly, P.

***Zalophus californianus* Lesson, 1828**. Cranium. LEPBLB-Z-ISM-228-050385. Male. Laboratorio de Ecologia de Pinnipedos ‘’Burney J. Le Boeuf’’. MorphoSource Specimen ID 000S22607. Uploaded by David Polly, P.

***Zalophus californianus* Lesson, 1828.** Cranium. LEPBLB-Z-CSL-550-201204. Male. Laboratorio de Ecologia de Pinnipedos ‘’Burney J. Le Boeuf’’. MorphoSource Specimen ID 000S22601 Uploaded by David Polly, P.

***Zalophus californianus* Lesson, 1828**. Cranium. LEPBLB-Z-CSL-469-230204. Female. Laboratorio de Ecologia de Pinnipedos ‘’Burney J. Le Boeuf’’. MorphoSource Specimen ID 000S22596. Uploaded by David Polly, P.

***Zalophus californianus* Lesson, 1828.** Cranium. LEPBLB-Z-CSL-554-301204. Female. Laboratorio de Ecologia de Pinnipedos ‘’Burney J. Le Boeuf’’. MorphoSource Specimen ID 000S22603. Uploaded by David Polly, P.

***Zalophus californianus* Lesson, 1828.** Cranium. LEPBLB-Z-LM-971-150204. Male. Laboratorio de Ecologia de Pinnipedos ‘’Burney J. Le Boeuf’’. MorphoSource Specimen ID 000S22611. Uploaded by David Polly, P.

***Zalophus californianus* Lesson, 1828**. Cranium. LEPBLB-Z-LP-405-220702. Female. Laboratorio de Ecologia de Pinnipedos ‘’Burney J. Le Boeuf’’. MorphoSource Specimen ID 000S22608. Uploaded by David Polly, P.

***Zalophus californianus* Lesson, 1828.** Cranium. LEPBLB-Z-CSL-580-300405. Male. Laboratorio de Ecologia de Pinnipedos ‘’Burney J. Le Boeuf’’. MorphoSource Specimen ID 000S22604. Uploaded by David Polly, P.

***Zalophus californianus* Lesson, 1828.** Cranium. LEPBLB-Z-CSL-456-080104. Male. Laboratorio de Ecologia de Pinnipedos ‘’Burney J. Le Boeuf’’. MorphoSource Specimen ID 000S22594. Uploaded by David Polly, P.

***Zalophus californianus* Lesson, 1828.** Cranium. LEPBLB-Z-SE-322-000697. Male. Laboratorio de Ecologia de Pinnipedos ‘’Burney J. Le Boeuf’’. MorphoSource Specimen ID 000S22615. Uploaded by David Polly, P.

***Zalophus californianus* Lesson, 1828.** Cranium. LEPBLB-Z-CSL-471-030304. Male. Laboratorio de Ecologia de Pinnipedos ‘’Burney J. Le Boeuf’’. MorphoSource Specimen ID 000S22597. Uploaded by David Polly, P.

***Zalophus californianus* Lesson, 1828.** Cranium. LEPBLB-Z-CSL-541-221104 Male. Laboratorio de Ecologia de Pinnipedos ‘’Burney J. Le Boeuf’’. MorphoSource Specimen ID 000S22600. Uploaded by David Polly, P.

***Zalophus californianus* Lesson, 1828.** Cranium. LEPBLB-Z-BM-361-080300 Male. Laboratorio de Ecologia de Pinnipedos ‘’Burney J. Le Boeuf’’. MorphoSource Specimen ID 000S22612. Uploaded by David Polly, P.

***Zalophus californianus* Lesson, 1828.** Cranium. LEPBLB-Z-CSL-553-201204. Male. Laboratorio de Ecologia de Pinnipedos ‘’Burney J. Le Boeuf’’. MorphoSource Specimen ID 000S22602. Uploaded by David Polly, P.

***Zalophus californianus* Lesson, 1828.** Cranium. LEPBLB-Z-CSL-477-060404. Female. Laboratorio de Ecologia de Pinnipedos ‘’Burney J. Le Boeuf’’. MorphoSource Specimen ID 000S22598. Uploaded by David Polly, P.

***Zalophus californianus* Lesson, 1828.** Cranium. LEPBLB-Z-CSL-484-230404. Female. Laboratorio de Ecologia de Pinnipedos ‘’Burney J. Le Boeuf’’. MorphoSource Specimen ID 000S22599. Uploaded by David Polly, P.

***Zalophus californianus* Lesson, 1828.** Cranium. LEPBLB-Z-L-712-000702. Male. Laboratorio de Ecologia de Pinnipedos ‘’Burney J. Le Boeuf’’. MorphoSource Specimen ID 000S22618. Uploaded by David Polly, P.

Fossils

***Kolponomos newportensis* Tedford et al., 1994**. USNM-215070. Early Miocene. NMNH Paleobiology Specimen Records. MorphoSource Specimen ID 0000S2720. Uploaded by Tseng,J.

***Proneotherium repenningi* Kohno et al., 1995**. LACM 124686. Collected from Oregon ,USA. Downloaded from www. phenome10k. org

***Neotherium mirum* Kellogg, 1931.** LACM 124686. Collected from USA. Downloaded from www. phenome10k. org

***Allodesmus Kernensis* Kellogg, 1922.** LACM 138167. Collected from USA. Downloaded from www. phenome10k. org

***Pteronarctos goedertae* Barnes, 1989**. LACM 123883. Collected from USA. Downloaded from www. phenome10k. org

2. 2 Methods

2. 2. 1. Geometric Morphometrics

Morphometrics can be defined as the quantitative study of shape, its variations, and its covariations with other variables (Webster and Sheets, 2010). The traditional morphometrics method is based on statistically analyzing measurements of length, width and depth, using multivariate techniques, such as distances, distant ratios and angles on the studied material without taking account of its shape and geometry (Marcus, 1990; Slice, 2007; Zelditch et al., 2012). That often results in an inability to represent the structural arrangement of the points in the anatomy on which the measurements are based (Slice, 2007).

On the other hand, geometric morphometrics tries to capture the shape of the studied material either in 2D or 3D coordinates using morphological landmark points (Rohlf and Marcus, 1993). The term shape is used as defined by Kendall (1977): All the geometric information that remains when location, scale and rotational effects are filtered out of an object. When these elements are removed and with the shape of the material intact through the process the only differences that remain are those of shape between comparable specimens (Zelditch et al., 2012).

Landmarks according to Dryden and Mardia (1998) are points of correspondence on each specimen that match between and within populations. The Cartesian coordinates of the landmarks are the ones that contain the necessary geometric information used in an analysis (Slice, 2007). Landmarks should be chosen based on some specific criteria according to Zelditch et al. (2012), with the first three being essential in any case and the following two situational depending on the material:

1)They have to be homologous

2)They must provide an adequate comprehensiveness of the specimen's morphology

3)They have to be found reliably and repeatedly on the specimens.

4)They do not switch positions relatively between them

5)If the study is in a 2D environment they have to be on the same plane.

There are three different categories of landmarks, defined by Bookstein (1991): Type 1 being based exclusively on clearly defined biological structures, while the other two, especially Type 3 are more loosely defined and placed on the researcher's will.

Geometric morphometrics were firstly introduced by Rohlf and Marcus (1993) with two points defining their approach to morphometrics :

1) Data are recorded to capture the geometry of the studied structure in 2D or 3D using homologous characters

2) Geometrical relationships among the landmarks are not inherent in the raw coordinates themselves.

The main techniques they proposed that are compatible with the theory were Relative warp analysis, Superimposition methods, Euclidean distance matrix analysis and finite element scaling analysis.

Later that year Corti (1993) proposed that shape coordinates was an additional viable method to be explored within Rohlf's and Marcus's and also was the first to use the term Geometric Morphometrics on a published paper (Slice, 2007).

Since their conception, Geometric morphometrics have been a very useful weapon in the arsenal of any scientific clade which focuses on studying animals, extant or extinct, based on their shape. There has been a plethora of publications in diverse clades of biology and paleontology like anthropology (Shin et al., 2021), entomology (Tatsuta et al., 2018), ostracology (Baltanas and Danielopol, 2011) and taphonomy (Courtenay et al., 2020) to mention just a few examples that use geometric morphometrics. Recently, Courtenay and Gonzalez-Aguilera (2020) published a paper discussing the possible usage of GANs (Generative Adversarial Networks), a model that is consisted of two rival neuron networks competing with each other, while are simultaneously trained with the aim to create new data that are based on the original training data (Goodfellow et al., 2014). They proposed this theory as an effective tool for data augmentation in geometric morphometrics,

proving that this clade still has untapped potential which can be explored in future studies.

In general superimposition methods seem to be the most popular among the different possible methods (Adams et al., 2004). The goal of these methods is to overlay at least two specimens so their homologous landmarks are found at the smallest possible proximity (Rohlf and Marcus, 1993).

Superimposition methods can be identified as Procrustes methods (Rohlf and Marcus, 1993). The goal of using these methods is to process the chosen landmarks so they end up having the same orientation and size so the shape of the specimens can be analyzed as purely as possible (Rohlf and Slice, 1990 ; Lawing and Polly, 2010). Procrustes analysis takes account of the coordinates of the shape that are generated by the least-squares superimposition of configurations of landmarks (Slice, 2007). The most used variant of this method is GPA (Generalized Procrustes Analysis). It was initially developed by Gower (1975) as a tool to be used in Psychometrics, with the purpose of analyzing the multivariate behavior of people and comparing it to what was considered as the average human behavior. In general, the basis of this theory is a combination of the basic Procrustes rotation with ANOVA (Analysis of Variants) to be used for modeling 3D data matrices (Grice and Assad, 2009). In the end, if a repeated method is used for the estimation of the mean form the whole process can be called a GPA (Zelditch et al., 2012).

2. 2. 1. 1. Geometric Morphometrics 3D Application

The first step for this study was to collect a number of 3D cranial models of both Pinnipedia and Mustelidae, with the highest diversity possible given the databases that we had access to.

The program that we used to place the landmarks on the 3D models was MorphoDig. MorphoDig is a free to use program developed by Renaud Lebrun of University of Montpelier with the intention of helping scientists like biologists and paleontologists to work with their 3D models on a digital environment specifically suited for them (Lebrun, 2018). MorphoDig is able to rotate the models so they can match their correct physical orientation, has a lasso function to remove unwanted or impractical parts of the models and save the project in different file types. The majority of the most common file types of 3D models, like . obj, . stl and . ply are compatible with MorphoDig.

Using MorphoDig 42 landmarks were placed on the cranial models. The list of the landmarks is presented on Figure 8. In total 56 3D cranial models were used, 1 skull of *P. valletoni*, 23 of them belonging to Pinnipedia and 32 to Mustelidae. There was one skull of *P. valletoni* availble to use, courtesy of www. phenome10k. org. The pinniped species that the models belonged to were *Kolponomos newportensis* (N=1), *Pteronarctos goedertae* (N=1), *Neotherium mirum* (N=1), *Proneotherium repenningi* (N=1), *Allodesmus kernensis* (N=1), *Mirounga angustirostris* (N=2), *Halichoerus grypus* (N=3), *Phoca vitulina* (N=1) *(Neo)Monachus tropicalis* (N=2), *Arctocephalus townsendi* (N=1), *Zalophus californianus* (N=6), *Odobenus rosmarus* (N=2) and *Hydrurga leptonyx* (N=1). Mustelidae models were of the species *Lontra canadensis* (N=2), *Enhydra lutris* (N=2), *Pteronura brasiliensis* (N=2), *Lontra felina* (N=1), *Aonyx capensis* (N=1), *Lutra lutra* (N=1), *Martes americana* (N=2), *Martes martes* (N=1), *Neovison vison* (N=3), *Mellivora ratel* (N=1), *Eira barbara* (N=1), *Gulo gulo* (N=3), *Mustela nivalis* (N=1), *Mustela eversmanii* (N=1), *Taxidea taxus* (N=3), *Lutrogale perspicillata* (N=1), *Meles meles* (N=3), *Mustela putorius* (N=2) and *Martes foina* (N=1).

The main influence for the position of each landmark was a study conducted by Kienle and Berta (2019), in which they studied the feeding of Pinnipeds through time using geometric morphometrics on specimens of both crown and stem Pinnipeds of a chronological range that spans from Miocene to today and they are placed in a way that could reflect the shape of the cranium. However, one key difference is that in this study landmarks are placed only on the left side of *P. valletoni's* skull. The reasoning behind this decision is based on a number of factors. First of all, the skull of specimen SG 692 from National Museum of Natural History in Paris is not complete on the right side with a hefty part of its zygomatic arch being absent. Despite this obstacle, the fact that *P. valletoni's* skull is symmetrical lets it be studied only on one of its sides without losing information about the shape of the skull. Symmetry in biology is defined as the repetition of parts in different positions and orientations to each other (Klingenberg, 2015). On most vertebrate skulls the midsagittal or medial plane passes through them, thus proving that there is bilateral symmetry with each half acting like a mirror image of the other half although small inconsistencies exist from specimen to specimen on their features (Klingenberg et al., 2002), with very few exceptions like the Cetacean suborder Odontocete for example having asymmetrical skulls (Fahlke et al., 2011). The second reason for only taking landmarks on the left side is to avoid the redundancy of having duplicate shape coordinates of the same landmarks on different cranial halfs that end up useless (Cardini, 2017). The final argument in favor of one sided landmarks is the fact that this technique saves time without sacrificing the quality of the shape it tries to impress (Cardini, 2017). The finalised list of landmarks is visible in Figure 8 and in the corresponding table.

After all the landmarks are placed on each 3D model separately, their coordinates are transformed on separate . tps files, through MorphoDig, one for each file. Then the final . tps file including all landmarks-es coordinates was created by combining all the individual files into one. For a specimen to be eligible for the analysis that follows it has to be added on its . tps text that LM3=42 instead of LM=42 with the 3 implying to the software used for the analysis that it should take the input file as a

3D project. The program used for the analysis was MorphoJ 1. 07a edition. MorphoJ is a software, designed by Christian Peter Klingenberg from University of Manchester with the goal to help scientist analyze shape in a variety of biological contexts, in environment specifically created for the study of geometric morphometrics without having any necessary previous experience in programming unlike other packages that work on programming environments (Klingenberg, 2011). It includes plenty of methods, from very standard multivariate techniques to more obscure and specific methods (Klingenberg, 2011).

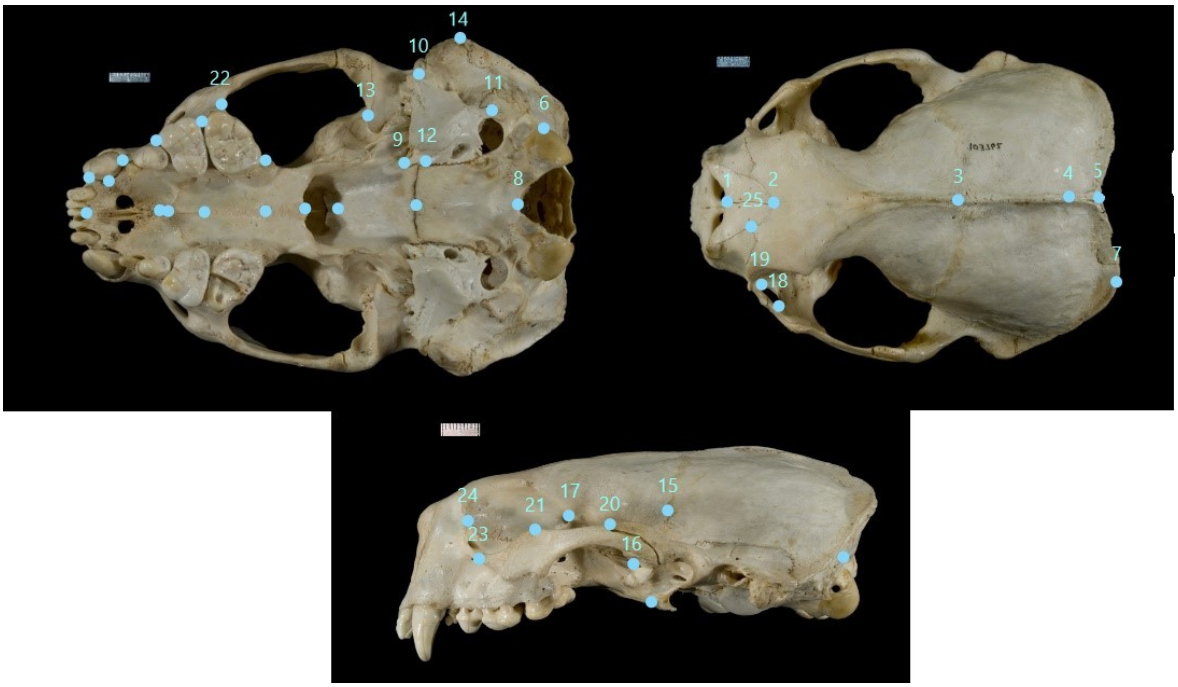

Figure 8: Cranial landmarks chosen for 3D geometric morphometrics analysis. Cranium of *Enhydra lutris* photographed by Phil Myers, Museum of Zoology, University of Michigan-Ann Arbor.

From the preliminaries menu on MorphoJ, the New Procrustes Fit option was the first action that had to be taken after the input of the . tps file in the software, as it was a necessary phase for the analyses that followed. Through this option, the data were projected to tangent space by the usage of Orthogonal Projection (Dryden and Mardia, 1998 ; Klingenberg, 2011). After that the covariance matrix based on the coordinates of the landmarks was created and the option Find Outliers was used to check for potential errors and deflections in the data. In general covariance matrices are used in a high number of different morphometric analyses and they can be used in a variety of biological contexts.

With all the prerequisite actions completed, a Principal Component Analysis (PCA) was performed. PCA is an ordination method which is used in geometric morphometrics for the simplification of patterns of variation and covariation which are present on the geometric shape variables, and make them more comprehensible by replacing the original variables with Principal Components (PC). Those are linear combinations of the original variables and they are independent from each other (Zelditch et al., 2012). It is used mainly for the investigation of morphological heterogeneity within the dataset and to reduce the dimensionality of the data and to describe the major axes of variation (Zelditch et al., 2012 ; Kienle and Berta, 2019).

Additional visualisation of the different PCs was conducted on SlicerMorph, an specialised extension for the 3D Slicer software, developed for Geometric Morphometrics analyses (Rolfe, 2021). 3D Slicer is an open source software mainly developed for medical images computing (Fedorov, 2012) and can be downloaded from http://www. slicer. org for free.

2. 2. 1. 2. Geometric Morphometrics on mandibles

The second analysis of this study revolves around the mandibles of *P. valettoni,* Pinnipedia and Mustelidae. To have a more complete understanding of the way *P. valletoni* fed itself, mandibles of both exant aquatic Mustelidae and Pinnipedia were collected for the analysis so a 2D morphometric analysis could be performed. The theoretical background of the analysis is the exact same as the one used in the 3D analysis and it is described in detail in the chapter relevant to it prior in the text. Mustelidae and *P. valletoni* mandibles were photographed from the collection of Natural History Museum of Basel (NHMB), while Pinniped mandibles were photographed from the collection of National Museum of Natural History of France (MNHN) with every photo taken from the left side of the mandible and with a fixed distance set between the lens of the camera and the specimen. In cases, that photos were taken from the right side of the mandible, TpsDig2, the program that was used for setting the landmarks in the final . tps file was used to mirror the images. In total 54 photos were apt for the analysis. Mustelidae jaws used in the examination were of *Aonyx capensis* (N=4), including 2 of the subspecies *congica, Aonyx cinerea* (N=4)*, Enhydra lutris* (N=1), *Hydrictis maculiocollis* (N=5*)*, *Lontra canadensis* (N=6) and *Lutra lutra* (N=8). Pinniped mandibles used, belonged to *Arctocephalus gazella* (N=1), *Erignathus barbatus* (N=1), *Cystophora cristata* (N=1), *Eumetopias jubatus* (N=1)*, Halichoerus grypus* (N=1)*, Hydrurga leptonyx* (N=2), *Leptonychotes weddelli* (N=1)*, Lobodon carcinophaga* (N=4), *Mirounga leonina* (N=2)*, Monachus monachus* (N=1), *Onomatophoca rosii* (N=1)*, Otaria flavescens* (N=1), *Phoca caspica* (N=1)*, Phoca groenlandica* (N=1), *Phoca hispida* (N=1), *Phoca vitulina* (N=3) and *Zalophus californianus* (N=1). Of *P. valletoni's* fossils, 2 mandibles were suitable to include in the analysis. The landmarks that were chosen reflected biological structures on the mandible which could help imprint the general shape of it and are listed on Figure 9.

Figure 9: Landmarks placed on the mandibles with the use of TpsDig. Taken from MNHM Paris collection. 1) Canine posterior edge/Dental bone intersection 2) Canine anterior edge/Dental bone Intersection 3) Vertical projection of landmark 2 to the mandible's body 4) Posterior edge of toothrow 5) Intersection of the Coronoid process and the Horizontal ramus 6) Vertical projection of landmark 5 to the mandible's body 7) Tip of the coronoid process 8) Anteroventral-most point between the condyloid and the coronoid process 9) Horizontal projection of landmark 8 to the coronoid process 10) Posteriormost point of condyloid process 11) Posteriormost point of angular process 12) Anteriormost point of the mandible's body.

To create a .tps file suitable for a 2D geometric morphometrical analysis the software used was TpsUtil, one of the programs available through the tps series of varied software, free to download and use, developed by James F. Rohlf (Rohlf, 2005). TpsUtil was built as a toolbox program, in which the user could perform different actions, that Rohlf called special operations, without having to resort on a number of different softwares. Instead all of these very specific actions can be done just by one program (Rohlf, 2005). For the needs of this study, TpsUtil was utilized to build the . tps file, which later was used as an input to TpsDig2, the program that was chosen for the landmarks placing. To build the file all the available photos have to be in the same folder and from TpsUtil's interface the user can choose any number or all of them to be part of the final . tps file under construction.

After the .tps file was created, the next step was to insert it in TpsDig2, the program used for placing the landmarks on the mandibles. TpsDig2 is another member of the tps series that Rohlf developed for public use (Rohlf, 2005). It was created with the intention of being a user-friendly program for processing .tps files, with functions as placing landmarks and measuring distances (Rohlf, 2005). Following the file insertion in TpsDig2, each photo that was used to build the file

has separately to be scaled according to the scale used while taking the original photo of each specimen. Photos that had an opposite direction from the intended one, were mirrored using the corresponding tool available in the program. With the scale on each photo set, the next action was to place the landmarks on the photos. 12 landmarks were chosen that portray an approximate form of the mandible's shape of Carnivora in general.

After each landmark is placed accordingly on each photo MorphoJ, the same software that was used for the analysis of the 3D landmarks is used for the statistical analysis and the same steps as the first analysis are followed. The first step was to select the option New Procrustes Fit and then create a covariance matrix based on the coordinates of the landmarks. Following this action, the option Find Outliers is used to check any problem with the data. Then a General Procrustes Analysis (GPA) has to be performed for the determination of differences of shape between the different groups that are established in the dataset as well as a Procrustes ANOVA. The data were examined for outliers. Principal Component Analysis (PCA) was executed from the covariance matrix for all the samples. After this procedure is completed for the total number of specimens, through MorphoJ's editing software it is possible to create a first sub-dataset in which only Mustelidae and P. valletoni's mandibles are included and a second dataset without the Mustelidae this time. On this dataset the previous actions are repeated. Then three different wireframe graphs were created by connecting the different landmarks to visualize the landmarks and their configuration by applying the thin plate splines.

2. 2. 2. Infraorbital Foramen

The infraorbital foramen (IOF) is positioned below and at a short distance from the infraorbital margin, on the maxilla of the cranium (Nanayakkara et al., 2016). In Figure 10 its placing on the cranium of *P. valletoni* is pointed. Its function is to act as a gateway for the infraorbital nerve and blood vessels to pass through it via the inferior orbital fissure and the inferior orbital canal and emerge to the face (Singh, 2011 ; Nanayakkara et al., 2016). There it branches into smaller threads that supply different parts of the face, like the skin of the upper lip, premolar teeth and the skin of the inferior eyelid (Lee et al., 2006). Based on studies conducted on human skulls it has been proven that different populations of the same species may have this foramen in a different location under the infraorbital margin based on their geographic diaspora (Singh, 2011 ; Przygocka et al., 2012), while the gender and the side of each studied individual should also be taken into account (Agthong et al., 2005). Populations that reside in colder environments seem to have more expanded foramens based on observations of a research conducted on foxes populations in Europe and America (Churcher, 1959). The overwhelming majority of extant mammals have one foramen per skull side, although some individual animals may have more than one as an anomaly (Muchlinski et al., 2020).

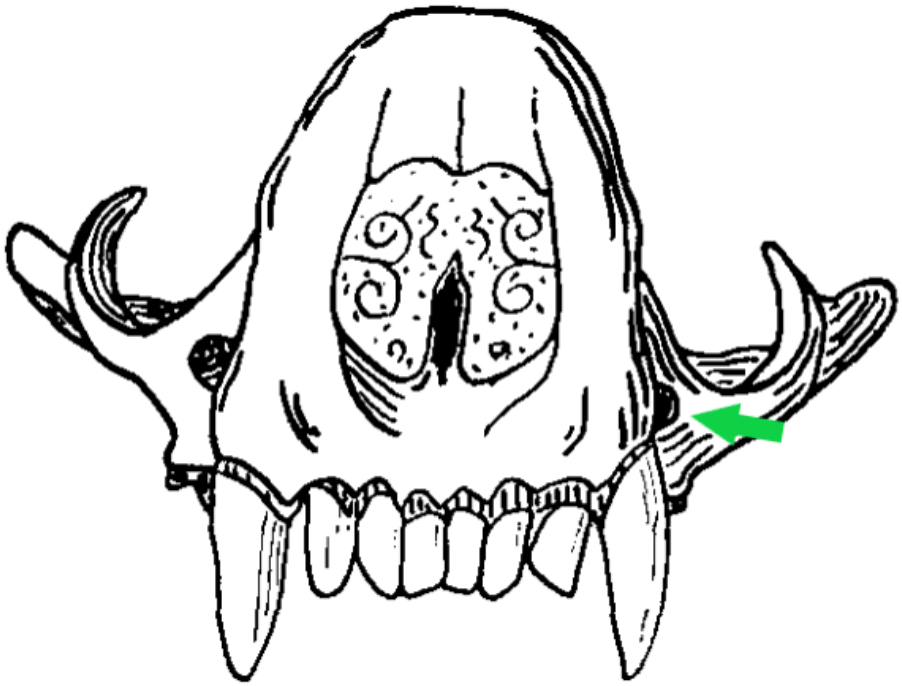

Figure 10: Position of Infraorbital Foramen on *P. valletoni*'s skull from anterior point of view. Modified after Savage (1957).

On pinnipeds IOF is important because it is channeling the blood vessels and the nerves that support their vibrissae, the commonly known whiskers, which are pretty developed on them, leading to a larger gap on their IOF's area because of this feature, as IOF size is analogous to the functional development of the vibrissae (Kay and Cartmill, 1977 ; Murphy et al., 2013). The predominant percentage of mammals have whiskers as they work like a sensory system, a radar that transfers information of the surrounding environment to the central nervous system through vibrations (Marshall et al., 2006). Although the raw number of vibrissae on Pinnipeds is lower than in other Carnivora (Milne et al., 2022), aquatic and semi-aquatic mammalian vibrissae are thicker and stiffer than those of terrestrial and arboreal mammals (Dougill et al., 2020), while also having more nerve endings leading to enhanced sensitivity (Marshall et al.,2006). Pinniped vibrissae are separated into subcategories based on their surface morphology: Undulated vibrissae that are found on the majority of Phocidae, the only family of animals that have whiskers of this type, and smooth vibrissae that

every member of Otariidae and Odobenidae has (Murphy et al., 2013). Odobenidae have the highest number of vibrissae while Otariidae's vibrissae are scarcer on their rostrum (Fay, 1982 ; Bauer et al., 2018) although Pinnipeds have the lowest total number of vibrissae among Carnivora despite their developed functionality (Milne et al., 2022). The main usage of Pinniped whiskers is to determine their circumambient objects while underwater (Bauer et al., 2018). Pinnipeds that actively hunt tend to have bigger IOF areas and move their whiskers around while they do, with this movement being a character that is connected with larger IOFs (Milne et al., 2020 ; Milne et al., 2022).

Of aquatic Mustelidae, *Pteronura brasiliensis* has a high number of long and stout whiskers which are used for locating its prey (Duplaix, 1980). Research on its brain and the parts that correspond to somatic sensory specialization has shown that its whiskers are extremely sensitive due to the size of the coronal gyrus (Radisnky, 1968). E*nhydra lutris'*s whiskers, while similar morphologically to those of Pinnipeds, are less sensitive than those of *P. brasiliensis* (Marshall et al., 2014). That is a result of the extended usage of the paws during its interactions with its prey and its environment, something that is also can be traced on the morphology of its brain that supports the usage of both forelimbs and vibrissae (Radinsky, 1968; Strobel et al., 2018). Terrestrial Mustelidae on the other hand are characterized by smaller IOF areas, with much less developed vibrissae compared to Pinnipeds (Milne et al., 2022).

For the third analysis, all the specimens used, were collected from the same sources utilized on the former two. 92 3D models of Pinnipeds and Mustelidae were eligible for this analysis as their infraorbital foramen and their total length and width were intact on their respective models. From pinnipeds *Zalophus califonianus* (N=17), *Odobenus rosmarus* (N=3), *Halichoerus grypus* (N=21), *Monachus tropicalis* (N=2), *Hydrurga leptonyx* (N=2) and *Mirounga angustirostris* (N=2) were included. From Mustelidae *Taxidea taxus* (N=4), *Pteronura brasiliensis* (N=2), *Mustela (Neovison) vison* (N=5), *Mustela sp.* (N=1), *Meles meles* (N=3), *Taxidea taxus* (N=4), *Martes foina* (N=1), *Mellivora capensis* (N=1), *Martes*

americana (N=1), *Lutrogale perspicillata* (N=1), *Lutra lutra* (N=2), *Lontra longicaudis* (N=1), *Lontra felina* (N=1), *Lontra canadensis* (N=4), *Hydrictis maculicollis* (N=1), *Gulo gulo* (N=6), *Enhydra lutris* (N=3), *Eira barbara* (N=1) and *Aonyx capensis* (N=1) were included. An analytic description of the specimens is presented in the Materials section of the study.

The basis for the method was a study conducted by Milne et al. (2022). The first action was to measure the maximum cranial length and the width of the available craniums. To measure the dimensions of the craniums in a 3D environment MeshLab was the software of choice. MeshLab is a free, open-source software released to the public in 2008 by Cignoni et al. (2008) members of the Visual Computing Lab of Institute of Information, Science and Technology ''Alessandro Faedo'' that allows its users to process 3D models in various ways making functions which were previously scarcely available to the public easier to find, especially in an academic environment.

With both measurements being repeatedly taken five times each on the models and with a median of those set as the absolute value the next step is the calculation of the Geometric Mean (GM) of each skull. Geometric Mean can be defined as the *n*th root of the product of all *n* variables (Jungers et al., 1995). To accomplish it Muchlinski's (2010) type of calculating the GM of cranial length and width is implemented by taking the square root of the absolute value of both measurements' multiplication result. To measure the maximum cranial length the distance between the most ventral and lateral points of the skull through the median plane were used, while for the maximum width the lateral-most points of the zygomatic arches of each side were used. For the calculation of IOF area MeshLab is used again. In their study Milne et al. (2022) created molds out of their physical specimens, so they could measure the dimensions of the IOFs of their specimens. In this study's case, the fact that all the craniums are 3D reconstructions of original specimens made the digital caliper that MeshLab provides a necessary tool. The measurements taken were the longest and the

shortest diameter of the IOF of each cranium. In general Pinniped skulls have IOFs that look approximately as an oval, making the type of calculating oval area (π x Length/2 x Width/2) valid as an option (Milne et al., 2022). The same could also be said about the IOF of the available models of Mustelidae ,even though in some species the shape of the IOF area was reminiscent of a circle but those cases were the ones with small diameters overall. With all the measurements set, the following step, based on Milne et al. (2022) methodology, was to calculate a normalized ratio by dividing the IOF area by the GM, with the result classified as normalized IOF area, an action that is instigated by the correlation between the correlation between GM and IOF area, a result that was also proven when correlation was tested in this study.

The next step was to compute a visual analysis of the results. PAST, a free software specifically designed for the needs of paleontologists was used. PAST offers an easy to use interface using spreadsheet data as input from the user to analyze a variety of univariate and multivariate statistics, phylogenetic analysis and other utility tools necessary for biological, ecological and paleontological needs (Hammer et al., 2001). Through this software, the plots that represent this part of the study were constructed so a clear picture of the IOF area compared to the whole skull's area could be visible.

2. 2. 3. Traditional Morphometrics Analysis

The final analysis was based on traditional morphometrics in an attempt to decipher if *P. valletoni* was a hand or mouth oriented predator, using measurements and data derived from Timm-Davis et al. (2015) and comparing it with the extant Lutrinae they used, two that are mouth oriented and two that are hand oriented.

Lutrinae skull can be classified under two categories that derive from characters related to their foraging strategies. Mouth oriented otters tend to have long rostrums and mandibles with long pterygoid hamuli, which favor bite velocity against bite force (Milne et al., 2022). On the other hand, hand oriented Lutrinae have shorter skulls and mandibles with teeth modified to crush the shells of their prey, as their bite is slanted towards bite force instead of velocity (Timm-Davis et al., 2015). This difference between the two is explained by focusing on the animals they feed on as the former tend to be omnivores or fish oriented hunters while the latter are durophagous that have to try to break the shells of their prey (Tseng et al., 2017).

Of the four species Timm-Davis et al., (2015) used in their study, *Pteronura brasiliensis* and *Lontra canadensis* are mouth oriented predators, while *Aonyx cinerea* and *Enhydra lutris* are hand oriented. Of the mouth oriented predators *L. canadensis* (North American River Otter) is a freshwater animal of North America and Mexico that mostly preys on slower fish which it hunts underwater, although crustaceans, amphibians, insects, mammals and birds constitute a portion of its diet (Melquist et al., 2003) and *P. brasiliensis* (Giant River Otter) is an exclusively South American species and the largest freshwater otter (Noonan et al., 2017) with its most common prey being fishes and at a lesser degree crustaceans and other animals that consumes headfirst, directly after catching them (Duplaix, 1980 ; Noonan et al., 2017).

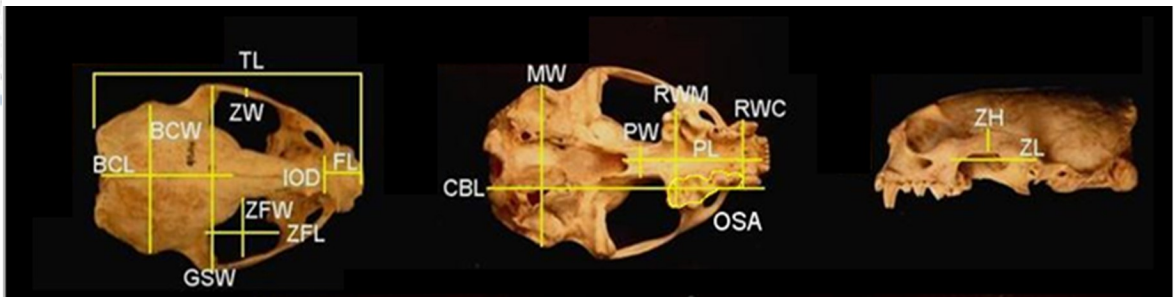

Figure 11: Cranial measurements calculated on the skull of *Potamotherium valletoni* to compare it with the other four Lutrinae. ZH: Zygomatic Height, ZL: Zygomatic Length, ZW: Zygomatic Width, ZFL: Zygomatic Fossa Length, ZFW: Zygomatic Fossa Width, BCL: Brain Case Length, BCW: Brain Case Width, GSW: Greater Skull Width, FL: Facial Width, IOD: Intra-Orbital Distance, TL: Total Length, CBL: Condylobassal Length, MW: Width between the Mastoids, PW: Palate Width, PL: Palate Length, RWM: Rostral Width between the Molars, RWC: Rostral Width between the Canines, OSA: Occlusal Surface Area of Post-canine Teeth. Figure modified after Timm-Davis et al., (2015).

Of the hand oriented predators *E. lutris* (Sea Otter) is a fully marine mammal and the heaviest member of Mustelidae (Estes, 1980), with a distribution spread along the coasts of Western and Eastern Pacific Ocean (Doroff et al., 2021). It forages by diving as its main prey, benthic invertebrates, live in the sea bottom, with the duration of the dive being proportional to the depth of the individual attempts (Bodkin et al., 2004). It captures its prey between his forepaws and then takes it to the surface, where it eats it, but in the case that the prey is a hard-shell invertebrate, use of tools, like rocks, have been heeded as a common phenomenon among sea otters, but pretty rare among mammals in general (Riedman and Estes, 1990). *A. cinerea* (Asian Small-clawed Otter) can be found in South and Southeast Asia in a variety of wetland systems, from shallow pools to rivers (Wright et al., 2021) and are the smallest extant otters (Perdue et al., 2013). What separates them from other otters is that they have short ,or in some fingers no, claws and quick fingers which they mechanically use to search, hunt and capture their prey with their front paws (Perdue et al., 2013). It is adapted to hunt invertebrates, mostly crustaceans, although fish are also consumed supplementary (Foster-Turley, 1992).

For this analysis, morphometric measurements of the skull of *P. valletoni* had to be calculated. 18 measurements were taken based on the study by Timm-Davis et al. (2015) that represent standard measurements for the cranium. The exact measurements are available on Figure 11. Of those measurements 17 were taken

using MeshLab's caliper tool, the same that was used on the previous analysis. The last measurement was that of the surface of the postcanine teeth (OSA). To calculate it, ImageJ was the preferable software. ImageJ is a free image processing program published by Wayne Rasband, of the Research Services Branch, National Institute of Mental Health in Bethesda, Maryland, with its first edition being released in 1997 (Abramoff et al., 2004). The goal of its creator was to make an open-source software for processing images that would be easy to use and massively available to the public (Abramoff et al., 2004; Schneider et al., 2012). Using the scaling tool to set a scale on isolated photos of the 3D model of *P. valletoni* and then encircling the post canine teeth using the freehand tool, which allowed to mark a part of the image, it became possible to determine their area by the calculate option in the Analyze section of the software.

After each measurement on *P. valletoni* was repeatedly taken 5 times each an average for each of the 18 measurements is calculated by LibreOffice Calc, the spreadsheet program offered by LibreOffice softwares. These linear measurements had to be transformed to their natural logarithm (ln) to reduce the skewness and the heteroscedasticity, a regular occurrence for linear distance data and to eliminate in general the size from influencing the results of the analysis (Sokal and Rohlf, 1995; Timm-Davis et al., 2015). The next action to be taken is the calculation of the natural log of the geometric mean size (GMS) for *P. valletoni* and the samples derived from Timm-Davis et al., (2015) database. While in their study, Timm-Davis et al., calculated GMS by using both cranium and mandible measurements, the fact that SG 692 has not a matching mandible, limited the extent of the measurements that were available. That led to an exclusion of all mandible measurements in addition to the cranial measures, which were originally excluded by Timm-Davis et al., (2015). These cranium measures are zygomatic height, zygomatic width and OSA, the first two because of their much smaller size in comparison to all other cranial dimensions and the latter, since it is an area contained within the other major cranial dimensions. Having the GMS calculated, we divided the cranium data, which were transformed through their natural logarithm, with their respective GMS for every different specimen. The reasoning

behind this action was to eliminate any negative influence of size in the analysis. With the numbers for each measurement being on the form they should, PAST was used to perform PCA and Discriminant Analysis with the inclusion of the samples collected on Timm-Davis et al. study and the *P. valletoni* skull's measurements.

3. Results

3. 1 Results of 3D Geometric Morphometrics Analysis

On MorphoJ, the first step for deciphering the results of the 3D geometric morphometric analysis was to conduct a Procrustes Anova including all the specimens used. For the centroid size F-statistic was calculated as 61,91 and p-value as smaller than 0,0001, meanwhile for the results for shape F-statistic was calculated as 12,81 and p-value as smaller than 0,0001. That means a great variation of both centroid size and shape between the total number of animal craniums used.

With the conduction of the first PCA on the total dataset and including every model used in the analysis, MorphoJ recognized 55 principal components, with any principal component having a value of 5% or more being meaningful in a biological context (Zelditch et al., 2012). By following this empirical rule, only the components whose value of the total variance exceeds 5% were interpreted. The reason behind it is the fact that the rest of the components represent such a small proportion of the complete variance each that they hardly can be used to describe anything meaningful on a biological level (Zelditch et al., 2012). For the total dataset PC1 represented 35,63% of the total variance, PC2 represented 12,24%, PC3 represented 7,51% and PC4 represented 6,3%, for a total accumulative variance of approximately 62% (Figure 12).

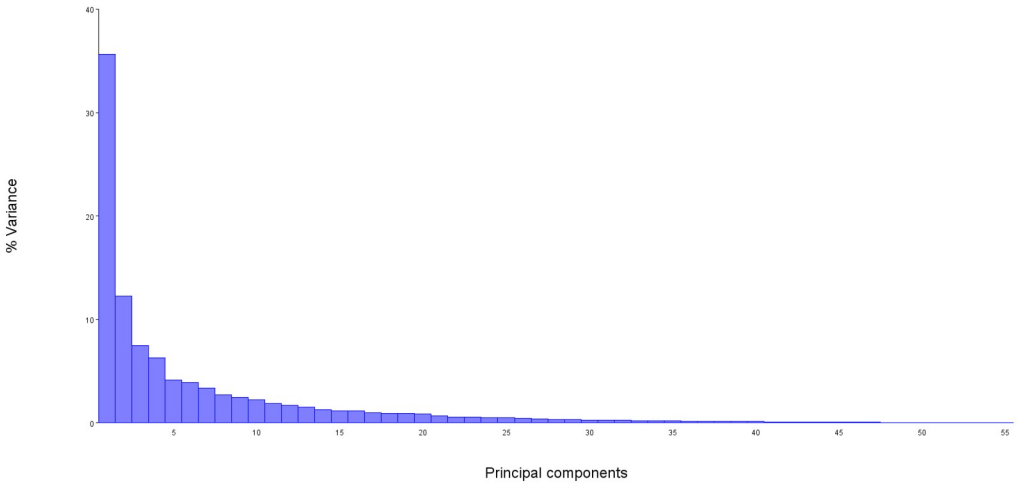

Figure 12: Eigenvalues of all the PCs among the two families and *P. valletoni* on the craniums. Only components with a value of 5% and more were taken into account as biologically important.

To explain what morphological tendencies influenced each of the most important principal components, the lollipop graph of PC shape changes created by MorphoJ is used. The lollipop graph shows how the position of landmarks change from the starting shape, indicated with a dot, to their target shape in which location and direction were designated by a straight line. MorphoJ allows the user to view the graph from different axes on 3D data. In this case Axis 1 vs Axis2 and Axis1 vs Axis3 gave the majority of information, although Axis2 vs Axis3 was also studied for additional insight. In 3D space, Axis1 vs Axis2 represented the dorsal view of the landmarks's placement, Axis1 vs Axis3 represented the lateral view and Axis 2 vs Axis 3 represented the anterior view.

While PC1 (Figure 13b) it is more often than not seems to be associated with size, in this case PC1 was associated with the length of the muzzle an observation mostly clear by the vectors of the landmarks on both Axis 1 vs Axis 2 and Axis 1 vs Axis 3, and the fact that there were both positive and negative values among the samples. On the opposite hand the neurocranium did not seem to have a clear association with PC1, although it was somewhat longer on smaller PC values.

Principal component 2 seemed to be characterized by alterations on the size of the cranium with low values showing a stouter, higher shape and high values

showing a lean and short shape. The width of the skull seemed to be disproportionate to the cranium's length (Figure 13c).

PC3 represented an enlargement of the neurocranium, while on the front it favored a smaller albeit thicker muzzle, leading to the conclusion that it characterized the contrast between the relative size of the neurocranium and the relative size of the splanchnocranium. Higher positive scores of this PC represented bigger neurocraniums.

PC4 was associated with a round shape of the neurocranium, while the muzzle tended to exhibit a leaner and sharper shape. On this PC the higher values showed a higher neurocranium, which simultaneously was less thick and flatter on the occipital bone. One thing that also could principal component 4 be associated with is the acoustic bulla. In Lutrinae, the acoustic bulla is more flattened than in terrestrial Mustelidae, and compared to modern Lutrinae, *P. valletoni's* bulla is more protuberant (Savage, 1957), a separation that the different scores of PC4 could support, with Lutrinae having negative scores and the majority of the rest of Mustelidae positive scores. *P. valletoni* sat confidently in the middle of this grouping based on this principal component.

On the PC scores graph (Figure 13a) of PC1 as the horizontal axis and PC2 as the vertical axis, as the two PCs with the highest total sum of variance, there were two groups that are clearly separated. The group that scored higher in PC1 are all the Pinnipeds, while *P. valletoni* scored inside the group that consisted of Mustelidae. On all other possible combinations between the different main PCs, there was not a clear distinction between groups on the graphical representation.

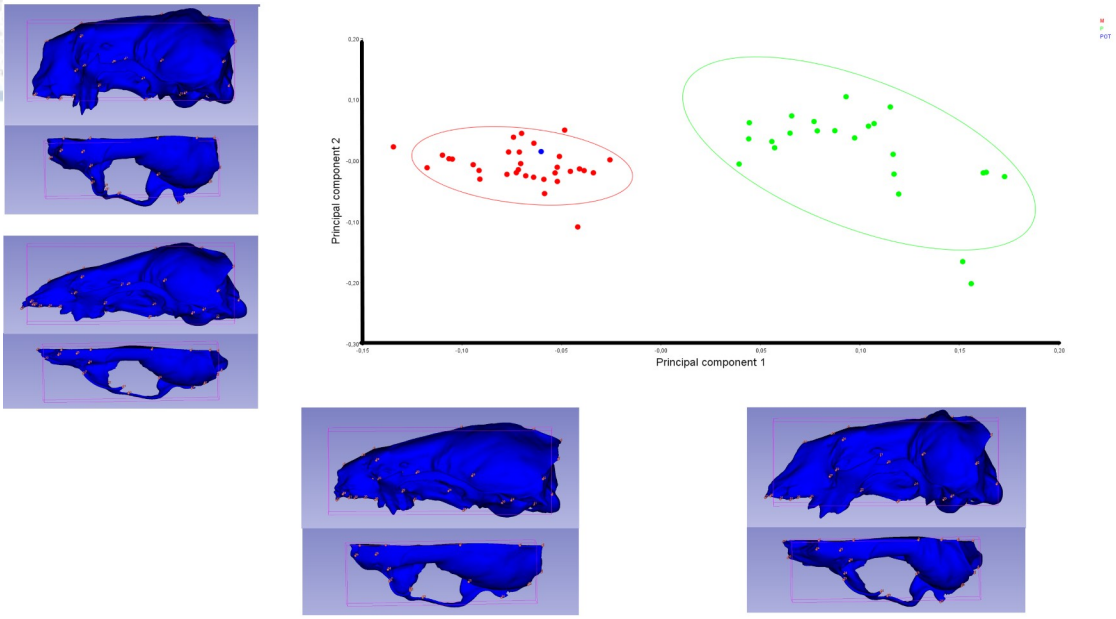

Figure 13a: Cranial PCA comparing PC1 and PC2. The two ellipses clearly separate two groups based on PC1 with a 90% confidence interval. On the graph, red dots represent Mustelidae, green dots represent Pinnipedia and the blue dot the cranium of *P. valletoni.*

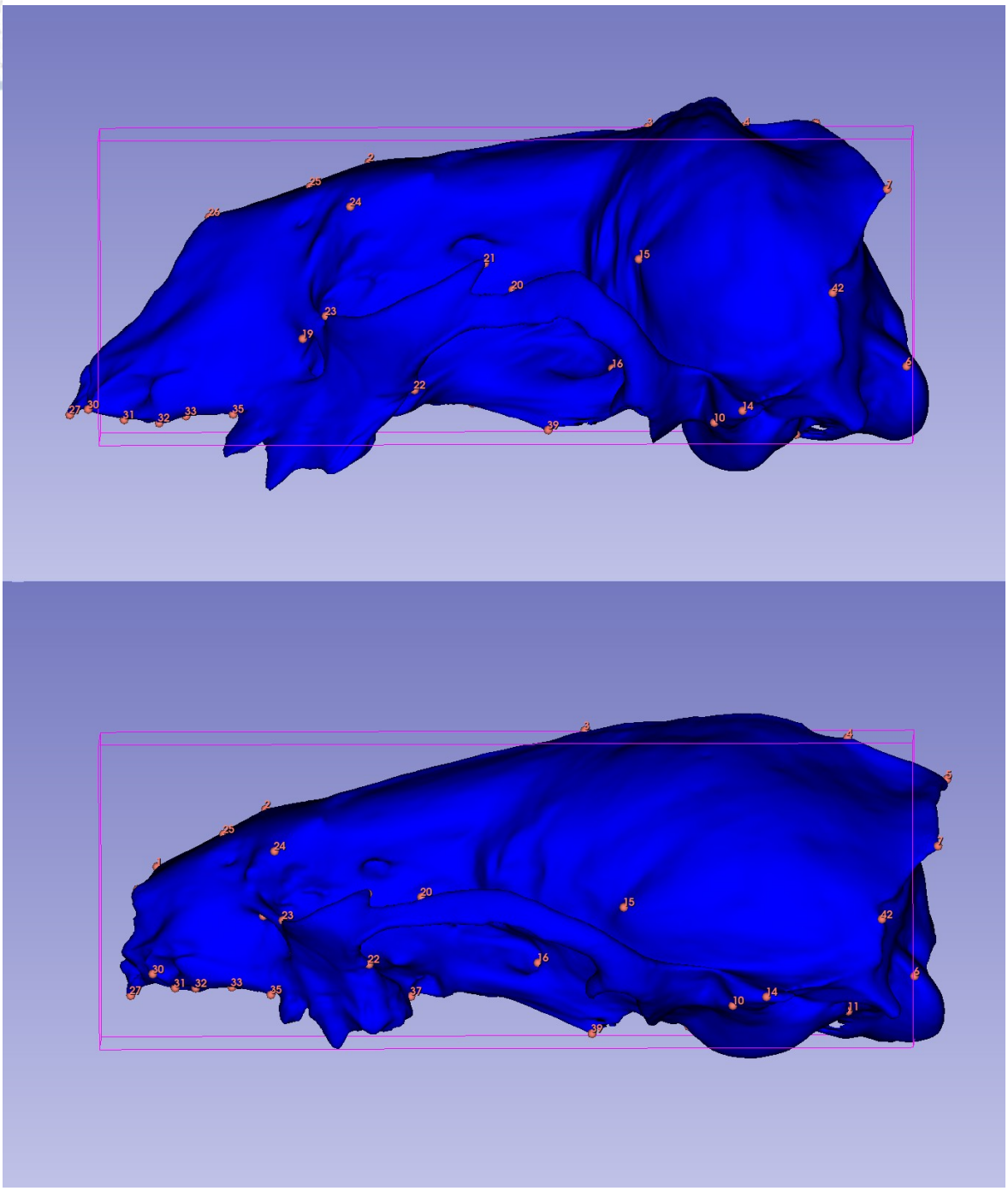

Figure 13b: Reconstruction of extreme positive and negative values respectively of PC1 between *P. valletoni*, Mustelidae and Pinnipedia, visualised through SlicerMorph.

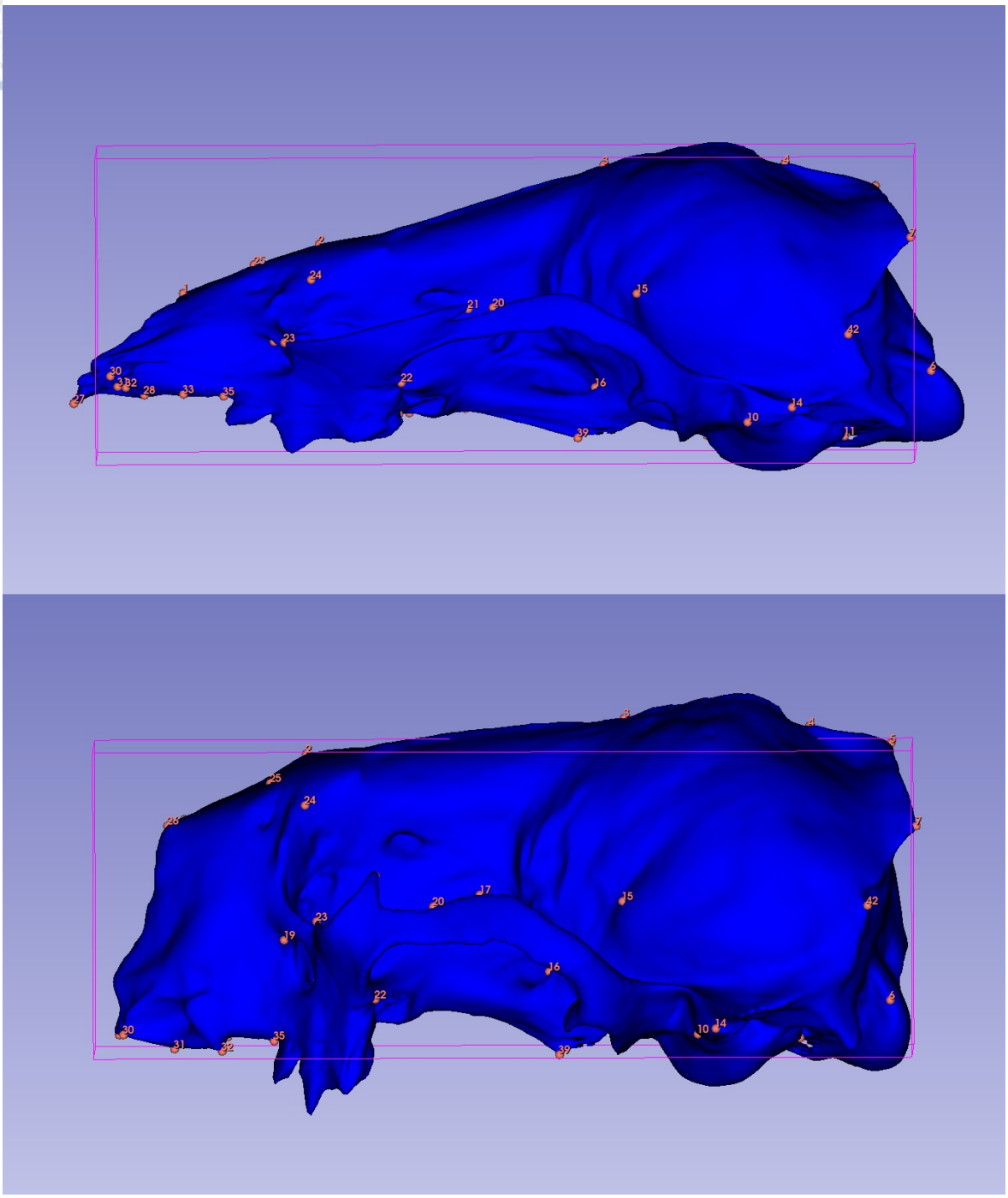

Figure 13c: Reconstruction of extreme positive and negative values respectively of PC2 between *P. valletoni*, Mustelidae and Pinnipedia, visualised through SlicerMorph.

On the ANOVA conducted with the exclusion of Pinnipedia F-statistic was calculated as 0,14 for centroid size and 1,05 for shape, whilst p-value was calculated as 0,707 on centroid size and 0,331 on shape, showing little variation

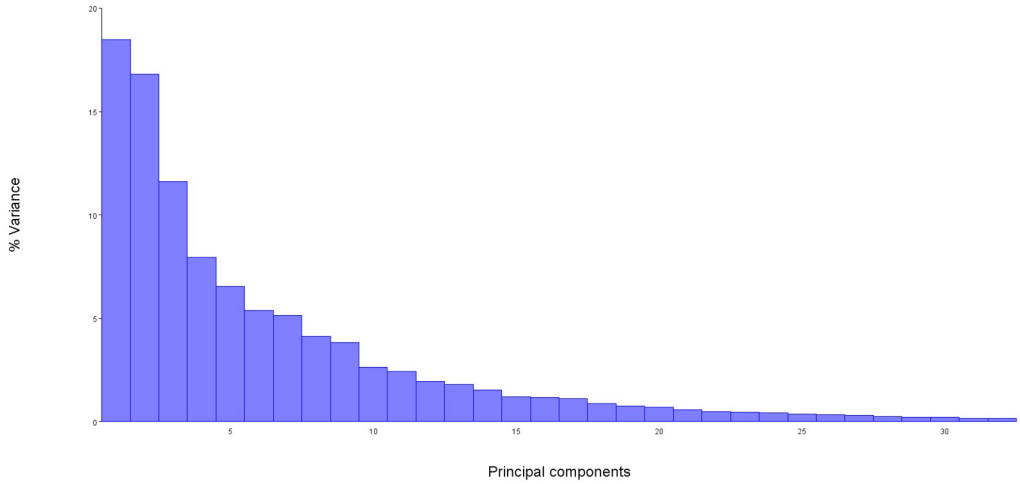

Figure 14: Eigenvalues of PCs of the PCA conducted between *P. valletoni* and Mustelidae craniums. In this case, as the number of PCs of a value higher than 5% are plenty, only the four first are used as they describe over 50% of the total variance.

on both between the studied specimens. In the isolated dataset, including only *P. valletoni* and Mustelidae, there were 7 principal components with a value of variance over 5% (PC=18,47%, PC2=16,8%, PC3=11,62%, PC4=7,94%, PC5=6,56%, PC6=5,38%, PC7=5,13%) (Figure 14). However, in this case it is possible for the results of the analysis to be described by using the first four principal components which include over 50% of the total variance, more particularly 54,83% instead of the 5% empirical rule used before as the rest can be considered redundant without any significant value.

Principal component 1, as before, was associated with the length of the muzzle and the height and roundness of the neurocranium, and also the width of the zygomatic arches, all visible on Figure 15a and Figure 15b. PC2 was characterized by a contrast of an elongation and enlargement tendency of the neurocranium in comparison to the viscerocranium and was presumably associated with the length of the frontal bone (Figure 15c). At the same time the maxillary bones showed elongated tendencies on higher scores. Higher scores were associated with elongated, low craniums and long frontal bones. PC3 again was dictated by a leaner palate on lower scores, while the neurocranium's shape was heading for a rounder shape reminiscent more of terrestrial Mustelidae on higher scores. PC4 unfurled an inclination towards an expansion of the occipital

bone's area, and also was influenced by the cranium's curvature with higher scores being associated with straighter craniums and low scores with a curvier shape.

On the PCA graph with PC1 as the horizontal axis and PC2 as the vertical axis, *P. valletoni* scored around the middle on PC1 which was connected with a lengthier and leanier splanchnocranium and a neither completely flat but also not heightened neurocranium.

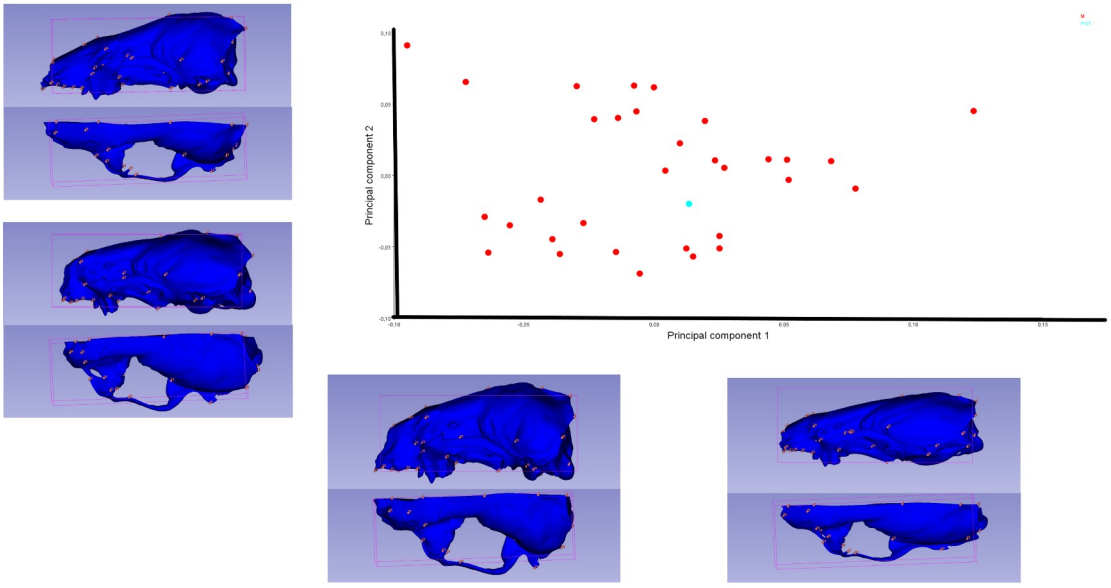

Figure 15a: PCA conducted between *P. valletoni* and Mustelidae, with comparison of PC1 and PC2. Red dots represent Mustelidae and the blue dot represents *P. valletoni.* It scored high on PC1 and around the middle on PC2 ,higher than most terrestrial Mustelidae, showing a lean shape and a frontal bone longer than terrestrial Mustelidae.

On PC2 it scored higher than the majority of terrestrial Mustelidae, while at the same time scored lower than the aquatic Mustelidae. This pointed to a smaller frontal bone, in comparison to Lutrinae but relatively longer than the remaining subfamilies.

On PC3 the palate of *P. valletoni* was again pointing to a leaner shape although it did not follow the neurocranium's shape modification. Principal component 4's score of *P. valletoni* had a positive value, and in fact one of the higher scores

which showed an expanded, leaner occipital bone and a low curvature of its shape.

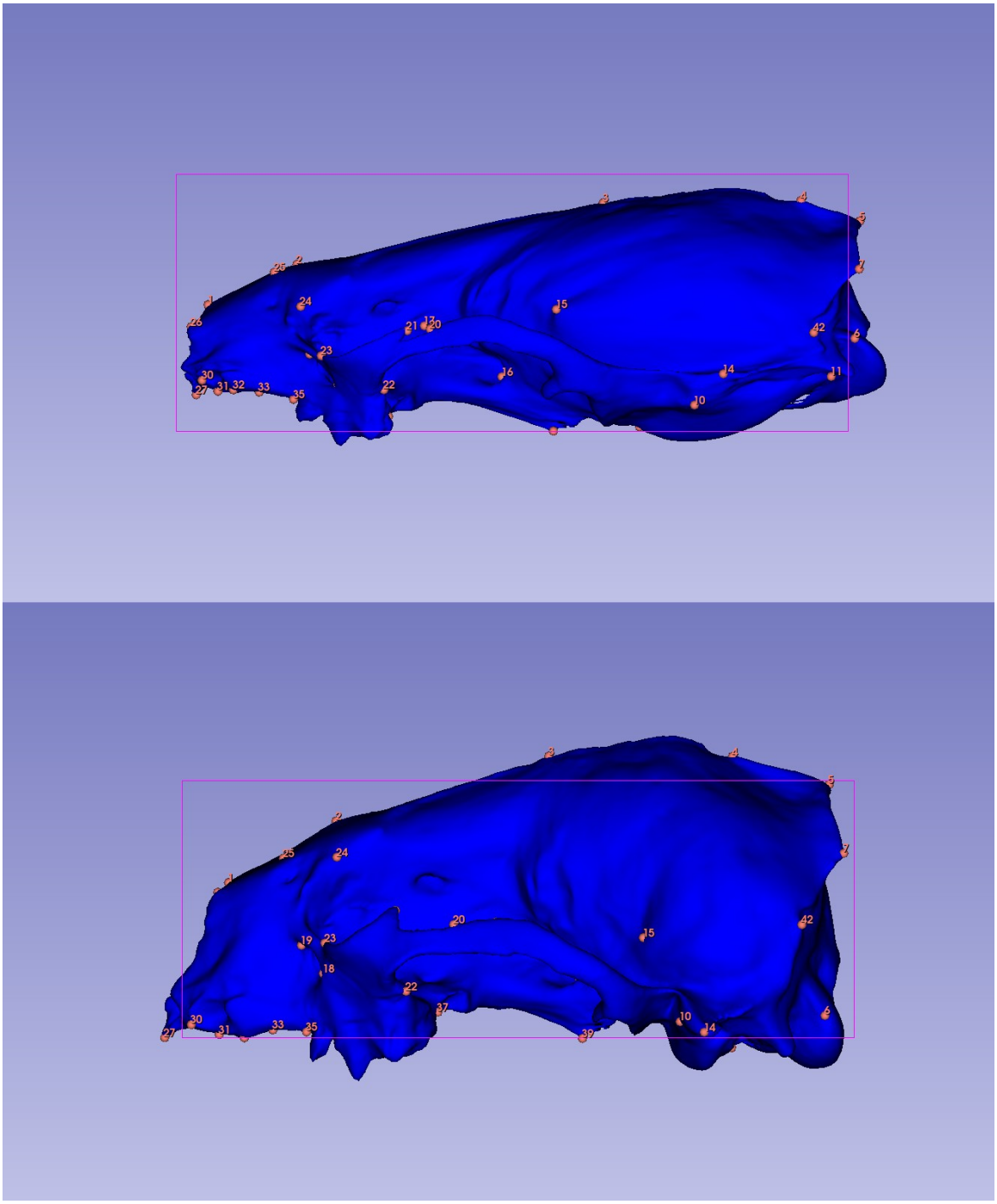

Figure 15b: Reconstruction of extreme positive and negative values respectively of PC1 between *P. valletoni* and Mustelidae, visualised through SlicerMorph.

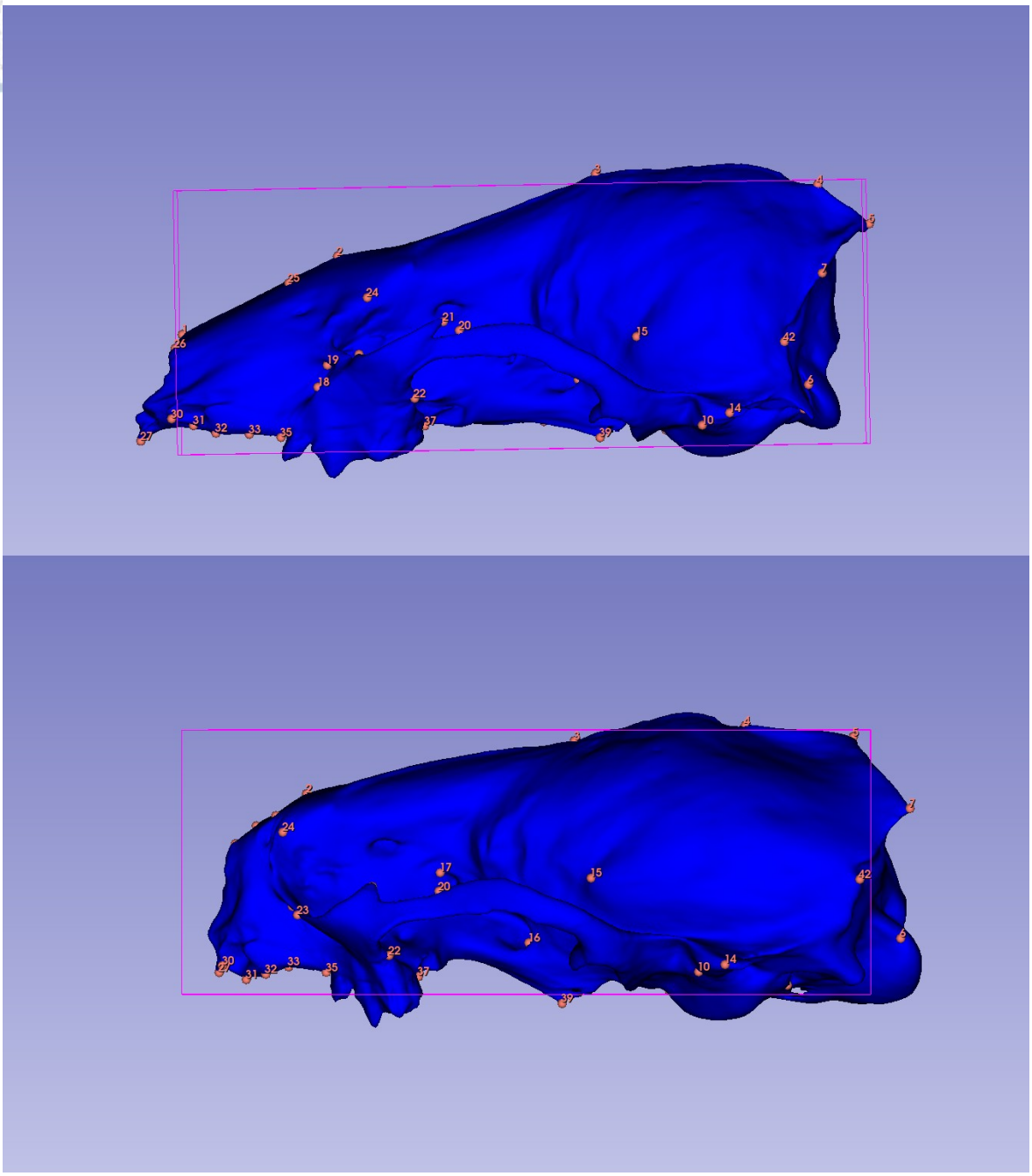

Figure 15c: Reconstruction of extreme positive and negative values respectively of PC2 between *P. valletoni* and Mustelidae visualised through SlicerMorph.

If the Mustelidae were excluded instead of Pinnipedia, the F-statistic was 4,36 and 1,61 for centroid size and shape respectively. P-value was calculated at 0,0486 for centroid size and at a number smaller than 0,0001 for shape, showing diversity among both centroid size and shape. There were 5 principal components with their variance calculated over 5% (PC1=29,33%, PC2=15,82%, PC3=11,58%, PC4=7,75%, PC5=5,15%) with a total variance of 69,65% (Figure 16).

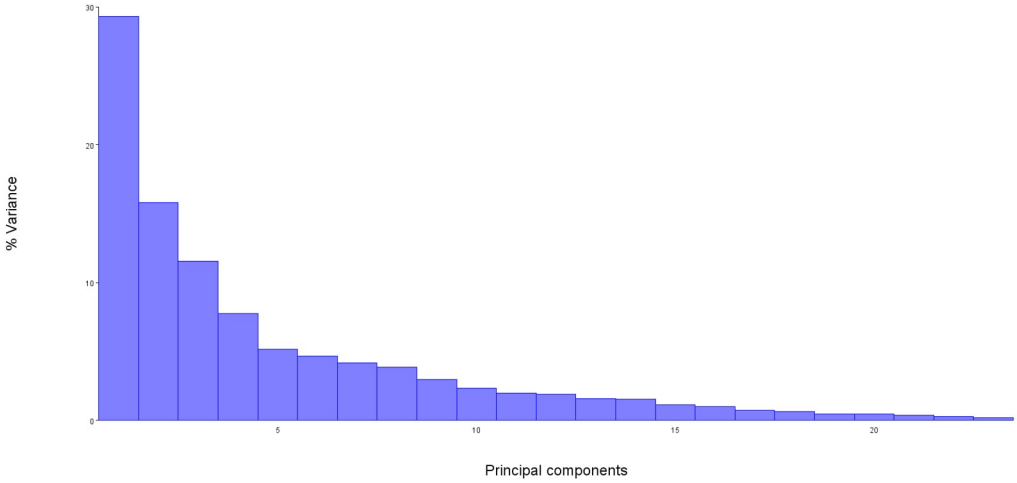

Figure 16: Eigenvalues of PCs between *P. valletoni* and Pinnipeds craniums.

Higher scores of PC1 represented a tendency of expansion from the starting shape, in almost every vector of the landmarks of the splanchnocranium, leading to more robust shapes. PC2 was associated with the relative width of the bones of the face and the general flatness of the cranium, with the splanchnocranium being more prominent in comparison to the neucroranium on higher values. On PC3, the neurocranium showed expansive tendencies from a dorsal view, meanwhile the splanchnocranium seemed to not be associated in any meaningful manner with this principal component. PC4 showed a tendency for a reduction of neurocranium's height while simultaneously becomes leaner, while the rostrum incorporates a rounder shape. On PC5 the tympanic bulla's shape and how inflated and wide it was and the neurocranium's and mastoid process's width had the biggest influence.

Graphically, *P. valletoni* had a negative value on PC1 something that is associated with a leaner shape of the splanchnocranium while almost every Pinniped, scored higher than it leading to the conclusion that its splachnocranium's shape is leaner than the Pinnipedian corresponding parts (Figure 17a & Figure 17b).

On PC2 *P. valletoni* had a positive value, one of the highest among the samples used, meaning its skull is flatter compared to Pinnipeds (Figure 17c). Principal component 3's positive values were associated with an expanded neurocranium which possibly had a connection with a toned sagittal crest, as indicated by the prevalence of *Z. californianus* as the highest scoring animal among the samples. On the other hand *P. valletoni* had a negative value, one of the lowest to be exact, which was associated with lower heights and more plain neurocraniums.

P. valletoni's PC4 value was positive and one of the highest among this grouping. It pointed to a leaner more straightforward neurocranium and a leaner splanchnocranium for *P. valletoni* with a smooth transition from one to another. The majority of the Pinnipeds seemed to follow a trend of more round and big neurocraniums with a more steep transition from the splanchnocranium with *Mirounga angustirostris* being the more common example, having the lowest score, out of all specimens with a negative value.

In principal component 5, *P. valletoni* had a negative value, inferior to all samples of Pinnipeds. This negative score was associated with smaller and flatter auditory bullae in comparison to Pinnipeds which tend to have wide and inflated bullae, and its mastoid processes were far smaller.

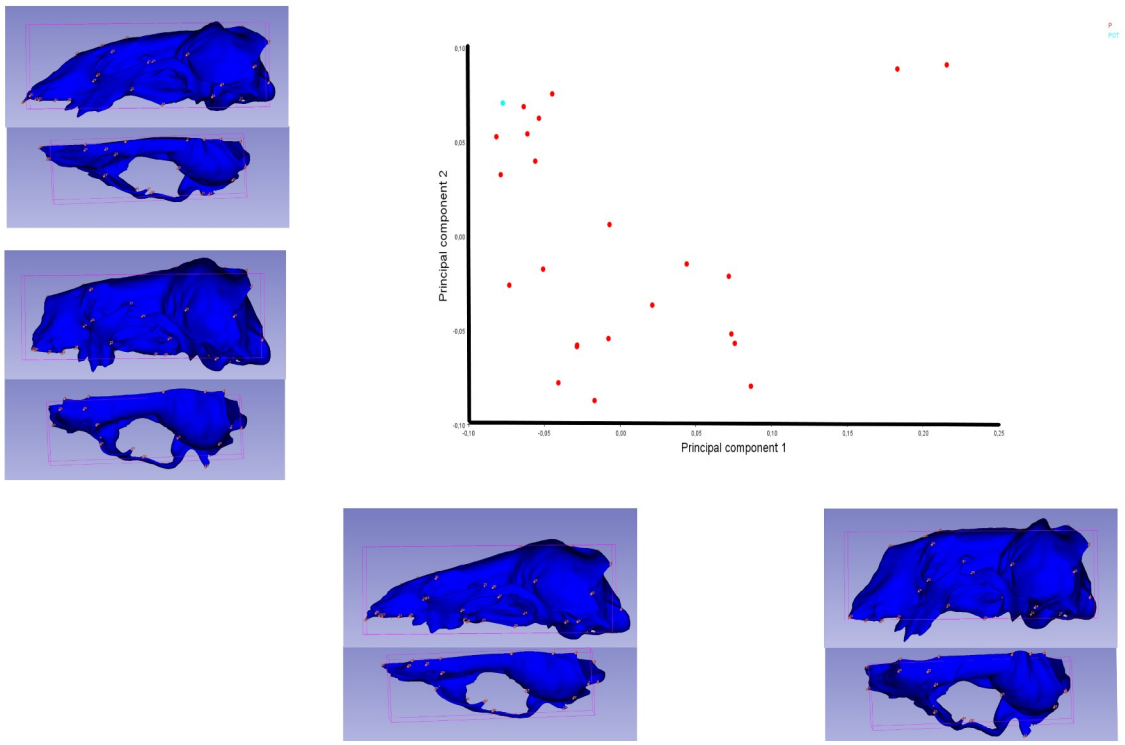

Figure 17a: PCA conducted between *P. valletoni* and Pinnipedia with graphical comparison of PC1 and PC2. *P. valletoni* scores low on PC1 and high on PC2 showing a cranium flatter and leaner than the Pinnipedian one.

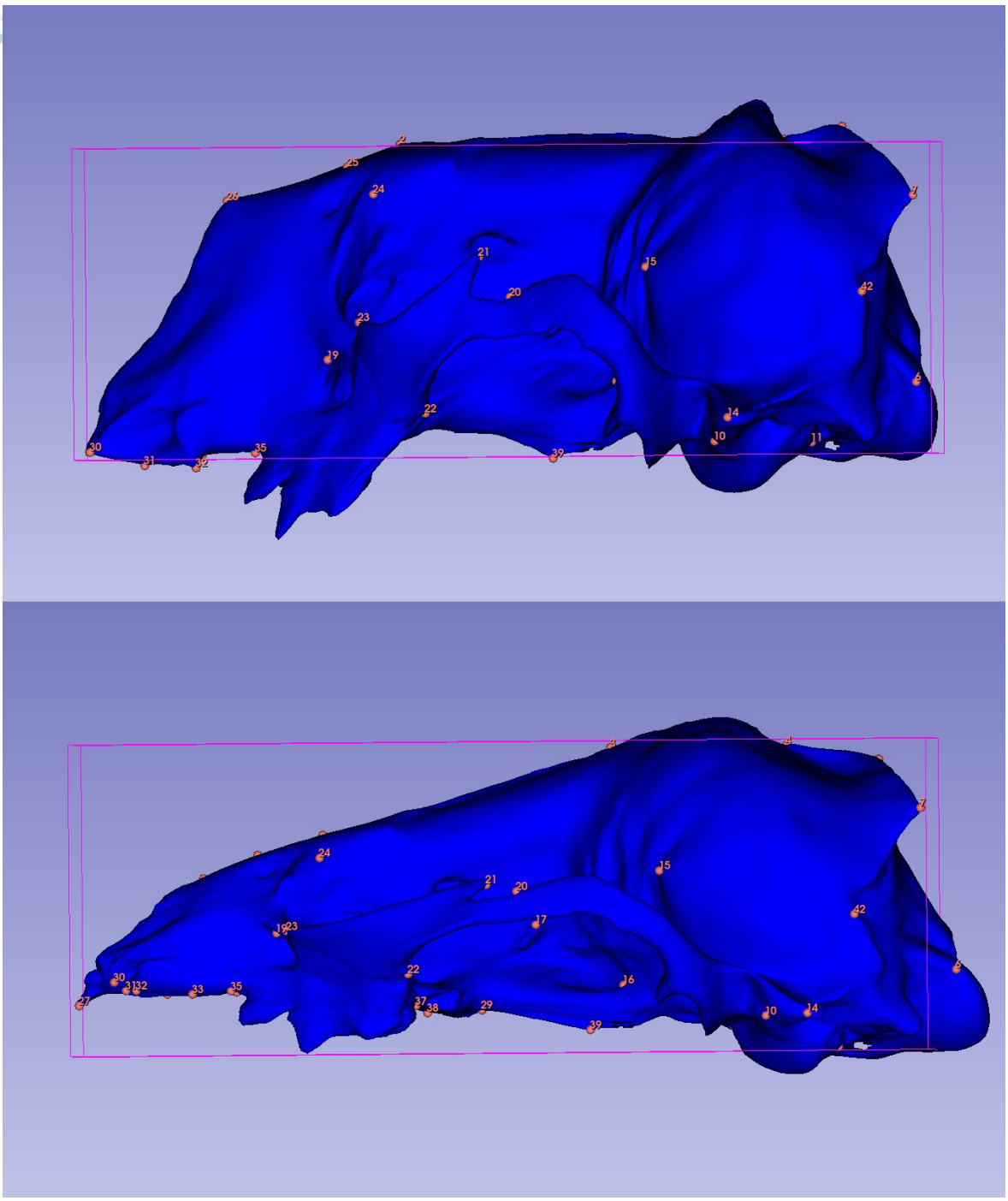

Figure 17b: Reconstruction of extreme positive and negative values respectively of PC1 between *P. valletoni* and Pinnipedia, visualised through SlicerMorph.

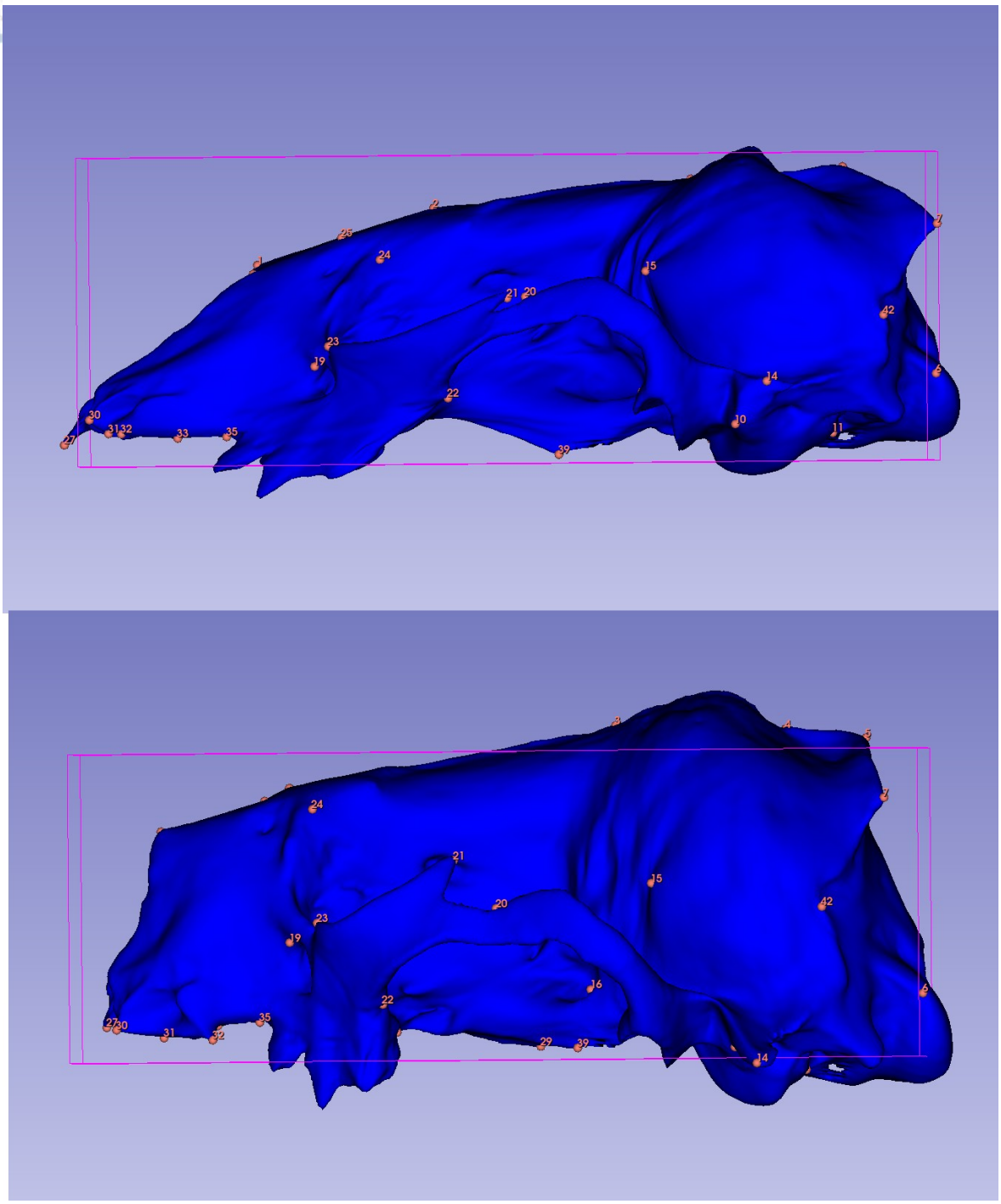

Figure 17c: Reconstruction of extreme positive and negative values respectively of PC2 between *P. valletoni* and Pinnipedia, visualised through SlicerMorph.

3. 2 Results of Geometric Morphometrics Analysis on mandibles

From the ANOVA conducted in MorphoJ, among all the species of Mustelidae, Pinnipedia and *P. valletoni* available, the F-statistic's value was calculated as 37,18 on centroid size and as 32,28 on shape, while p-value was of a value smaller than 0,0001 on both. That showed a great division between the shape and the centroid size of the total of the specimens.

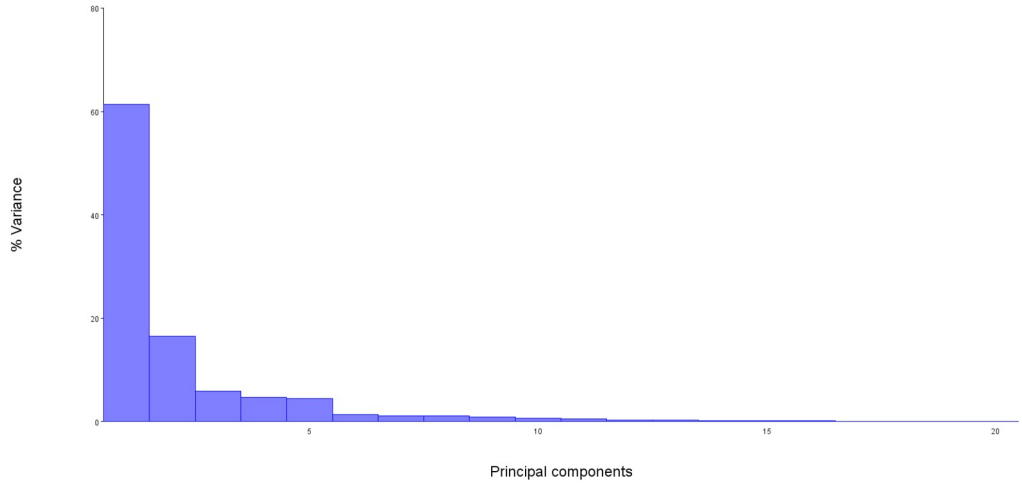

Figure 18: Eigenvalues extracted from the PCA conducted among *Potamotherium*, Mustelidae and Pinnipedia mandibles. Principal components with a value of 5 and higher were taken into account for the variation of shape.

MorphoJ recognized 20 principal components on the total mandible dataset after the PCA was run on the dataset. As it was done prior in the 3D study, only principal components with an individual value that exceeds 5% were taken into account, for the same reasons as stated prior in the text (Zelditch et al., 2012). From the collective PCA, the first two Principal Components composed around 78% of the total variance, while PC3 also exceeded the 5% mark for a total of 83,77% (Figure 18). By checking on the wireframe of the mandibles, PC1, the most important of the principal components as it was the one with the highest absolute value, composed 61,43% of the variance and it seemed to be associated

with the tip of the mandible's coronoid process in comparison to its body and the corner it makes at the frontal end with the main body of the mandible. PC2 composed 16,48% of the variance. After the imposition of PC2 wireframe on the total wireframe, it became apparent that it is associated with the rostral depth of the mandible. PC3 composed 5,86% of the variance. By checking on the wireframe imposition and the lollipop diagram, it seems that it was influenced by the direction of the coronoid process's tip and the angular process's shape, which was more prevalent the higher any specimen score on this principal component.

On the main PCA graph in Figure 19, with PC1 as the horizontal axis and PC2 as the vertical axis, two groups are clearly defined with Pinnipedia being completely separate from Mustelidae and *P. valletoni* being approximate to Mustelidae. Mustelidae are defined by positive values of PC1 indicating higher coronoid processes that end up on a more perpendicular corner to the body of the

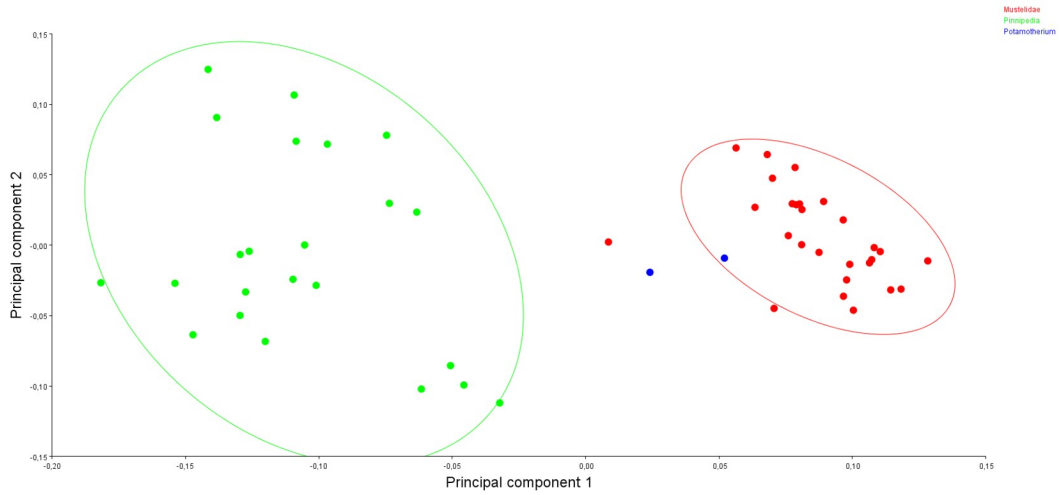

Figure 19: Mandibular PCA comparing PC1 with PC2. The ellipses represent 90% confidence intervals between the two families and *Potamotherium valletoni.*

mandible. Pinnipedia show lower values of PC1, mostly negative leading to the result that their coronoid process is lower in comparison to Mustelidae and instead of a steep corner upwards the transition from the main hull of the mandible to the coronoid process is gradual. *P. valletoni* is confidently placed closer to Mustelidae, having a positive value. but not as distant to Pinnipedia as the majority of Mustelidae. PC2 and PC3 did not offer any clear separation between the two

groups graphically with both Mustelidae and Pinnipedia having samples with positive and negative values among them.

P. valletoni PC2's value was negative showing a lower rostral depth. On the other hand, it scored high on PC3 which denoted a longer angular process.

Between the Mustelidae and *P. valletoni's* Procrustes ANOVA, the F-statistic's value was calculated at 0,42 for the centroid size and 3,04 for the shape. P-value was calculated at 0,5219 for the centroid size and it was smaller than 0,001 for the shape. That means small variation in size and big variation in shape between the samples.

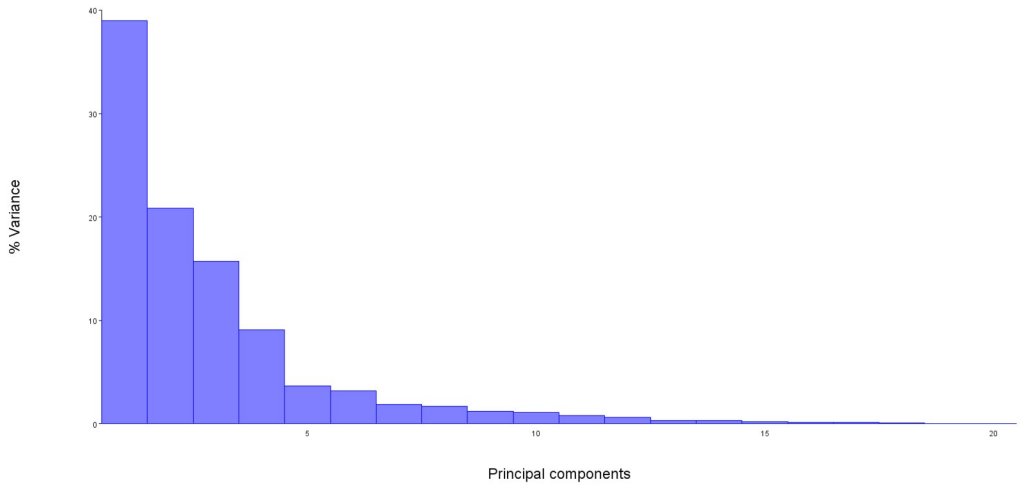

Figure 20: Eigenvalues of PCA between *Potamotherium* and Mustelidae mandibles.

On the isolated PCA conducted between only Mustelidae and *P. valletoni*, MorphoJ again recognized 20 Principal Components with PC1 to PC4 explaining 84,57% of the total variance (Figure 20). PC1 consists of 38,96% of the total variance. By inspecting the wireframe and the lollipop diagram, it was again associated with the tip of the coronoid process. PC2's value was 20,83%. Based on the wireframe it seems that it was associated with the back side of the coronoid process and the prominence of the angular process. PC3 covered 15,7% of the total variance. It was determined by the depth of the rostral part of the mandible.

PC4 was measured at 9,08% and was associated with alterations of the mandible's base and how curvy its shape appears to be.

On the PCA graph (Figure 21), again with PC1 as the horizontal axis and PC2 as the vertical axis *P. valletoni* scored positive and could be traced closer to *L. lutra*, some specimens of *A. cinerea* and *L. canadensis* at PC1. Higher PC1 scores were associated with higher coronoid processes and *P. valletoni*'s placement seemed to follow the trend.

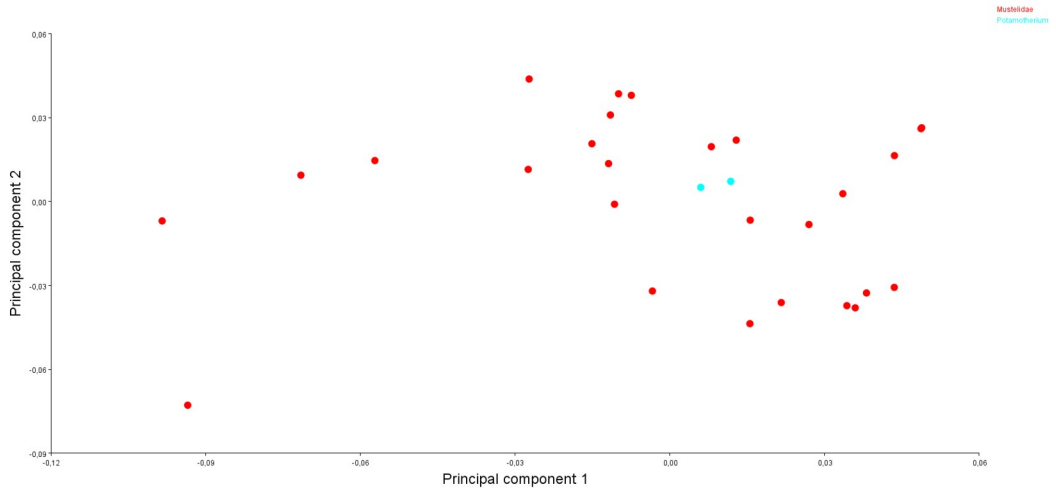

Figure 21: Mandibular PCA including only *Potamotherium* and Mustelidae comparing the first two Principal Components. *Potamotherium* and the majority of mouth-oriented predators have positive directions on the first and most important PC.

At PC2. *P. valletoni* had a positive score indicating a developed angular process although not as much as the major bulk of the Lutrinae samples .

PC3 is interesting as *P. valletoni* seemed to score far from the rest of the specimens. Both *P. valletoni* samples had positive values of PC3 which by inspecting the graph of the principal components are much higher than all of Mustelidae samples used in the analysis These higher values were associated with the leaner shape of its mandible.

On PC4 the two specimens of *P. valletoni* scored with some distance between them with the one with higher value (SG 2629) showing a less curvy base than the other, although multiple samples of the same species, like *L. lutra* and *L.*

canadensis seem to score in a similar way with different samples of the same species having divergent scores.

On the Procrustes ANOVA conducted with Pinnipedia and P. valletoni, for the centroid size F-statistic had a value of 4,62 and p-value had a value of 0,0419, while for shape F-statistic was calculated at 3,86 and p-value was smaller than 0,001, showing big variation both in shape and centroid size.

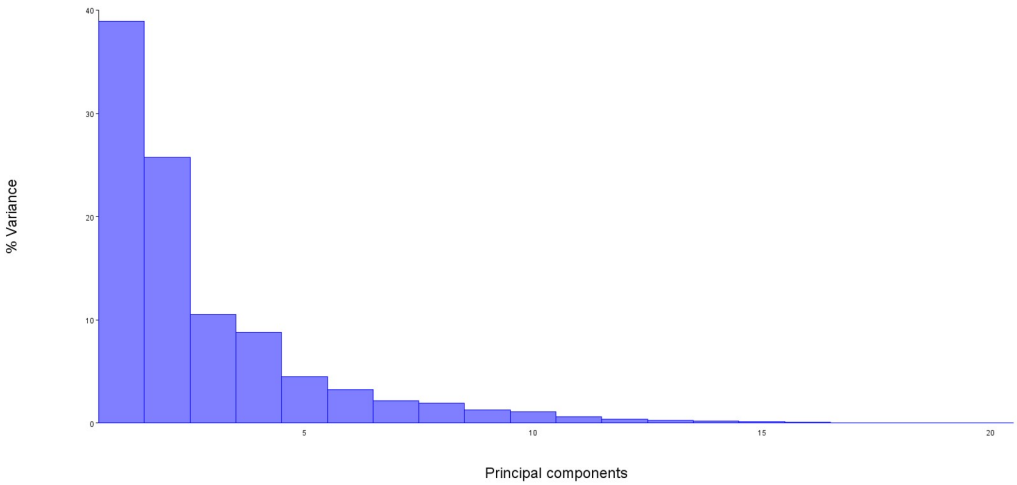

Figure 22: Eigenvalues of the PCA conducted between *Potamotherium* and Pinnipedia mandibles.

The last PCA was concluded by isolating the Pinnipedia mandibles and *P. valletoni* mandibles. MorphoJ traced 20 principal components with PC1 to PC4 having an absolute value of over 5%, with their total value calculated at 83,97% (Figure 22). PC1 had a value of 38,9% and was influenced by the general shape of the mandible, mainly the lateral width of its main body and the transition to the ramus. PC2 had a value of 25,73% and it is governed by the tip of the coronoid process and the lateral width of the front-end of the mandible. PC3 was estimated at 10,51%. and it was associated with the lateral width of the mandible compared to the coronoid process's height and the development of the angular process. PC4 was estimated at 8,81%, and it was associated by the curvature of the mandible.
By looking through the values of each principal component, *P. valletoni* scored low on both PC1 and PC2 in comparison to Pinnipeds, with the exception of *L.*

carcinophagus on PC1 (Figure 23). Its negative values on both principal components can lead to the conclusion that its mandible was not as wide laterally as the mandibles of Pinnipeds and has a more steep rise from the main body to the coronoid process.

On PC3, *P. valletoni* was clustered along the middle of the allocation. This shows that *P. valletoni* had a big coronoid process on a relatively slim mandible's body in comparison to Pinnipeds like *M. leonina*, of which the lateral width is pretty expanded while its coronoid process small.

On PC4 *P. valletoni* had a positive value indicating a mandible with not so much curvature and a clear distinction of the ramus. Samples with positive values have more complicated mandibles, while the ones with negative values have mandibles that show a seamless transition from the frontal to the distal parts.

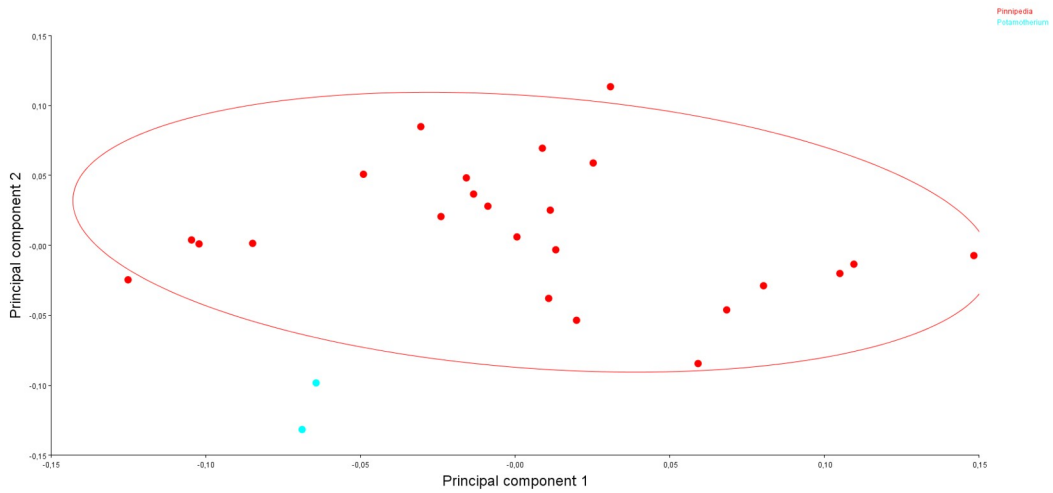

Figure 23: PCA of *Potamotherium* and Pinnipedia mandibles. PC1 and PC2 are compared. *Potamotherium* has an apparent distance on PC2 and on PC1 it scores at a negative direction, while most Pinnipeds score on a positive direction.

3. 3. Infraorbital Foramen analysis results

The IOF Area was highly correlated with the GM (p<0,5), especially in pinnipeds, an observation shared with Milne et al., 2022. As expected the IOF areas of pinnipeds and aquatic Mustelidae, especially Lutrinae were larger compared to those of terrestrial Mustelidae (Figure 24). The one glaring exception was that of the European badger, *M. meles*, which has a wider IOF compared to the dimensions of its skull in comparison to other terrestrial Mustelidae, or even other species of the genera *Meles,* like *M. iberica*, an animal from the Pliocene and Pleistocene of Spain (Arribas and Garrido, 2007). This can be explained if its fossorial lifestyle is taken into account. Especially in northern latitudes and forests, like Britain, *M. meles* is specialized in excavating earthworms that it needs to hunt by burrowing underground (Kruuk and Parish, 1985). On the other hand the majority of Mustelidae are active hunters with a slew of different prey and hunting methods within the group as mentioned earlier in the study.

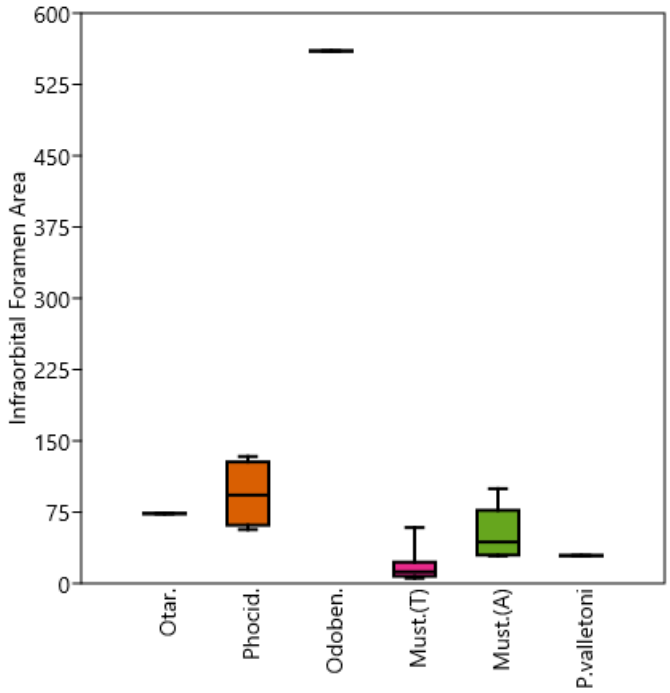

Figure 24: Boxplot of calculated IOF areas among the studied families.

By creating an XY graph (Figure 26) by having GM on the X axis and the IOF area

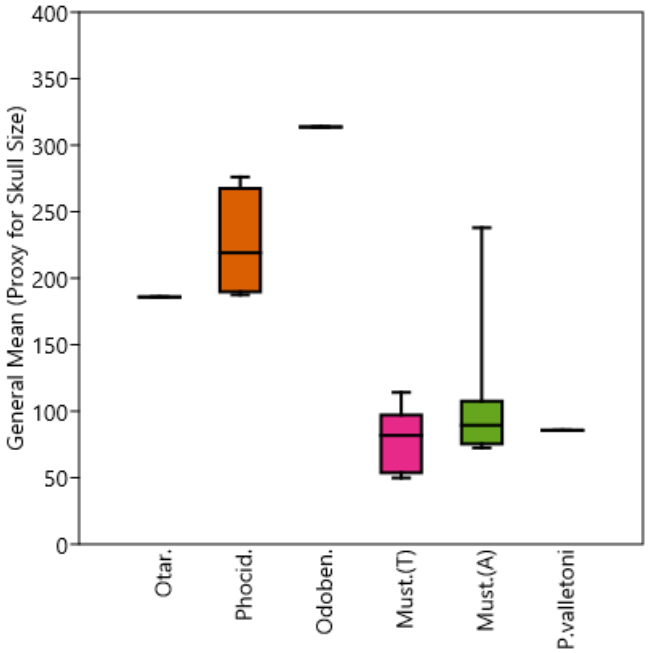

Figure 25: Boxplot of the calculated GMs of the different families craniums.

on the Y axis the placement of *P. valletoni* among the species used in the analysis is traced (Figure 26 & Figure 27). In the graph, *P. valletoni* was approximate to members of Lutrinae, with its IOF being close in area to the IOF of smaller Lutrinae, like *L. felina*. Simultaneously, while its size and GM was significantly smaller than some terrestrial Mustelidae, like *G. gulo* and *T. taxus*, its IOF area was still bigger, showing greater sensitivity around the vibrissal area. However, *P. valletoni's* IOF area was significantly smaller than other Lutrinae of comparable GM, like *L. lutra* and *L. canadensis*. This is a possible indicator of the fact that it used its whiskers to understand the environment around it. Radinsky (1968) studied the brain of *P. valletoni* using endocranial casts and recognized enlargement of the coronal gyrus, which in modern Lutrinae is associated with vibrissae specialization. The most prominent observation is that *P. valletoni* seemed to have similar sized IOF areas with smaller Lutrinae, while similar sized Lutrinae tend to have larger IOF areas (Figure 28).

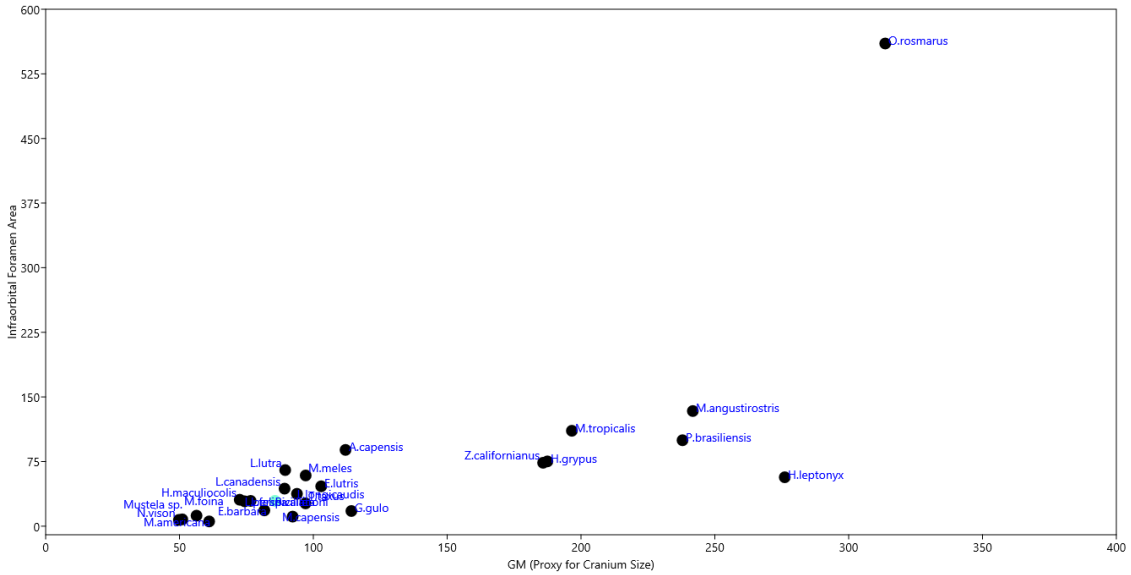

Figure 26: Scatter graph for the IOF area and the geometric mean (GM) of the cranium measured in mm². *Odobenus rosmarus* IOF area is exceptionally large in comparison to all other species skewing the graph.

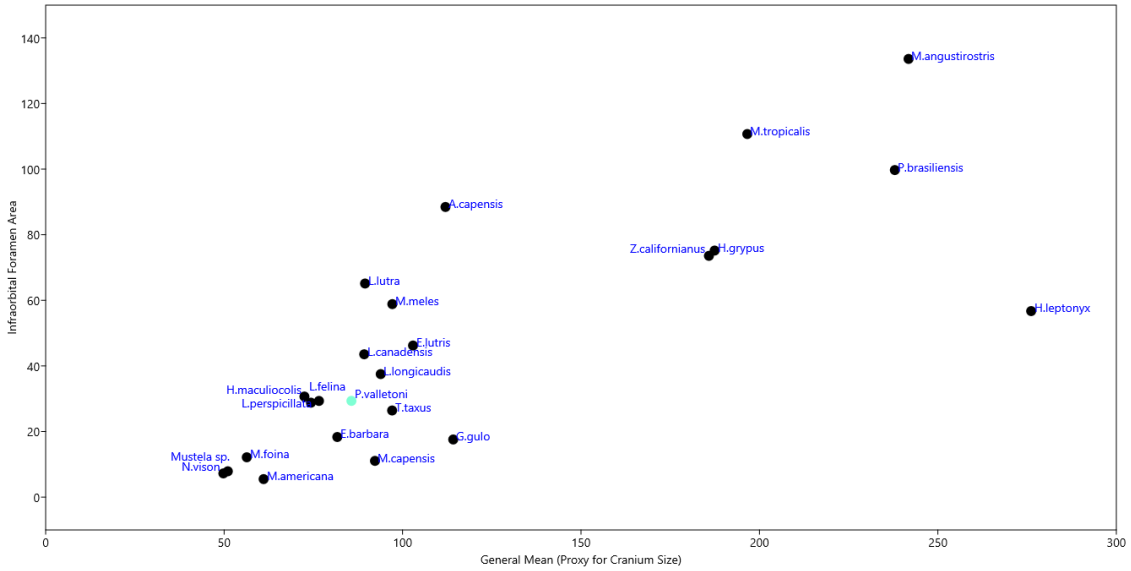

Figure 27: Excluding *Odobenus rosmarus* from the previous graph the exact placements of *Potamotherium* and all the other species got distinguishable.

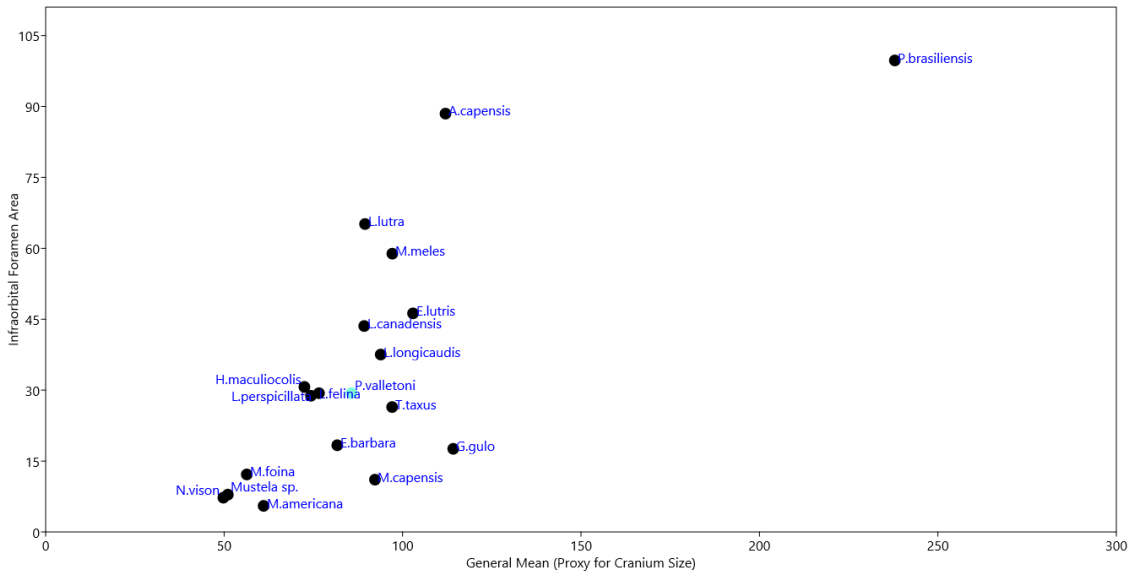

Figure 28: Excluding Pinnipedia, the area of *Potamotherium*'s IOF in comparison to Mustelidae is similar to Lutrinae of smaller size, while simultaneously is smaller to those of the same size.

3. 4. Traditional Morphometrics results

P. valletoni's skull tends to resemble the category of Lutrinae skulls which are mouth-oriented predators, based on the skull MNHM SG692 and Savage's (1957) description of its skeleton. It had a long rostrum with short nasal bones and a steep premaxilla. The frontal bone was long and formed a bridge-like structure which led to the parietal, which covered a narrow neurocranium. Zygomatic bones were thin and did not form a wide arc dorsal to the glenoid fossa. On a ventral view the most important character of *P. valletoni* was the elongated, slim palate.

From the new PCA with both Timm-Davis et al.,(2015) data and the transformed measurements of *P. valletoni* conducted for this study, visible in Figure 29, the first conclusion is that interorbital distance is clearly lengthier in *E. lutris* than any of the other species, while *P. valletoni* seems to be on the lower end of that spectrum. The next thing that is visible was that based on the measurements of the palate, *P. valletoni* seems to match very well with the two mouth oriented predators, as both species and *P. valletoni* seem to have lengthy but thin palates, while the two hand oriented predators tend to have wide, short ones. On the zygomatic arch, length favors mouth-oriented otters and width hand-oriented predators with bigger orbital cavities. The backside of the cranium did not seem to influence the foraging way. The surface of the post-canine teeth of *P. valletoni* was aligned with those of mouth-oriented otters as it is significantly smaller than the surface of hand oriented predators. This observation is consistent with the rest of the measurements, as mouth-oriented otters are not calibrated towards crushing the prey. On the contrary post-canine surface of *E. lutris* is consistent with other durophagous animals that intend to crush the shells of their prey, having bunodont type teeth, an adaptation by durophagous animals that assists them to break the shells of their prey (Popowics, 2003).

With the initial results leading to a proximity of *P. valletoni* with the mouth-oriented otters, a new PCA and a discriminant analysis with an isolated group of only those samples were commenced. *P. valletoni* seemed to have a smaller zygomatic arch than *P. brasiliensis*, while it has smaller interorbital distance and post-canine teeth

surface than *L. canadensis*. The palate of *P. valletoni* appeared to be longer than both of the other two species, while the width of it was smaller. In the discriminant analysis *P. valletoni* consisted a group by itself, not matching with either *P. brasiliensis* or *L. canadensis*, with the palate being the main element that differentiates *P. valletoni* from *P. brasiliensis* and *L. canadensis*. The interorbital distance and the surface of the post-canine teeth separated it from *L. canadensis* as both are smaller compared to the *L. canadensis*. Juxtaposed to *P. brasiliensis,* the height and the width of the bones of the zygomatic arch are the main measurements that divaricated the two in the discriminant analysis(Figure 31).

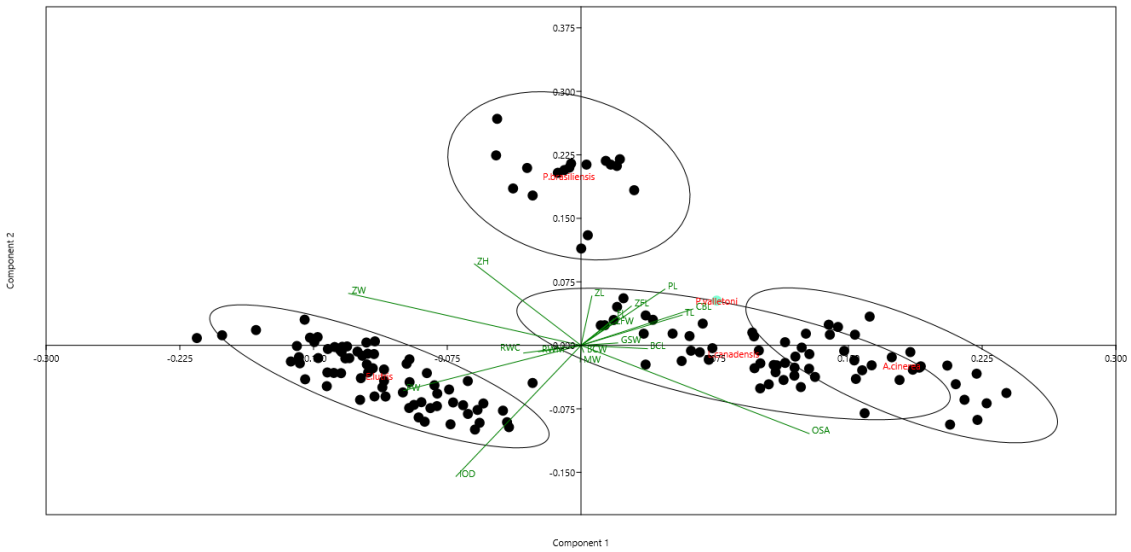

Figure 29: PCA including *Potamotherium* and the four Lutrinae. *P. valletoni* is closer to the mouth-oriented predators with longer, muzzles, zygomatic arches and palates but not as wide as the hand-oriented predators especially *E. lutris*.

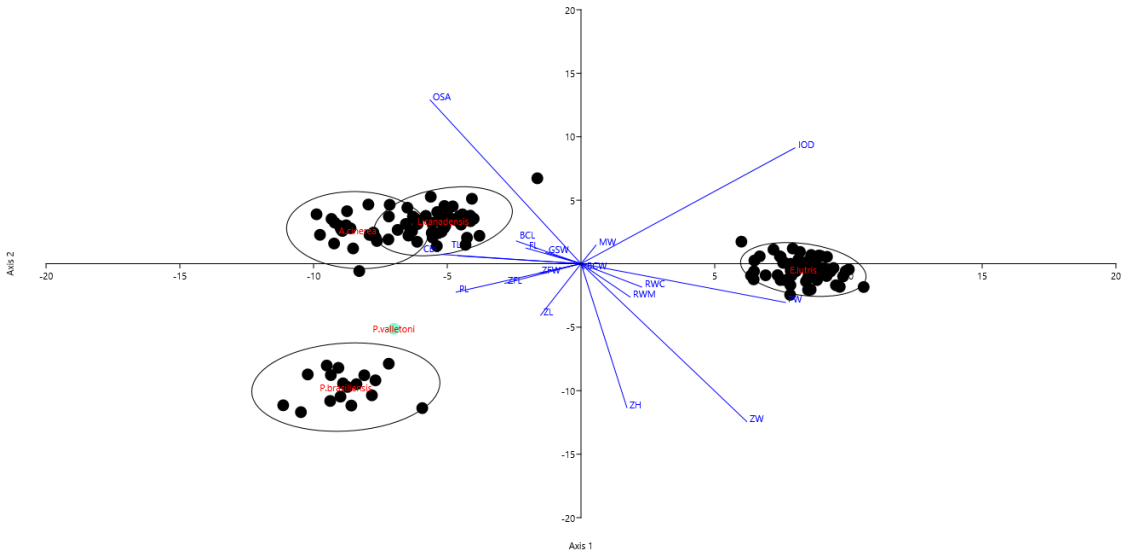

Figure 30: Discriminant analysis between the four species. *P. valletoni* scores closer to the mouth-oriented predator *Pteronura brasiliensis*.

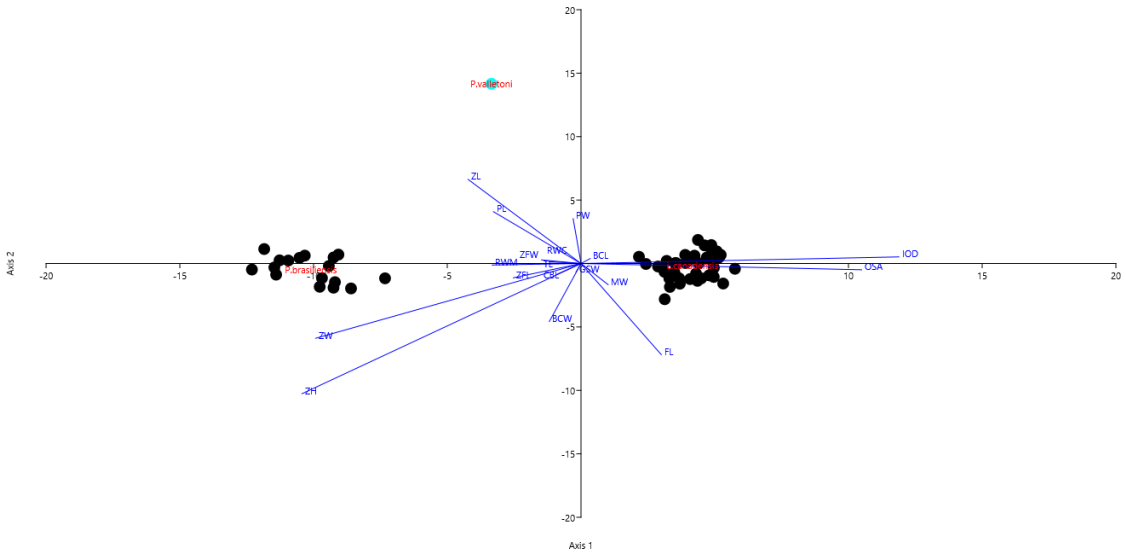

Figure 31: Discriminant analysis graph of only *Potamotherium* and the two mouth-oriented predators. *P. valletoni* is mainly distinguished based mostly on the length of its palate and its zygomatic arch in comparison to the other two species.

4. Discussion

The goal of this study is to understand how *P. valletoni* used to hunt. The different analyses of the skull of *P. valletoni* led to an interesting bundle of conclusions.

4. 1 Shape of the Skull: Proximity to Mustelidae or Pinnipedia?

From the results of the geometric morphometrics analyses, both on 2D and 3D, it was easily concluded that the skull of *P. valletoni* is more reminiscent of Mustelids than Pinnipeds. More specifically, the splanchnocranium of *P. valletoni* is short in comparison to the Pinnipeds with short nasal and maxillary bones, while concurrently it has a long frontal which transitions smoothly into the parietal bone (Savage, 1957). On the other hand the frontal bones of Pinnipeds tend to be wide but not lengthy and do not consist a large part of their facial structure, while their maxillary bones tend to be elongated (Hafed et al., 2020).

The neurocranium of *P. valletoni* is smaller in height compared to pinnipeds and lacks a sagittal crest, a character that varies from just traceable to utterly prominent in Pinnipeds, depending on the family (Hafed et al., 2020). Furthermore, the absence or the underdevelopment of the sagittal crest is also a character found on most Lutrinae skulls, although species like *E. lutris* still retain a prominent one. The tympanic bulla of *P. valletoni* is somewhat flattened although not as much as the Lutrinae, and far smaller than the inflated bullae of pinnipeds. One pretty distinct element of *P. valletoni's* skull morphology, the elongated, lean shape of its palate became visible when compared only to Mustelidae, a unique character that was not present on other samples used in the study in a way that betrays direct similarities.

Its occipital crest is not wide, whilst the paroccipital processes and condyles were on the larger end in comparison to most Mustelidae. Occipital condyles are connected to the atlas thus forming the atlantoccipital joint (Harode and Gupta, 2022). Large occipital condyles and paroccipital processes are correlated with carnivorous diets as it help them redistribute the strain the atlas and the axis could

be subjected under while feeding to the rest of the cervical vertebrae, protecting them from dislocations (Mead, 1906). The morphology of its zygomatic arch is long and narrow, though it does not seem to influence the feeding habits as it is proven that its shape has not an effect on feeding, rather it is a complimentary adaptation to the other cranial adaptations and the distribution of forces inflicted upon the skull while feeding, despite its importance in mastication (Smith and Grosse, 2016) The area the infraorbital foramen of *P. valletoni* covered on its face was estimated as larger than terrestrial subfamilies of Mustelidae, while when compared to Pinnipeds was far smaller. When it was weighed against Lutrinae IOFs its foramen was smaller than the ones which were around the same Geometric Mean. On the contrary, smaller Lutrinae had an area of similar dimensions.

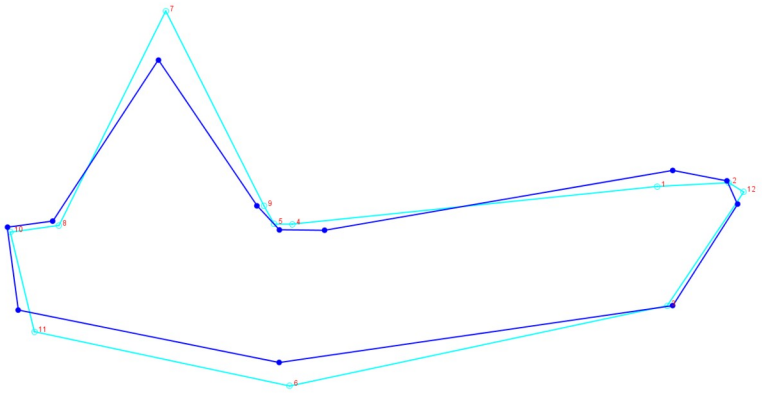

Figure 32: Impression of the wireframes of Mustelidae mandibles on P. valletoni mandibles based on the landmarks taken.

On the mandible, *P. valletoni* again showed similar traits with Lutrinae rather than Pinnipedia (Figure 32). In general, Pinnipedia have differences on their mandible's shape depending on which family they belong to: Odobenidae and Otariidae tend to have lower ramuses with small coronoid processes although the former's ramuses are thick meanwhile the latter's are thinner and narrower, and Phocidae have differences within their family depending on the subfamilies or the species they belong to (Hafed et al., 2020), but in general their ramuses are shorter compared to their corpuses (Meloro and Tamagnini, 2021). On the other hand Mustelidae's mandibles shape is influenced not only by their subfamilies, but by

their type of prey available around them and the adaptations their jaws go through under the environmental pressure of different biomes (Romaniuk, 2018). In the Palearctic region the ramus of the Mustelidae mandibles can be divided into two types, narrow and long, reminiscent of sea otters, and wide and short similar to those of badgers (Romaniuk, 2018).

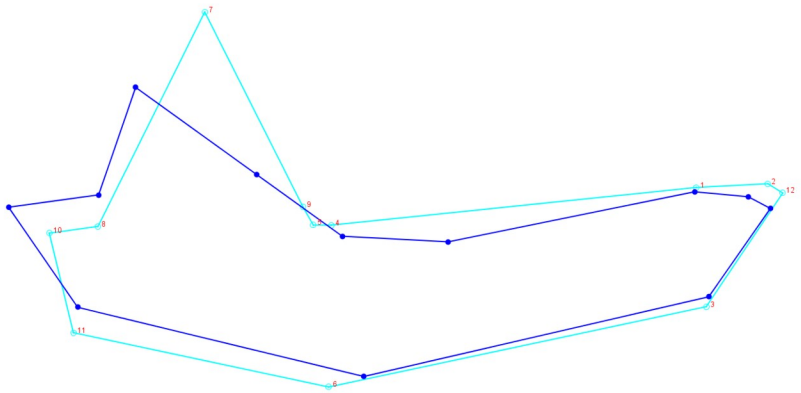

Figure 33: Impression of the wireframes of Pinnipedia mandibles on *P. valletoni* mandibles based on the landmarks taken.

Compared to Pinnipeds, the body of *P. valletoni*'s mandible is not as curvy, while the ramus makes a steeper corner where it connects to the body and it is notably higher than in Pinnipeds (Figure 33). The ramus has an almost vertical direction to the body, and the condyloid process is on a level close to the upper parts of the main hull of the body. On the other hand, on the majority of Pinnipeds the condyloid process is higher than the Lutrinae, sometimes on the same level as the coronoid process. The proximity of the condyloid and the coronoid process is an aquatic adaptation, indicating that Pinnipeds's temporalis attachment area is short (Meloro and Tamangini, 2022), as the coronoid process is where the temporalis and the masseter, the most important muscles used by mammals for mastication are jointed (Patil et al., 2022). That is explained by the fact that Pinnipeds do not masticate, meaning these muscles do not need to be especially developed (Jones et al., 2013).

The ramus of *P. valletoni*'s mandibles creates a steep corner with the main body of the mandible while also the tip of the coronoid process has a similar morphology and direction with the Lutrinae, although it is lower in height. The angular process of *P. valletoni's* mandibles is not in any way prominent in comparison to the Lutrinae's, while it is not underdeveloped. The body of the mandible is pretty similar to the average Lutrinae one.

In general, extant Mustelidae's skull shape has undergone a reduction on temporal fossa width, teeth row length, jaw length, moment arm of masseter, orbits and condyle to carnassial distance, and a prominent development on occipital's width (Radinsky, 1982). The results of both traditional and geometric morphometrics on *P. valletoni* seem to mostly agree with it.

All of these observations on the geometric morphometrics analyses are consistent with previous descriptions of *P. valletoni*'s skulls shape, mainly Savage's (1957), that conclude its proximity to a Lutrinae morphology, without making any assumptions for its phylogenetic placement, if it was closer to a Pinniped or a Mustelidae.

4. 2 *Potamotherium* skull functions and diet

In most published works *Potamotherium* is compared with the Eurasian otter *L. lutra. L. lutra* hunts by diving downwards vertically, with a preference to shallow waters as their fauna is richer and easier to catch (Kruuk and Moorhouse, 1990). Its diet is mostly composed of fish, however in Mediterranean habitats, *L. lutra*'s diet is pretty diverse with the percentage of invertebrates and reptiles which it consumes is significantly higher (Clavero et al., 2003). Their skull's shape is also influenced by their habitat as *L. lutra* which hunt fish in freshwater deposits tend to have slender and smaller muzzles than the ones which hunt in the open sea (Russo et al., 2022). In Saint-Gerand-le-Puy, based on the associated fossil fauna, it is theorized that it was mainly a freshwater habitat, but also included parts with brackish water (Cheneval, 1989).

The first feature of *P. valletoni's* skull which leads to a conclusion about its feeding is the small, almost absent, sagittal crest. An enlarged sagittal crest is a reflection of a developed temporalis muscle. This is the muscle that is primarily used in Carnivora, to close the jaw, and it is an evolutionary adaptation that helps in redistributing the strain the skull of an animal with a high bite force is put under (Curtis et al., 2018). Knowing this, it is obvious that *P. valletoni* did not have a strong bite, which it used to grip its prey, nor it hunt hard shelled animals that required additional force to smash their shell. Combining this information with the fact that *P. valletoni's* coronoid process had a shape approximate to those of Lutrinae it seems it hunted smaller prey than it with a moderate bite force for its size. Modern Lutrinae of size and skull morphology comparable to *P. valletoni's* also seem to use moderate force on their bites and their diets are mostly piscivorous (Christiansen and Wroe, 2007). Thus, taking also into consideration the palaeoenvironment of Saint Gerand-le-Puy, a diet mainly consisting of fish can be attributed to *P. valletoni.*

It could have utilized its whiskers as modern freshwater Lutrinae do, using them as a scanner of its surroundings to compensate for the lower visibility insider the bodies of water, something that as it is was referenced earlier was also evident by endocasts of its brain and the enlargement of the coronal gyrus (Radinsky, 1968), and partially confirmed by the results of the measurements of its infraorbital foramen. Lyras et al. (2023) reinforced this assumption by comparing the coronal gyrus of *P. valletoni*'s brain to both modern and extinct carnivores. Their results exhibited the enlargement of *P. valletoni*'s coronal gyrus. Unfortunately, the number of its vibrissae can not be estimated, as they are impossible to count on an extinct animal and there can not be a speculation as the vibrissae number is not predictable just from the area the IOF covers, as the dimensions of the vibrissae should be taken into account (Muchlinski, 2010), although the IOF has been positively correlated with the number and the shape of whiskers an animal may have and their sensory abilities (Mucklinski, 2008). However, a large IOF area and a wide infraorbital nerve can be associated with the action of whisking, the deliberate, rhythmic movement of the whiskers to scan the surrounding area, as

those animals have typically larger IOFs (Muchlisnki et al., 2020). By the results of the analysis and having the previous theory as a basis, it could be hypothesized that *P. valletoni's* whiskers had similar functionality as modern Lutrinae, although it was more primitive in its usage of them as it tried to sense its surrounding environment.

Concluded by the results of the traditional morphometrics analysis, and having already established that its skull shape and function was similar to Lutrinae it was concluded that the skull of *P. valletoni* was reminiscent of Lutrinae mouth-oriented predators. Knowing that *P. valletoni's* palate had an elongated and narrow shape on the palate, while the skull's shape being leaner to begin with in comparison to hand-oriented animals like *Enhydra lutris ,*the main example of hand-oriented Lutrinae predator, with the shape of its skull and palate being short and wide, while simultaneously having an ample post-canine teeth surface and the prevalence of a sagittal crest, characters completely opposite to those of *P. valletoni*, it can be hypothesized that its foraging behavior was similar to mouth-oriented Lutrinae. *P. valletoni* possibly captured its prey with a swift bite and if it is to compared with the preferences of modern Lutrinae in environments with freshwater deposits, like *Lutra lutra* (Nolet et al., 1993), it should prefer shallow waters, as its efficiency on finding prey should be higher, since it would require less energy and time.

5. Conclusions

The main goal of this study was to investigate the ecomorphological adaptations of *Potamotherium valletoni*'s skull using four different methodologies.

The results of the geometric morphometrics analysis showed the morphological proximity of the skull of P. valletoni to that of Lutrinae. It had a lean, low cranium with an elongated palate suitable for hunting underwater. The cranium of terrestrial Mustelidae was thicker and wider, while Pinnipedia cranium showed a completely different morphology than Mustelidae. The mandible was also reminiscent of Lutrinae, with a much steeper transition from the body to the ramus and a longer coronoid process, compared to Pinnipedia. This trait of the mandible could be attributed to the fact that Pinnipedia do not tend to masticate, leading to weaker masseter muscles and smoother, lower shapes.

Its Infraorbital foramen was bigger than terrestrial Mustelidae, smaller than Lutrinae of similar size and approximately the same size as modern Lutrinae smaller than it. That led to the conclusion that while it hunted in the water, it possibly used a more unrefined whisking, the deliberate movement of its whisker, a characteristic of both Lutrinae and Pinnipedia, to locate its prey while it hunted, as the infraorbital foramen is the passage which the nerves acquainted to the sensitivity of whiskers use to connect to the outer side of the face.

Comparing different dimensions of its cranium to other extant Lutrinae, two hand-oriented predators and two mouth-oriented, it was discerned that its morphology was closer to the later, with the lean palate and the narrow shape being the most important characteristics. Those were considered as proof of its foraging methods as a mouth-oriented predator. *P. valletoni*'s palate is renowned for its unique thin and long shape, a trait shared with modern mouth-oriented predators. Hand-oriented predators, especially *Enhydra lutris* tend to have bigger, wider skulls and a bigger post-canine teeth surface which help them shatter their prey's shells, which they prefer as prey, instead of fish, the common prey of most mouth-oriented predators.

Thus, it is concluded that *P. valletoni*'s ecomorphological adaptations were reminiscent of the modern freshwater Lutrinae and not Pinnipeds. The shape of its cranium indicates that it was hunting in a similar way as modern aquatic Mustelidae that hunt mostly fish by using their mouth.

References

Abramoff, M. D., Magahles, P. J., Ram, S. J., 2004. Image processing with ImageJ. Biophotonics International 11(7), 36-42.

Adam, P. J., Berta, A., 2002. Evolution of prey capture strategies and diet in the Pinnipedimorpha (Mammalia, Carnivora). Oryctos 4, 83-107.

Adams, D. C., Rohlf, F. J., Slice, D. E., 2004. Geometric morphometrics: ten years of progress following the 'revolution'. Italian Journal of Zoology 71, 5-16.

Agthong, S., Huanmanop, T., Chentanez, V., 2005. Anatomical variations of the supraorbital, infraorbital, and mental foramina related to gender and size. Journal of Oral and Maxillofacial Surgery 63, 800-804.

Arribas, A., Garrido, G., 2007. *Meles iberica n. sp.,* a new Eurasian badger (Mammalia, Carnivora, Mustelidae) from Fonelas P-1 (Plio-Pleistocene boundary, Guadix Basin, Granada, Spain). Comptes Rendus Palevol 6, 545-555.

Baltanás, A., Danielopol, D. L., 2011. Geometric morphometrics and its use in ostracod research: a short guide. Joannea-Geologie und Palaontologie 11, 235-272.

Baskin, J. A., 1998. Mustelidae, in: Janis, C. M, Scott, K. M., Jacobs, L. L. (Eds.), Evolution of Tertiary Mammals in North America. Cambridge University Press, Cambridge, pp. 152-173.

Bauer, G. B., Reep, R. L., Marshall, C. D., 2018. The tactile senses of marine mammals. International Journal of Comparative Psychology 31.

Berta, A., 1991. New *Enaliarctos* (Pinnipedomorpha) from the Oligocene and Miocene of Oregon and the role of ''Enaliarctids'' in Pinniped phylogeny. Smithsonian Contributions to Paleobiology 69, 1-33.

Berta, A., Churchill, M., Boessenecker, R. W., 2018. The origin and evolutionary biology of pinnipeds: seals, sea lions ,and walruses. Annual Review of Earth and Planetary Sciences 46, 203-228.

Berta, A., Lanzetti, A., 2020. Feeding in marine mammals: an integration of evolution and ecology through time. Palaeontologia Electronica 23(2), a40.

Bodkin, J. L., Esslinger, G. G., Monson, D. H., 2004. Foraging depths of sea otters and implications to coastal marine communities. Marine Mammal Science 20(2), 305-321.

Boessenecker, R. W., Churchill, M., 2018. The last of the desmatophocid seals: a new species of *Allodesmus* from the upper Miocene of Washington, USA, and a revision of the taxonomy of Desmatophocidae. Zoological Journal of the Linnean Society 183, 211-235.

Bolliger, T., 2000. Wiesholz (canton of Schaffhausen, Switzerland), a peculiar mammal fauna from mica-rich sands (Upper Freshwater Molasse, Miocene, early MN6). Revue de Paléobiologie 19, 1-18.

Bookstein,F. L., 1991. Morphometric Tools for Landmark Data: Geometry and biology. Cambridge University Press, Cambridge.

Byrom, A. E., Caley, P., Paterson, B. M., Nugent, G., 2015. Feral ferrets (*Mustela furo*) as hosts and sentinels of tuberculosis in New Zealand. New Zealand Veterinary Journal 63, 42-53.

Cardini, A., 2017. Left, right or both? Estimating and improving accuracy of one-side-only geometric morphometric analyses of cranial variation. Zoological Systematics and Evolutionary Research 55(1), 1-10.

Cheneval, J., 1989. Fossil bird study, and paleoecological and paleoenvrionmental consequences: example from the Saint-Gerand-Le-Puy deposits (Lower Miocene, Allier, France). Palaeogeography, Palaeoclimatology, Palaecology 73, 295-309.

Christiansen, P., Wroe, S., 2007. Bite forces and evolutionary adaptations to feeding ecology in carnivores. Ecology 88, 347-358.

Churcher, C. S., 1959. The specific status of the new world red fox. Journal of Mammalogy 40(4), 513-520.

Cignoni, P., Callieri, M., Corsini, M., Dellepiane, M., Ganovelli, F., Ranzuglia, G., 2008. MeshLab: an open-source mesh processing tool, in: Scarano, V., De Chiara, R., Erra, U. (Eds.), Eurographics Italian Chapter Conference 2008. The Eurographics Association, pp. 129-136.

Clavero, M., Prenda, J., Delibes, M., 2003. Trophic diversity of the otter (*Lutra lutra L.*) in temperate and Mediterranean freshwater habitats. Journal of Biogeography 30, 761-769.

Corti, M., 1993. Geometric morphometrics: an extension of the revolution. Tree 8(8), 302-303.

Courtenay, L. A., Huguet, R., González-Aguilera, D., Yravedra, J., 2020. A hybrid geometric deep learning approach for cut and trampling mark classification. Applied Sciences 10, 150.

Courtenay, L. A., González-Aguilera, D, 2020. Geometric morphometric data augmentation using generative computional learning algorithms. Applied Sciences 10, 9133.

Curtis, A. A., Orke, M., Tetradis, S., van Valkenburgh, B., 2018. Diet-related differences in craniodental morphology between captive-reared and wild coyotes, *Canis latrans* (Carnivora: Canidae). Biological Journal of the Linnean Society 123, 677-693.

Davies, J. L., 1958. The Pinnipedia: an essay in zoogeography. Geographical Review 48(4), 474-493.

Deméré, T. A., Berta, A., 2001. A reevaluation of *Proneotherium repenningi* from the Miocene Astoria Formation of Oregon and its position as a basal Odobenid (Pinnipedia: Mammalia). Journal of Vertebrate Paleontology 21, 279-310.

Derežanin, L., Blažytė, A., Dobrynin, P., Duchêne, D. A., Grau, J. H., Jeon,S., Kliver, S., Koepfil, K. -P., Meneghini, D., Preick, M., Tomarovsky, A., Totikov, A., Fickel, J., Förster, D. W., 2022. Multiple types of genomic variation contribute to adaptive traits in the mustelid subfamily Guloninae. Molecular Ecology 31, 2898-2919.

Doroff, A., Burdin, A., Larson, S., 2021. *Enhydra lutris*. The IUCN Red List of Threatened Species 2021, e. T7750A164576728.

Dougill, G., Starostin, E. L., Milne, A. O., van der Heijden, G. H. M., Goss, V. G. A., Grant, R. A., 2020. Ecomorphology reveals Euler spiral of mammalian whiskers. Journal of Morphology 281, 1271-1279.

Dryden, I. L., Mardia, K. V., 1998. Statistical Space Analysis. John Wiley and Sons, Chichester.

Dumont, M., Wall, C. E., Botton-Divet, L., Goswami, A., Peigné, S, Fabre A-C., 2016. Do functional demands associated with locomotor habitat, diet and activity pattern drive skull shape evolution in musteloid carnivorans?. Biological Journal of the Linnean Society 117, 858-878.

Duplaix, N., 1980. Observations on the ecology and behavior of the giant otter *Pteronura brasiliensis* in Suriname. Revue d'Ecologie, Terret et Vie, Société national de protection de la nature 34(4), 495-620.

Estes, J. A., 1980. *Enhydra lutris.* Mammalian Species 133, 1-8.

Fabre A-C., Cornette, R., Slater, G., Argot, C., Peigné, S., Goswami, A., Pouydebat, E., 2013. Getting a grip on the evolution of grasping in musteloid carnivorans: a three-dimensional analysis of forelimb shape. Journal of Evolutionary Biology 26, 1521-1535.

Fahlke, J. M., Gingerich, P. D., Welsh, R. C., Wood, A. R., 2011. Cranial asymmetry in Eocene archaeocete whales and the evolution of directional hearing in water. PNAS 108(35), 14545-14548.

Fay, F. H., 1982. Ecology and biology of the pacific walrus, *Odobenus rosmarus divergens* Illiger. United States Department of the Interior Fish and Wildlife Service. Washington D. C.

Fay, F. H., 1985. *Odobenus Rosmarus*. Mammalian Species 238, 1-7.

Fedorov, A., Beichel, R., Kalpathy-Cramer, J., Finet, J., Fillion-Robin, J. -C., Pujol, S., Bauer, C., Jennings, D., Fennessy, F., Sonka, M., Buatti, J., Aylward, S., Miller, J. V., Pieper, S., Kikinis, R., 2012. 3D Slicer as an image computing platform for the quantitative imaging network. Magnetic Resonance Imaging 30, 1323-1341.

Filhol, M. H., 1879. Etude des mammiferes fossiles de Saint-Gerand le Puy (Allier) par M. H. Filhol. Bibliothèque de l'Ecole des Hautes Etudes, Sciences Natural, Paris.

Finarelli, J. A., 2008. A total evidence phylogeny of the Arctoidea (Carnivora : Mammalia): Relationships among basal taxa. Journal of Mammalian Evolution 15, 231-259.

Foster-Turley, P., 1992. Conservation ecology of sympatric Asian otters *Aonyx cinerea* and *Lutra perspicillata*. Ph. D. Thesis, University of Florida.

Ginsburg, L., Bonneau, Mi., 1995. La succession des faunes de mammifères miocènes de Pontigné (Maine-et-Loire), France. Bulletin of National Museum of Natural History of Paris 16, 313-328.

Goodfellow, I. J., Pouget-Abadie, J., Mirza, M., Xu, B., Warde-Farley, D., Ozair, S., Courville, A., Benglo, Y., 2014. Generative adversial nets, in: Ghahramani, Z., Welling, M., Cortes, C., Lawrence, N., Weinberger, K. Q. (Eds.), Advances in Neural Information Processing Systems 27. Curran Associates Inc., New York.

Gower, J. C., 1975. Generalized procrustes analysis. Psychometrika 40(1), 33-51.

Grice, J. W., Assad, K. K., 2009. Generalized procrustes analysis: a tool for exploring aggregates and persons. Applied Multivariate Research 13(1), 93-112.

Hafed, A., Koretsky, I., Rahmat, S., 2020. Current status of pinnipeds phylogeny based on molecular and morphological data. Historical Biology 33(6), 1-15.

Hammer, Ø, Harper, D. A. T., Ryan, P. D., 2001. PAST: paleontological statistics software package for education and data analysis. Palaentologia Electronica 4(1), 4.

Harode, H. A., Gupta, S. D., 2022. Analysis of occipital condyles on dry human skulls. International Journal of Health Sciences 6, 1428-1434.

Heizmann, E.P.J., Ginsburg, L., Bulot, C., 1980. Prosansanosmilus peregrinus, ein neuer machairodontier Felide aus dem Miocän Deutschlands und Frankreichs. Stuttgarter Beiträge zur Naturkunde 58, 1-27

Herr, 1876. The Primeval World of Switzerland. Taylor and Franics, London.

Higdon, J. W., Bininda-Emonds, O. R. P., Beck, R. M. D., Ferguson, S. H., 2007. Phylogeny and divergence of the pinnipeds (Carnivora: Mammalia) assessed using a multigene dataset. BMC Evolutionary Biology 7, 216.

Hocking, D. P., Fitzgerald, E. M. G., Salverson, M., Evans, A. R., 2016. Prey capture and processing behaviors vary with prey size and shape in Australian and subantarctic fur seals. Marine Mammal Science 32(2), 568-587.

Hocking, D. P., Marx, F. G., Park, T., Fitzgerald, E. M. G., Evans, A. R., 2017. A behavioural framework for the evolution of feeding in predatory aquatic mammals. Proceedings of the Royal Society B 284, 20162750.

Hugueney, M., Poidevin, J. L., Bodergat, A. M., Caron, J. B., Guérin, C., 1999. Des mammifères de l'Aquitanien inférieur à La Roche-Blanche-Gergovie (Puy-de-Dôme, France), révélateurs de l'activité post-oligocène du rift en Limagne de Clermont. Earth & Planetary Sciences 328, 847-852.

Hugueney, M., Berthet, D., Escuille, F., Rival, J., 2006. Eomyids (Rodentia, Mammalia) in the St-Gerand-le-Puy Area (Allier, France; MN2a). Beiträge zur Paläontologie 30, 205-221.

Jiang, H., Deng, T., Li, Y., Xu, H., 2015. Neogene tectonics and climate forcing of carnivora dispersals between Asia and North America. Solid Earth Discussions 7, 2445-2479.

Jones, K. E., Ruff, C. B., Goswami, A., 2013. Morphology and biomechanics of the Pinniped jaw: Mandibular evolution without mastication. The Anatomical Record 296, 1049-1063.

Jungers, W. L., Falsetti, A. B., Wall, C. E., 1995. Shape, relative size, and size-adjustments in morphometrics. Yearbook of Physical Anthropology 38, 137-161.

Kargopoulos, N., Valenciano, A.,Abella, J., Kampouridis, P., Lechner, T., Böhme, M., 2022. The exceptionally high diversity of small carnivorans from the Late Miocene hominid locality of Hammerschmiede (Bavaria, Germany). PloS ONE 17, e0268968.

Kay, R. F., Cartmill, M., 1977. Cranial morphology and adaptations of *Palaechthon nacimienti* and other Paronomyidae (Plesiadapoides, ? Primates), with a description of a new genus and species. Journal of Human Evolution 6, 19-53.

Kellogg, E., 1922. Pinnipeds from Miocene and Pleistocene deposits of California. Bulletin of the Department of the Geological Sciences, University of California Publications 13(4), 23-132.

Kendall, D. G.,1977. The diffusion of shape. Advances in Applied Probability 9, 428-430.

Kienle, S. S., Berta, A., 2016. The better to eat you with: the comparative feeding morphology of phocid seals (Pinnipedia, Phocidae). Journal of Anatomy 228, 396-413.

Kienle, S. S., Law, C. J., Costa, D. P., Berta, A., Mehta, R. S., 2017. Revisiting the behavioural framework of feeding in predatory aquatic mammals. Proceeding of the Royal Society B 284, 20171035.

Kienle, S. S., Berta, A., 2019. The evolution of feeding strategies in phocid seals (Pinnipedia, Phocidae). Journal of Vertebrate Paleontology e1559172.

King, J. E., 1956. The monk seals (genus Monachus). Bulletin of the British Museum (Natural History) Zoology 3(5),201-256.

Klingenberg, C. P., Barluenga, M., Meyer, M., 2002. Shape analysis of symmetric structures: quantifying variation among individuals and asymmetry. Evolution 56(10), 1909-1920.

Klingenberg, C. P., 2011. MorphoJ: an integrated software package for geometric morphometrics. Molecular Ecology Resources 11, 353-357.

Klingenberg, C. P., 2015. Analyzing fluctuating asymmetry with geometric morphomertrics: concepts, methods and applications. Symmetry 7, 843-934.

Koepfli, K. -P., Deere, K. A., Slater, G. J., Begg, C., Begg, K., Grassman, L., Lucherini, M., Veron, G., Wayne, R. K., 2008. Multigene phylogeny of the Mustelidae: Resolvin relationships, tempo and biogeographic history of a mammalian adaptive radiation. BMC Biology 6, 10.

Kruuk, H., Parish, T., 1985. Food, food availability and weight of badgers (*Meles meles*) in relation to agricultural changes. Journal of Applied Ecology 22(3), 705-715.

Kruuk, H., Moorhouse, A., 1990. Seasonal and spatial differences in food selection by otters (*Lutra lutra*) in Shetland. Journal of Zoology 221, 621-637.

Lavrov, A. V., Tarasenko, K. K., Vlasenko, A. N., 2018. *Semantor macrurus* Orlov, 1931 (Carnivora: Mustelidae): Morphology of the hind limb and a new view on its paleobiology. Paleontological Journal 52, 1637-1646.

Law, C. J., Slater, G. J., Mehta, R. S., 2018. Lineage diversity and size disparity in Musteloidea: Testing patterns of adaptive radiation using molecular and fossil-based methods. Systematic Biology 67, 127-144.

Lawing, A. M., Polly, P. D., 2009. Geometric morphometrics: recent applications to the study of evolution and development. Journal of Zoology 280, 1-7.

Lebrun, R., 2018. MorphoDig, an open source 3D freeware dedicated to biology. IPC5 Paris, France.

Lyras, G. A., Werdelin, L., van der Geer, B. G. M., van der Geer, A. A. E., 2023. Fossil brains provide evidence of underwater feeding in early seals. Nature Communications Biology 6, 747.

Marcus, L., 1990. Traditional Morphometrics, in: Rohlf, F. J., Bookstein, F. L. (Eds.), Proceedings of the Michigan Morphometrics Workshop. University of Michigan Special Publication 2, Michigan, pp. 77-122.

Marshall, C. D., Amin, H., Kovacs, K. M., Lydersen, C., 2006. Microstructure and innervation of the mystacial vibrissal follicle-sinus complex in bearded seals, *Erignathus barbatus* (Pinnipedia: Phocidae). The Anatomical Record Part A 288A, 13-25.

Marshall, C. D., Rozas, K., Kot, B., Gill, V. A., 2014. Innervation patterns of sea otter (*Enhydra lutris*) mystacial follicle-sinus complexes. Frontiers in Neuroanatomy 8, 121.

Mead, C. S., 1906. Adaptive modifications of Occipital condyles in Mammalia. The American Naturalist 40, 475-483.

Meloro, C., Tamagnini, D., 2021. Macroevolutionary ecomorphology of the Carnivora skull: adaptations and constraints in the extant species. Zoological Journal of the Linnean Society 196, 1054-1068.

Melquist, W. E., Polechla Jr., P. J., Toweill, D., 2003. River Otter (*Lontra canadensis*), in: Feldhamer, G. A., Thompson, B. C., Chapman, J. A. (Eds.), Wild Mammals of North America: Biology, Management and Conservation, 2nd Edition. Johns Hopkins University Press, Baltimore and London, pp. 708-734.

Milne, A. O., Smith, C., Orton, L. D., Sullivan, M. S., Grant, R. A., 2020. Pinnipeds orient and control their whiskers: a study on Pacific walrus, California sea lion and Harbor seal. Journal of Comparative Psychology A 206, 441-451.

Milne, A. O., Muchlinski, M. N., Orton, L. D., Sullivan, M. S., Grant, R. A., 2022. Comparing vibrissal morphology and infraorbital foramen area in pinnipeds. The Anatomical Record 305, 556-567.

Morlo, M., 1996. Carnivoren aus dem Unter-Miozän des Mainzer Beckens (2. Mustelida, Pinnipedia, Feliformia, *Palaeogale*). Senckenbergiana Lethaea 76(1/2), 193-249.

Mörs, T., von Koenigswald, W., 2000. Potamotherium valletoni (Carnivora, Mammalia) aus dem Oberoligozän von Enspel im Westerwald. Senckenbergiana Lethaea 88, 257-273.

Mörs, T., von der Hocht, F., Wutzler, B., 2000. Die erste Wirbeltierfauna aus der miozänen Braunkohle der Niederrheinischen Bucht (Ville-Schichten, Tagebau Hambach). Paläontologische Zeitschrift 74(1/2), 145-170.

Muchlinski, M. N., 2008. The relationship between the Infraorbital foramen, Infraorbital nerve, and maxillary mechanoreception: implications for interpreting the paleoecology of fossil mammals based on infraorbital size. The Anatomical Record 291, 1221-1226.

Muchlinski, M. N., 2010. A comparative analysis of vibrissa count and infraorbital foramen area in primates and other mammals. Journal of Human Evolution 58, 447-473.

Muchlinski, M. N., Wible, J. R., Corfe, I., Sullivan, M., Grant, R. A., 2020. Good vibrations: the evolution of whisking in small mammals. The Anatomical Record 303, 89-99.

Murphy, C. T., Eberhardt, W. C., Clhoun, B. H., Mann, K. A., Mann, D. A., 2013. Effect of angle on flow-induced vibrations of pinniped vibrissae. PloS ONE 8(7), e69872.

Nanayakkara, D., Peirie, R., Mannapperuma, N., Vadysinghe, A., 2016. Morphometric analysis of the infraorbital foramen: the clinical relevance. Anatomy Research International 2016, 7917343.

Noonan, P., Prout, S., Hayssen, V., 2017. *Pteronura brasiliensis* (Carnivora: Mustelidae). Mammalian Species 49(953), 97-108.

Orlov, J. A., 1932. *Semantor macrurus* (Ordo Pinnipedia, Fam. Semantoridae Fam. Nova) aus den Neogen-Ablagerungen Westsibiriens. Travaux de l'Institute Paleozoologique de l'Académie des Sciences de l'Urss 1, 165-268.

Paterson, R. S., Rybczynski, N., Kohno, N., Maddin, H. C., 2020. A total evidence phylogenetic analysis of Pinniped phylogeny and the possibility of parallel evolution within a monophyletic framework. Frontiers in Ecology and Evolution 7, 457.

Patil, K., Sanjay, C. J., Mahima, V. G., Surya, L. K., 2022. Human unilateral bifid coronoid process- Report of a rare accidental radiographic finding. European Journal of Anatomy 26, 231-236.

Penney, R. L., Lowry, G., 1967. Leopard seal predation of Adelie penguins. Ecology 48(5), 878-882.

Perdue, B. M., Snyder, R. J., Maple, T. L., 2013. Cognitive research in Asian small-clawed otters. International Journal of Comparative Psychology 26, 105-113.

Popowics, T. E., 2003. Post Canine dental form in the mustelidae and viverridae(Carnivora: Mammalia). Journal of Morphology 256, 322-341.

Przygocka, A., Podgórski, M., Jędrzejewski, K., Topol, M., Polguj, M., 2012. The location of the infraorbital foramen in human skulls, to be used as new anthropometric landmarks as a useful method for maxillofacial surgery. Folia Morphologica 71(3), 198-204.

Rabi, M., Bastl, K., Botfalvai, G., Evanics, Z., Peigné, S., 2018. A new carnivoran fauna from the late Oligocene of Hungary. Palaeobiodiversity and Palaeoenvironments 98, 509-521.

Radinsky, L. B., 1968. Evolution of somatic sensory specialization in otter brains. Journal of Comparative Neurology 134, 495-506.

Radinsky L. B., 1982. Evolution of skull shape in carnivores. 3. The origin and early radiation of the modern carnivore families. Paleobiology 8, 177-195.

Riedmand, M. L., Estes, J. A., 1990. The sea otter (*Enhydra lutris*): Behavior, ecology, and natural history. Biological Report 90(14), 1-127.

Riisgård, H. U., 2015. Filter-feeding mechanisms in crustaceans, in: Thiel, M., Watling, L. (Eds.), Lifestyles and Feeding Biology. Oxford University Press, Oxford. pp. 418-463.

Rohlf, F. J., Slice, D., 1990. Extensions of the procrustes method for the optimal superimposition of landmarks. Systematic Zoology 39(1), 40-59.

Rohlf, F. J., Marcus, L. F., 1993. A revolution in morphometrics. Tree 8(4), 129-132.

Rohlf, F. J., 2005. The Tps series of softwares. Hystrix 26(1), 1-4.

Rolfe, S., Pieper, S., Porto, A., Diamond, K., Winchester, J., Shan, S., Kirveslahti, H., Boyer, D., Summers, A., Maga., A. M., 2021. SlicerMorph: an open and extensible platform to retrieve, visualize and analyse 3D morphology. Methods in Ecology and Evolution 12, 1816-1825.

Romaniuk, A. 2018. Shape variation of Palearctic mustelids (Carnivora: Mustelidae) mandible is affected both by evolutionary history and ecological preference. Hystrix 29(1), 87-94.

Russo, L. F., Meloro, C., De Silvestri, M., Chadwick, E. A., Loy, A., 2022. Better sturdy or slender? Eurasian otter skull plasticity in response to feeding ecology, PloS ONE 17,e0274893.

Rybczynski, N., Dawson, M. R., Tedford, R. H., 2009. A semi-aquatic Arctic mammalian carnivore from the Miocene epoch and origin of Pinnipedia. Nature 458, 1021-1024.

Sabol, M., Holec, P., 2002. Temporal and spatial distribution of Miocene mammals in the Western Carpathians (Slovakia). Geologica Carpathica 53, 269-279.

Sato, J. J., Wolsan, M., Prevosti, F. J., D'Elía, G., Begg, C., Begg, K., Hosoda, T., Campbell, K. L., Suzuki, H., 2012. Evolutionary and biogeographic history of weasel-like carnivorans (Musteloidea). Molecular Phylogenetics and Evolution 63(3), 745-757.

Savage, R. J. G., 1957. The anatomy of *Potamotherium* an Oligocene Lutrinae. Proceedings of the Zoological Society of London 129(2), 151-244.

Schneider, C. A., Rasband, W. S., Eliceiri, K. W., 2012. NIH Image to ImageJ: 25 years of image analysis. Nature Methods 9, 671-675.

Shin, J. Y., Alias, A., Chung, E., Ng, W. L., Wu, Y. S., Gan, Q. F., Thu, K. M., Choy, K. W., 2021. Identification of race: a three-dimensional geometric morphometric and conventional analysis of human fourth cervical vertebrae in adult Malaysian population. Journal of Clinical and Health Sciences Special Issue 6(1), 17-31.

Singh, R., 2011. Morphometric analysis of infraorbital foramen in indian dry skulls. Anatomy & Cell Biology 44, 79-83.

Slice, D. E., 2007. Geometric Morphometrics. Annual Review of Anthropology 36, 261-281.

Smith, A. L., Grosse, I. R., 2016. Biomechanics of zygomatic arch shape. The Anatomical Record 299, 1734-1752.

Sokal, R. R., Rohlf, F. J., 1995. Biometry: the Principles and Practice of Statistics in Biological Research. 3rd Edition. W. H. Freeman and Co., New York.

Stirling, I., 1983. The evolution of mating systems in pinnipeds, in: Eisenberg, J. F., Kleinman, D. G. (Eds.), Recent Advances in the Study of Mammalian Behavior. American Society of Mammalogists, Pittsburgh, pp. 489-527.

Strobel, S. M., Sills, J. M., Tinker, M. T., Reichmuth, C. J., 2018. Active touch in sea otters: in-air and underwater texture discrimination thresholds and behavioral strategies for paws and vibrissae. Journal of Experimental Biology 221, jeb181347.

Szabó, N., Botfaval, G., Kocsis, L., Carnevale, G., Sztano, O., Evanics, Z., Rabi, M., 2017. Upper Oligocene marine fishes from nearshore deposits of the Central Paratethys (Máriahalom, Hungary). Palaeobiodiversity and Palaeoenvironments 97, 747-771.

Tatsuta, H., Takahashi, K. H., Sakamaki, Y., 2018. Geometric morphometrics in entomology: basics and applications. Entomological Science 21, 164-184.

Tedford, R. H., Relationships of Pinnipeds to other carnivores (Mammalia). Systematic Zoology 25, 363-374.

Timm-Davis, L. L., DeWitt, T. J., Marshall, C. D., 2015. Divergent skull morphology supports two trophic specializations in otters (Lutrinae). PloS ONE 10(2), e0143236.

Tseng, Z. J., Grohe, C., Flynn, J. J., 2016. A unique feeding strategy of the extinct marine mammal Kolponomos: convergence on sabretooths and sea otters. Proceedings of the Royal Society B 283, 20160044.

Tseng, Z. J., Su,D. F., Wang, X., White, S. C., Ji, X., 2017. Feeding capability in the extinct giant Siamogale melilutra and comparative mandibular biomechanics of living Lutrinae. Nature Scientific Reports 7, 15225.

Qiu, Z., 2003. Dispersals of Neogene carnivorans between Asia and North America. Bulletin of the American Museum of Natural History 279, 18-31.

Webster, M., Sheets, H. D., 2010. A practical introduction to landmark-based geometric morphometrics, in: Alroy, J., Hunt, G. (Eds.), Quantitative Methods in Paleobiology. The Paleontological Society, pp. 163-188.

Werth, A., 2000. Feeding in marine mammals, in: Schwenk, K. (Ed.), Feeding: Form, Function and Evolution in Tetrapod Vertebrates. Academic Press, San Diego, pp. 487-526.

Willemsen, G. F., 1992. A revision of the Pliocene and Quaternary Lutrinae from Europe. Scripta Geologica 101, 1-115.

Wolsan, M., 1993. Phylogeny and classification of early European *Mustelida* (Mammalia: Carnivora). Acta Theriologica 38(4), 345-384.

Wright, L., de Silva, P. K., Chan, B., Reza Lubis, I., Basak, S., 2021. Aonyx cinereus. The IUCN Red List of Threatened Species 2021, Et44166a164580923.

Yu, L., Peng, D., Liu, J., Luan, P., Liang, L., Lee, H., Lee, M., Ryder, O. A., Zhang, Y., 2011. On the phylogeny of Mustelidae subfamilies: analysis of seventeen nuclear non-coding loci and mitochondrial complete genomes. BMC Evolutionary Biology 11, 92.

Zelditch, M. L., Swiderski, D. L., Sheets, H. D., 2012. Geometric Morphometrics for Biologists: A Primer (Second Edition). Elsevier, New York.

Abbreviations

AMNH: American Museum of Natural History

CMNH: Cleveland Museum of Natural History

DUNUC: University of Dundee

LACM: Los Angeles Museum of Natural History

IMNH: Idaho Museum of Natural History

LEPBLB: Laboratorio de Ecologia de Pinnipedos ‘’Burney J. Le Boeuf’’.

MNHN: Muséum national d’Histoire naturelle, Paris

MRI-PAS: Mammal Research Institute, Polish Academy of Sciences

MSU: Michigan State University

MZB: Museu de Ciències Naturals de Barcelona

N-C: California Academy of Sciences

NHMUK: Natural History Museum, London

NMBA : Naturhistorisches Museum Basel

RISD: Rhode Island School of Design

SMNS: Staatliches Museum für Naturkunde

UAM: University of Alaska Museum

UMZC: University Museum of Zoology, Cambridge

USNM: United States National Museum

YPM: Yale Peabody Museum of Natural History

List of Figures

Table of Cranial Landmarks

1) Anterior-most point of Nasal bones at medial plane

2) Nasal and Frontal bone intersection

3) Frontal and Parietal bone intersection at medial plane

4) Parietal and Interparietal bone intersection at medial plane

5) Nuchal Crest at median plane

6) Lateral-most point of left Occipital condyle

7) Lateral-most point of left Superior Nuchal line

8) Occipital condyle's caudal margin

9) Auditory bulla's rostral-most tip

10) External auditory meatuses lateral-most tip

11) Auditory bulla's caudal-most tip

12) Auditory bulla's medial-most point at the suture of Basisphenoid and Basioccipital bones

13) Parietal and Squamosal suture

14) Mastoid process's lateral-most point at left side

15) Parietal's rostral-most projection

16) Inferior Orbital Fissure

17) Optic canal foramen

18) Infraorbital foramen's lateral-most point

19) Infraorbital foramen's caudal-most point

20) Dorsal-most junction of Squamosal and Jugal bones

21) Zygomatic arch's tip

22)Dorsocaudal-most suture of Maxilla and Jugal bones

23) Dorsal junction of Maxilla and Jugal bones

24) Junction of Lacrimal, Maxilla and Frontal bones

25) Junction of Maxilla, Frontal and Nasal bones

26) Anteriolateral-most point of left Nasal bone

27) Dorsorostral-most tip of the rostrum

28) Ventral junction of Premaxilla and palatine process of maxilla bones at medial plane

29) Caudal-most point of palate's midline

30) Rostral edge of left canine along lingual palatine border

31) Caudal-most edge of left canine

32) Rostral-most edge of first left post-canine tooth

33) Rostral-most edge of second left post-canine tooth

34) Projection of landmark 33 to the palate midline

35) Rostral-most edge of third left post-canine tooth

36) Projection of landmark 35 to the palate midline

37) Caudal-most edge of last left post-canine tooth

38) Ventral junction of Palatine process of Maxilla and Palatine bones at medial plane

39) Rostral-most point of the Pterygoid at its suture with palatine bones

40) Junction of Presphenoid and Basisphenoid bone at medial plane

41) Junction of Basisphenoid and Basioccipital bones at medial plane

42) Caudal-most suture of left side's Squamosal, parietal and Supraoccipital bones